TECHNISCHE UNIVERSITÄT MÜNCHEN

Lehrstuhl für Ernährungsphysiologie

Colonic expression of the intestinal peptide transporter PEPT1 is not associated with inflammatory bowel diseases in humans and mouse models

Tilo Wünsch

Vollständiger Abdruck der von der Fakultät Wissenschaftszentrum Weihenstephan für Ernährung, Landnutzung und Umwelt der Technischen Universität München zur Erlangung des akademischen Grades eines

Doktors der Naturwissenschaften

genehmigten Dissertation.

Vorsitzender: Univ.-Prof. Dr. M. Schemann
PrüferIn der Dissertation: 1.   Univ.-Prof. Dr. H. Daniel
                                              2.   Univ.-Prof. Dr. D. Haller

Die Dissertation wurde am 23.03.2012 bei der Technischen Universität München eingereicht und durch die Fakultät Wissenschaftszentrum Weihenstephan für Ernährung, Landnutzung und Umwelt am 29.07.2012 angenommen.

ZUSAMMENFASSUNG

Der intestinale Peptidtransporter PEPT1 findet sich in der apikalen Membran von Dünndarmzellen. Er ermöglicht die Aufnahme von Di- und Tripeptiden, welche bei der Proteinverdauung anfallen und trägt damit zur Aminosäureversorgung des Organismus bei. Neben den aus der Proteinverdauung hervorgegangenen Peptiden ist PEPT1 auch in der Lage immunmodulierende und entzündungsfördernde bakterielle Peptide wie N-Formyl-Methionyl-Leucyl-Phenylalanine (fMLP) oder Muramyldipeptid (MDP) zu transportieren und ihnen somit den Kontakt zum Immunsystem zu ermöglichen. Zudem wurde PEPT1 als Suszeptibilitätsgen für chronisch entzündliche Darmerkrankungen beschrieben und es wurde eine erhöhte PEPT1-Expression im entzündeten Colon von Patienten mit chronisch entzündlichen Darmerkrankungen postuliert, während angenommen wird, dass PEPT1 im gesunden Colon nicht exprimiert ist.

Ziel dieser Arbeit war es die PEPT1-Expression systematisch im gesunden Colon von Mäusen, Ratten und Menschen zu erforschen und seine Expression während Darmentzündung in Mausmodellen und an humanen Gewebeproben von Patienten mit chronisch entzündlichen Darmerkrankungen zu untersuchen.

Mit Hilfe spezialangefertigter Antikörper gelang erstmalig die Detektion von PEPT1 im gesunden Colon von Mäusen, Ratten und Menschen. Dabei zeigte PEPT1 ein differentielles Verteilungsmuster entlang der proximal-distalen Achse des Colons. Während PEPT1 im proximalen Teil nicht detektierbar war, stieg seine Expression vom mittleren Teil bis zum Rektum deutlich an. Funktionelle Analysen am intakten Mausdarm zeigten seine Transportaktivität und ein erhöhter Wassergehalt im Fäzes von Pept1-defizienten ($Pept1^{-/-}$) Mäusen deutet auf den physiologischen Wert von PEPT1 zur adequaten Flüssigkeitsresorption hin. Das PEPT1-Protein aus dem Colon zeigt ein höheres Molekulargewicht als die Dünndarm-Variante, was auf einen erhöhten Glykosylierungszustand im Dickdarm zurück geführt werden konnte.

Während Darmentzündung, sowohl bei Morbus Crohn-ähnlicher Ileitis in $TNF^{\Delta ARE/WT}$-Mäusen, als auch Colitis-ähnlicher Entzündung in $IL\text{-}10^{-/-}$-, $IL\text{-}10XTLR2^{-/-}$- oder $Rag2^{-/-}$-Mäusen wurde nur eine verminderte PEPT1-Expression im entzündeten Gewebe festgestellt. Auch humanes Darmgewebe zeigte in der aktiven Entzündungsphase eine verminderte PEPT1 Expression. Weiterhin zeigten $Pept1^{-/-}$-Mäuse im Vergleich zu Wildtyp-Mäusen keine veränderte Anfälligkeit gegenüber einer mit Dextrannatriumsulfat (DSS) induzierten Colitis und PEPT1 war in Wildtyp-Mäusen nach DSS-Behandlung nur vermindert detektierbar.

Zusammenfassend zeigen die Ergebnisse erstmals die segmentspezifische PEPT1-Expression im gesunden Colon von Mäusen, Ratten und Menschen und seine verminderte Expression im entzündeten Darmgewebe. Die Gesamtheit der Ergebnisse deutet – entgegen bisheriger Annahmen – nicht auf eine vermehrte Bildung von PEPT1 im entzündeten Colon hin und läßt daher auch keinen zentralen Zusammenhang zwischen PEPT1 und der Entstehung oder dem Verlauf chronisch entzündlicher Darmerkrankungen vermuten.

ABSTRACT

The intestinal peptide transporter PEPT1 is expressed in the brush border membrane of enterocytes and contributes to adequate amino acid supply from dietary protein digestion. Additionally, PEPT1 has been shown to transport bacterial peptides with immunomodulatory activities, like N-formylmethionyl-leucyl-phenylalanine (fMLP) or muramyl dipeptide (MDP). PEPT1 has been identified as a susceptibility gene in IBD and is proposed to be expressed at high levels in the inflamed but not in healthy normal colon. By its capability to transport bacteria-derived proinflammatory di- and tripeptides, PEPT1 has been proposed to act as an amplifier of inflammatory processes.

Although prominent PEPT1 expression in the small intestine is consistently found, data about its expression level in colonic tissues in health and disease conditions are highly controversial. We therefore reassessed the presence and function of PEPT1 in healthy and inflamed colon and found that PEPT1 is expressed in epithelial cells of normal distal colon and rectum but not in proximal colon of mice, rats and humans. Basal colonic PEPT1 expression is not influenced by the intestinal microbiota, as germfree mice show identical PEPT1 expression patterns as conventionally housed mice. In contrast to small intestinal PEPT1, colonic PEPT1 shows a higher molecular weight which can be attributed to higher glycosylation status. Colonic PEPT1 was demonstrated to be functional in intact colonic mouse tissues of wildtype mice and PEPT1-deficient ($Pept1^{-/-}$) mice showed an increased fecal water content suggesting that PEPT1 contributes to electrolyte and water homeostasis.

During intestinal inflammation, as studied in four animal models, resembling Crohn's-like ileitis ($TNF^{\Delta ARE/WT}$) and colitis ($IL\text{-}10^{-/-}$, $IL\text{-}10XTLR2^{-/-}$, $Rag2^{-/-}$), and in human intestinal tissues from IBD patients, severity of inflammation correlated with lowered PEPT1 expression levels. Moreover, in $Pept1^{-/-}$ mice susceptibility to dextran sodium sulfate (DSS)-induced colitis was unaltered and PEPT1 expression in wild-type mice treated with DSS decreased significantly.

The totality of the data unequivocally showed that PEPT1 is expressed in healthy colon from mice, rats and humans and is down-regulated during small intestinal and colonic inflammation in mouse models and human IBD. These findings contradict previous findings suggesting that PEPT1 is not expressed in healthy colon but may be up-regulated during intestinal inflammation.

Taken together, the current studies argue against a contribution of colonic PEPT1 expression in exacerbating proinflammatory processes and thus strongly suggest that PEPT1 is not associated with the development of intestinal inflammation or IBD severity.

TABLE OF CONTENTS

1 INTRODUCTION

1.1 Discovery of the peptide transporter PEPT1 and its main structural features

The oligopeptide transporter PEPT1 belongs as member 1 to the solute carrier (SLC) family 15A, also tagged as proton-coupled oligopeptide transporters (POT). Other POT members are PEPT2 (SLC15A2), and the peptide/histidine transporter (PHT) 1 (SLC15A4) and PHT2 (SLC15A3). Proton-dependent peptide transport across intestinal brush border membranes was already shown in the 1980's [1] and the gene encoding the responsible PEPT1 protein was first cloned in 1994 from a rabbit cDNA library based on a functional screening in *Xenopus laevis* oocytes [2, 3]. The amino acid sequence of rabbit-PEPT1 comprises 707 amino acids with 12 predicted transmembrane domains (TMDs), a large extracellular loop between TMD 9 and 10 and cytosolic amino- and carboxy-termini [2]. Cloning of the human, rat and mouse PEPT1 predicted similar membrane arrangements with 12 TMDs as described before for rabbit-PEPT1 [4-6]. The rat-PEPT1 (rPEPT1) isoform, encoded on chromosome 15, consists of 710 amino acids and the large extracellular loop between TMD 9 and 10 has 5 potential canonical N-linked glycosylation sites and in the inside loop between TMD 8 and 9 two predicted phosphorylation sites; one for protein kinase A (PKA; Thr-362) and one for protein kinase C (PKC; Ser-357) [5, 7]. The mouse PEPT1 (mPEPT1) isoform is encoded on chromosome 14, consists
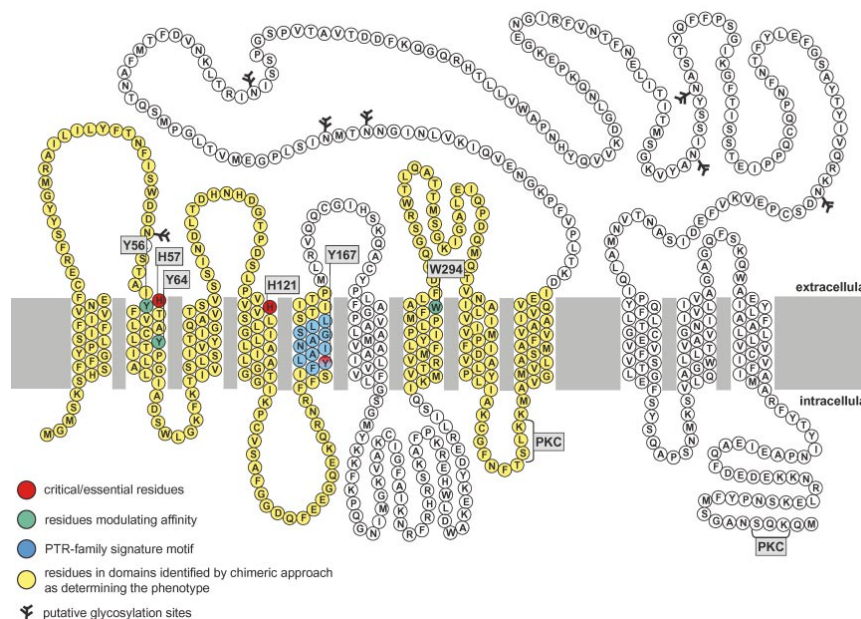

Figure 1. Secondary structure model of hPEPT1.
(Adopted from Daniel H 2004 [8]) Topology organization of hPEPT1 showing 12 TMDs, intracellular C- and N-terminus and the large extracellular loop between TMD 9 and 10. Furthmore, single amino acids or distinct regions representing important functional domains or individual residues relevant for function are color-coded.

of 709 amino acids, the large extracellular loop between TMD 9 and 10 with 5 potential N-linked glycosylation sites, one cAMP-dependent protein kinase phosphorylation site (Thr-362) and one PKC-dependent phosphorylation site (Ser-357) [6]. While the human PEPT1 (hPEPT1) protein carries two potential PKC phosphorylation sites but none for PKA-dependent phosphorylation (**Figure 1**) [4]. The hPEPT1 isoform consists of 708 amino acids, encoded on chromosome 13. The three-dimensional structure of the mammalian peptide transporter proteins is not available, as none of the proteins has been crystallized yet. So the current models of PEPT1 structures are based on hydrophobicity plots and *in silico* molecular modeling approaches on the basis of recently crystallized bacterial transporters [9, 10].

1.2 Characteristics of the transport process and substrates of PEPT1

Fei YJ and coworkers expressed rabbit-PEPT1 in *Xenopus laevis* oocytes and described the proton driven, electrogenic nature of PEPT1-mediated transport processes, which occurs independent from sodium, potassium or chloride ions, but is energized by a negative membrane potential [2]. PEPT1 transport was found to cause a decrease of the intracellular pH from 7.22 to 7.0 and membrane depolarization in *Xenopus laevis* oocytes. And PEPT1 mediated transport (at low substrate concentrations) was found to be maximal at an extracellular pH of 5.5, compatible with an acidic micro-environment on the outside of the brush border membrane [11]. The transport properties of PEPT1 have been well characterized in small intestine of several species [12, 13] and *in vitro* test systems like cell cultures or heterologous expression in *Xenopus leavis* oocytes [14, 15]. They all revealed PEPT1 to serve as a high capacity, low affinity (Km ~1.1 mM for the prototypical PEPT1 substrate glycylsarcosine (Gly-Sar)) transporter [16]. PEPT1 transports di- and tripeptides as well as peptidomimetics such as the β-lactam antibiotics cefadroxil and cyclacillin, whereas transport of a tetrapeptide consisting of glycine was hardly detectable and free amino acids are not transported at all. From Gly-Sar uptake and simultaneous proton flux measurements Fei YJ and colleagues calculated a substrate to proton flux-stoichiometry of 1:1 [2].

PEPT1 function *in vivo* depends on the inwardly directed proton gradient with the cell interior less acidic than the lumen. To maintain this gradient, PEPT1 function requires the proton-sodium exchanger (NHE) 3, which exports protons out of the cell by utilizing the sodium ion-gradient as a driving force. When the proton gradient is disrupted, peptide uptake is reduced. This functional connection and the necessity of NHE3 for adequate transport function of PEPT1 has been shown *in vitro* in the transfected human embryonic kidney cell line 293 (HEK293), the human colorectal epithelial adenocarcinoma cell line Caco-2 and hPEPT1-expressing *Xenopus laevis* oocytes [17-19]. Finally, the basolateral sodium-potassium ATPase is required to maintain the intracellular sodium ion

concentration, defining PEPT1 as a tertiary-active transporter [20]. PEPT1 has a wide substrate spectrum as it transports virtually all naturally occurring di- and tripeptides. Based on 20 proteinogenic amino acids, far over 8.000 di- and tripeptide combinations are possible. And together with numerous peptidomimetic drugs, PEPT1 accepts a wide range of heterogenic substrates with respect to the molecular weight (MW; 132-577 kDa), charge, polarity and conformation [8]. After transport into cells, most peptides undergo intracellular hydrolysis to free amino acids for delivery into portal blood, mediated by amino acid transporters on the basolateral site [21]. However, as intact peptides seem to pass the basolateral membrane, the existence of a further peptide transporter has been proposed, but no protein has yet been identified as such (**Figure 2**) [22].
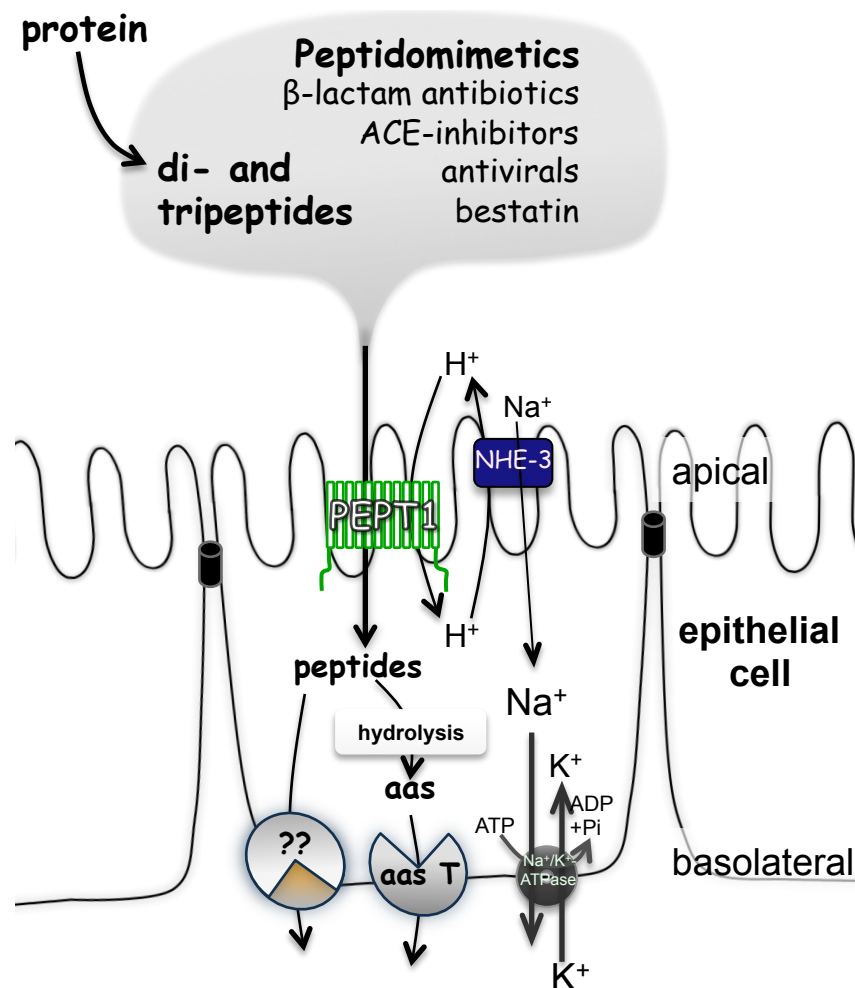
Figure 2. Schematic illustration of the physiological PEPT1 transport process.
PEPT1, expressed in the apical brush border membrane of intestinal epithelial cells, accepts nutrient derived di- and tripeptides as well as certain peptidomimetic drugs as substrates and arranges intracellular uptake. Intracellularly peptides become hydrolysed and free amino acids are transported via different amino acid transporting systems (aas T) into the blood. Peptides not undergoing hydrolysis can exit the cell by a basolateral peptide transporting system which has still to be identified.

In addition to nutrient derived peptides, PEPT1 has been shown to transport β-lactam antibiotics of the cephalosporine and aminopenicillin group, antiviral drugs like valacyclovir, the anticancer agent bestatin and certain angiotensin-converting enzyme inhibitors like fosinopril or ramipril [5, 14, 23-26]. Other substrates include bacterial structures originating from the intestinal commensal bacterial flora or even pathogens [27-29]. And even the anti-inflammatory acting tripeptide lysine-proline-valine (KPV) has been described as PEPT1 substrate [30]. Beside physiological substrates or substrates with therapeutical benefit, a fluorophore-conjugated dipeptide derivative D-Ala-Lys-N(epsilon)-7-amino-4-methylcoumarin-3-acetic acid (D-Ala-Lys-AMCA) was found and offered the possibility to visualize peptide transporter-mediated uptake into cells [31, 32].

1.3 Tissue distribution of PEPT1

The well characterized transport properties and its distinct expression in surface layers within the body makes PEPT1 a target for drug delivery approaches. PEPT1 is known as the "intestinal" peptide transporter isoform because it is primarily expressed in the brush border membrane of enterocytes, although it is also expressed in other tissues, like the nasal epithelium, kidney, bile duct epithelium and macrophages [2, 33-36]. In contrast, PEPT2 is defined as the „renal" PEPT isoform, as it is primarily expressed in the kidney, but can be also found in enteric glia cells, thyroid follicular cells, lung epithelial cells and mammary gland and the choroid plexus [37-41].

About PEPT1 expression along the entire small and large intestine, controversial data exist. It is well established that PEPT1 is expressed in the brush border membrane of enterocytes of the small intestine with increasing expression along the crypt-villus axis and highest expression level on cells of the villus tip [42, 43]. For colonic expression conflicting findings are reported. Several reports describe colonic tissue as free of PEPT1 expression [2, 44-46], while other studies showed low mRNA expression levels in colonic tissue from healthy humans and rodents [42, 47, 48]. Meier Y et al. reported a markedly increasing *Pept1* mRNA abundance along the human colon from the ascending to the descending part [42]. Increased *Pept1* mRNA in distal colon in comparison to the proximal part was also found in mice by Jappar D et al., however they found no PEPT1 protein in distal colon [45]. Finally, although the presence of PEPT1 in healthy colon has so far never been systematically addressed, PEPT1 is proposed to be substantially up-regulated during colonic inflammation in IBD patients [49, 50], in IL-10$^{-/-}$ mice [51] or during chemical induced colitis in rats [52].

1.3.1 Expression of other nutrient transporters in colon

Recent reports focusing on other intestinal transport proteins like the sodium-dependent glucose transporter 1 (SGLT1), the insulin-independent glucose transporter 1 (GLUT1),

NHE3 or the chloride/bicarbonate exchanger, down-regulated in adenoma (DRA) demonstrated their small intestinal and also colonic presence [53, 54]. Furthermore, NHE3 and DRA showed contrasting expression profiles along the proximal-distal axis of rat colon [53]. While DRA was found to be abundantly expressed in distal colon and the cecum but not in the proximal part of the colon, NHE3 was found to be expressed in the proximal part of the colon but not in distal colon or cecum. These findings extend the knowledge about the physiological role of the colon in electrolyte and water absorption and pH regulation [53].

Notably, with respect to the colonic SGLT1 expression found in mice, studies on rats failed to detect either the protein or SGLT1-mediated transport in the colon [55, 56]. Whether these are typical species differences remains unclear.

1.4 Physiological importance of PEPT1 and characteristics of *Pept1* knockout (*Pept1*^{-/-}) mice

Under physiological conditions PEPT1 seems to be dispensable, as the capacity of small intestinal amino acid transporters seems not to limit the uptake of adequate amounts of amino acids. However for enteral nutrition in patients, peptide solutions which have a lower osmolarity than solution containing free amino acids proved to be beneficial [57].

The importance of PEPT1 as a back-up system becomes obvious when functions of intestinal amino acid transporters are impaired or deleted. One example is a genetic defect in the SLC6A19 gene encoding the sodium-dependent neutral amino acid transporter B(0)AT1. Patients with an inherited defect in this transporter, called Hartnup disease do not suffer from inadequate amino acid supply of typical SLC6A19 transporter substrates such as tryptophane or phenylalanine, as the defect can be compensated by uptake of peptides, including those containing the critical amino acids, via PEPT1 [58]. The other way round, deletion of the *Pept1* gene in *Pept1*^{-/-} mice did not lead to any obvious phenotypical abnormalities in these mice under basal conditions [59]. Nevertheless, *Pept1*^{-/-} mice show reduced dipeptide absorption and an altered ability to handle large protein loads [59, 60]. Furthermore, the Gly-Sar induced acid load in small intestinal enterocytes from wild-type mice was abolished in *Pept1*^{-/-} mice and PEPT1 function was found to significantly contribute to intestinal fluid transport. [61].

1.5 PEPT1-regulating factors and the transcriptional control

Regulation of PEPT1 has been described by different stimuli and conditions, including dietary protein intake, fasting, diurnal rhythm, proinflammatory cytokines, vitamin D3, leptin, L-thyroxine, butyrate and certain bacteria; most of them modulating *Pept1* expression on the transcriptional level [12, 51, 62-71].

Transcriptional regulation of *Pept1* in mammals has been studied in various models. Beside experimental data, bioinformatic approaches were used to determine putative transcription factor binding sites upstream near the transcription start site of the *Pept1* gene. Fei YJ et al. presented the first overview of potential *Pept1* regulating transcription factors [6]. They proposed the essential regulating elements within 1140 bp upstream the transcription start and possible transcription factors are Sp1, AP-1/Jun-B, Cdx2, c-Myb, c-Myc, GATA-1, NFE1 and AARE. Sp1 was considered to be crucial for basal *Pept1* transcription [72, 73]. Computational analyses showed the lack of a TATA or CAAT box near the transcription start but several GC-rich regions [6, 73]. The *Pept1* promotor region showed additionally binding sites for AP-1, CREB, myeloid zinc finger 1 (Mzf1) and caudal-related homeobox transcription factor Cdx A [73]. Shimakura J et al. showed substantial regulation of *Pept1* expression after mutagenesis of an element till -172 bp downstream of the transcription start and electrophoretic mobility shift assays (EMSA) revealed Sp1 to bind to two of the predicted binding sites. The Sp1 binding has been shown to be responsible for recruiting TATA-binding proteins and fixing the transcription start site [74, 75]. Thus, Sp1 seems to play a significant role as basal transcription factor for *Pept1*. In addition, Shimakura J et al. showed by reporter gene assays that Sp1 interacts with the transcription factor Cdx2 and both synergistically activate *Pept1* expression [72]. Shiraga T et al. found further upstream of -172 bp before the transcription start of the *Pept1* gene in rats a TATA-like box, further GC-rich regions and an amino acid-responsive element [62]. Initially, Shiraga T et al. detected increased Gly-Sar transport rates in ileal brush border membrane vesicles (BBMV) after protein feeding to rats and *Pept1* mRNA levels were found to be increased. Their analysis of potential regulatory factors by reporter gene assays revealed AP-1 as one factor. AP-1 was indeed shown to be involved in gene expression regulation by amino acid starvation [76]. Beside AP-1, Shimakura J et al. found an amino acid responding-element -277 to -271 bp of the rat *Pept1* promotor, which might be a link to direct regulation of *Pept1* transcription by the intracellular amino acid pool [73].

A further study showing *Pept1* regulation by leptin revealed the necessity of the transcription factors CREB and Cdx2 for this regulation [67]. Furthermore it was shown by co-immunoprecipitation that a direct interaction of both transcription factors, CREB and Cdx2, occur [67]. The same mechanism was reported to be responsible for the butyrate-induced *Pept1* expression [68]. Pathogenic bacteria have also been shown to transcriptionally regulate *Pept1* expression. Here, Nguyen HT et al. showed that Cdx2 is required for *Pept1* expression induced by the pathogenic bacterium *citrobacter (c.) rodentium*. Together with their previous studies on butyrate and leptin-regulated *Pept1*

expression - in inflammation-associated states - Cdx2 appears as the key factor in controlling pathophysiological *Pept1* expression [68, 69].

In addition to transcriptional *Pept1* regulation, so far only one study found a posttranscriptional regulation of PEPT1 expression by small noncoding RNA, microRNA. This microRNA was found to be inversely correlated with the expression levels of PEPT1 during the differentiation of the human epithelial colorectal adenocarcinoma cell line Caco2-BBE *in vitro* [77]. In context with intestinal proliferation and differentiation the evolutionary conserved zinc finger-containing transcriptional factor family of Krüppel-like factors (klfs) has also been described [78, 79]. One study in zebrafish showed that klf4 is required for intestinal epithelia development, including *Pept1* expression [80].

1.6 Inflammatory bowel disease and its etiology

Inflammatory bowel diseases (IBD) are a group of spontaneously relapsing, chronic inflammatory disorders of the gastrointestinal tract. The two primary forms of IBD are Crohn's disease (CD) and ulcerative colitis (UC). While UC is limited to the colon and characterized by diffuse mucosal inflammation, CD may affect any part of the gastrointestinal tract and is characterized by a patchy distribution and the transmural nature of the inflammation. Typical clinical symptoms of IBD include abdominal pain, fever, diarrhea with blood and mucus, and increased risk of colon cancer [81-83].

IBD have a multifactorial etiology with four major factors contributing to the development, namely environmental factors, the intestinal microbiota, the individual genetic make-up, and disturbances in the innate and adaptive immune responses. These factors lead to a disturbed intestinal homeostasis, driven by the dynamic interplay between intestinal epithelial cells (IEC), the intestinal microbiota and the host's immune system. A combination of all these factors is necessary for the clinical manifestation of the disease. However, the clinical picture displayed by the patients is not homogenous for both, clinical symptoms as well as response to therapy [84].

1.7 The intestinal epithelium as the first line of defense

An intact intestinal epithelial layer is required to maintain intestinal homeostasis [85]. The intestinal epithelium represents a single cell layer consisting of different cell types, which are connected thightly to each other to form a highly selective barrier between the luminal environment and underlying lamina propria immune cells and cappilaries. Beside barrier formation, epithelial cells secrete compounds that influence bacterial colonization, e.g. mucins, defensing and trefoils peptides as well as secretory IgA (sIgA) from specialized cells, namely Paneth and Goblet cells. The latter produce and secrete mucins which form – together with the cell surface glycocalyx – a biofilm thought to prevent the unselected attachement of intestinal bacteria to the epithelium [86, 87]. The intestinal mucus

secretion is a direct response of the epithelium to the intestinal microbiota, as germfree rats show altered gut mucin contents as compared to conventionally housed rats [88, 89]. An intact mucus-producing Goblet cell system has a crucial role in intestinal homeostatsis, as mice lacking the major mucin protein MUC2 develop spontaneous colitis [90]. Comparable results were observed in mice lacking an enzyme important for sufficient mucin core protein production, the 3 beta1,3-N-acetylglucosaminyltransferase. These mice show increased susceptibility towards chemically induced colitis and colorectal adenocarcinoma genesis [91]. The second cell type producing and secreting defense compounds are Paneth cells. These cells are located at the base of the small intestinal crypts and produce antimicrobial peptides, called defensins. In contrast to the general mucin production from Goblet cells, Paneth cells act in inducible fashion. Impaired Paneth cell function (defensin secretion) has been shown to contribute to CD susceptibility, as for example CD patients or those with Nucleotide-Binding Oligomerization Domain 2 (NOD2)-susceptibility alleles showed reduced α-defensin expression [92, 93]. However, if this is a cause or a consequence of IBD is still a matter of debate [94]. Furthermore, Paneth cells are able to sense commensal bacteria by Toll-like receptors (TLRs) inducing defensin production and secretion [95].

The intestinal epithelium is forced to interact with and has to adapt and respond to the constant changing environment by processing the combined biological information of luminal enteric bacteria and host-derived signals in order to maintain gut homeostasis. This tightly regulated homeostatsis between oral tolerance and immune response is called hyporesponsiveness. Hyporesponsiveness vs. (chronic) intestinal inflammation is determined by the presence or absence of appropriate control mechanisms, like conditioning cytokines that terminate mucosal immune responses to the constant antigenic drive of luminal enteric bacteria and food antigens. Appropriate function of the innate immune system is required to regulate tolerance to commensal intestinal microbiota and thus maintain the peaceful coexistence of commensal bacteria in the gut, so called symbiosis [96, 97].

1.8 Crosstalk between luminal bacteria and the immune system

IEC directly interact with the luminal microbiota as they express molecules specialized to recognize bacterial structures, so called pattern recognition receptors (PRRs). PRRs are the first structures of the hosts innate immune system that get in contact with and sense luminal microbial content and they have the ability to discriminate between pathogenic and non-pathogenic (commensal) bacteria and to initiate adequate immune responses [98]. Important members of PRRs are NOD-like receptors (NLRs) or TLRs, both expressed in IEC [99, 100].

NLR proteins, like NOD1 and NOD2 contain a NOD domain in the C-terminal domain linked to a leucine-rich repeat (LRR) domain and linked on the N-terminal side to two tandem caspase recruitment domains (CARDs). The LRR domain acts as microbe-associated molecular pattern recognition region and the CARD domains are the responsible regions for downstream signaling by Nuclear Factor-κB (NF-κB). NF-κB can act through a protein–protein interaction of CARD with the serine-threonine kinase receptor-interacting protein 2 (RIP2) and can in turn cause expression of various proinflammatory cytokines like Interleukin (IL)-1β, IL-18 or IL-23, which in turn activate helper T (T_H) cells to produce IL-17 (T_H17) and cause T_H1 cell responses [101-106]. Several bacterial structures and moieties have been identified as PRR agonists. Amongst those, muramyl dipeptide (MDP), part of bacterial peptidoglycan, was found to get recognized by LRRs of NOD2 and shown to activate NF-κB [104, 107]. In case of NOD1 the bacterial peptide l-Ala-γ-D-Glu-meso-diaminopimelic acid (Tri-DAP) was demonstrated to interact with the LRR domain of NOD1 to mediate downstream NF-κB activation [108].

TLRs are transmembrane receptors that are characterized by an extracellular domain containing LRRs and the intracellular domain containing the adapter molecules Toll/IL-1R and myeloid differentiation factor 88 (MyD88) [109]. TLRs were found to sense a broad spectrum of bacterial structures from gram-positive and gram-negative bacteria with ligand-specific binding to TLRs, providing the basis for differentiated activation of downstream cascades and responses [110-112]. TLRs promote signals by interaction of the cytoplasmic TIR domain with various adaptor proteins (MyD88, MAL/TIRAP, TRIF/TI-CAM-1, TRAM/TIRP/TICAM-2) and subsequent activation of effector kinases such as the mitogen-activated kinases (MAPK), extracellular signal-regulated kinase (ERK) or c-Jun NH$_2$-terminal kinase (JNK), which finally activate NF-κB-dependent gene expression [113, 114]. Most of the downstream signaling of PRRs in IEC involves the transcription factor NF-κB [115, 116]. And commensals have been shown to dampen the proinflammatory response by inhibition of the inhibitory protein (IκBα) degradation and enhanced nuclear export of the transcriptionally active NF-κB subunit RelA [117].

The importance of adequate PRR function on maintaining intestinal homeostatsis becomes obvious as transgenic mice with modified PRR expression or signaling function are more susceptible to develop intestinal inflammation. However, most of the mouse models with genetic modifications of PRRs or associated proteins do not develop spontaneous inflammation but display increased susceptibility towards inflammation when induced by certain stimuli like pathogenic bacteria or chemicals. For example, NOD2^{-/-} mice do not develop spontaneous intestinal inflammation but are more susceptible to intra-oral *Listeria* infection [118]. And in the same mice, probiotic therapy ameliorates intestinal inflammation, pointing to the importance of bacterial colonization [119].

Furthermore, NOD1$^{-/-}$ and NOD2$^{-/-}$ mice showed defects in defensin secretion and an increased susceptibility to dextran sodium sulfate (DSS) induced colitis [120]. The PRR effects seem to be a synergistic action of several PRRs as shown by the observation that NOD2$^{-/-}$ mice become susceptible to colitis as a result of increased TLR2 responses with increased production of IL-23 and IL-12p70 [121]. Another evident finding showed a directed crosstalk between TLR2 and NOD2, as MDP suppressed TLR2-induced IL-12 production in wild type but not in NOD2$^{-/-}$ mice after the stimulation with peptidoglycan. This suggests a negative feedback mechanism of the NOD signaling pathway on TLR-mediated T_H1 immune activation [122]. In general, peptidoglycan is recognized by several PRRs including TLR2 or NOD2 [123]. However, loss of signaling by one innate PRR seems to disrupt an appropriate innate immune response leading to dys-regulated adaptive responses [124]. Another cellular protection process, by degradation of potential pathogenic agents, is autophagy. NOD2 stimulates autophagy by interacting directly with the autophagy-related protein 16-1 (ATG16L1), which allows recruitment of ATG16L1 to the side of bacterial entry [125, 126]. Dendritic cells (DCs) expressing mutant forms of NOD2 or ATG16L1 showed reduced autophagy in response to MDP, and this led to impaired antigen presentation and bacterial killing [125].

Other transgenic mice, lacking the TLR receptors *Tlr2*, *Tlr4*, *Tlr5*, *Tlr9* or the shared TLR-adapter protein MyD88 show increased susceptibility to DSS colitis [127]. TLR5$^{-/-}$ mice for example developed spontaneous colitis with altered colonic bacteria flora, increased intestinal permeability and increased colonic expression of hematopoietic-derived proinflammatory cytokines, like TNF-α, IFN-γ, IL-1β, and IL-23. Surprisingly, the additional TLR4 knockout in TLR5$^{-/-}$ mice rescued the colitis in these TLR4 X TLR5$^{-/-}$ mice underpinning the importance of PRRs for both, pro- and anti-inflammatory processes [128]. In case of TLR2$^{-/-}$ and TLR4$^{-/-}$, these mice do not develop intestinal inflammatory tissue pathology, but double-knockout mice, when crossbred with IL-10$^{-/-}$ mice exhibit in case of IL-10 X TLR2$^{-/-}$ mice severe colonic inflammation due to ER stress-associated cellular responses, while IL-10 X TLR4$^{-/-}$ mice are significantly less affected by colonic inflammation [129].

Furthermore, disruption of donwstream molecules of PRR recognition and sensing also leads to impaired intestinal homeostasis. Transgenic mice lacking MyD88, a TLR-linked adapter protein required for NF-κB activation, exhibit increased susceptibility to DSS-induced colitis, similar like TLR2$^{-/-}$ or TLR4$^{-/-}$ mice, suggesting a protective role of these PRRs towards chemically induced colitis [130, 131]. And finally, mice with a deletion of the NF-κB essential modulator NEMO in IEC develop severe spontaneous colitis; possibly caused by decreased production of antimicrobial peptides and an impaired intestinal barrier in these mice [132].

The importance of the integrity of the intestinal barrier was also shown, as an altered barrier function was found as a potential pathway to IBD [133]. Experimental data supporting this hypothesis show that the commensal bacteria strain of *Enterococcus faecalis* contributes to development of chronic intestinal inflammation in genetically susceptible IL-10$^{-/-}$ and TNF$^{\Delta ARE/WT}$ mice, by impairing epithelial barrier integrity [134]. Finally, it has become clear from numerous studies in IBD patients and in animal models of experimental colitis that enteric bacteria are a critical component in the development and prevention/ treatment of IBD in genetically susceptible hosts [135, 136].

Beside columnar IEC further cell populations monitor luminal bacteria content. These include specialized M cells capable of transporting macromolecules, IgA complexes and microbes to present them to professional antigen-presenting cells, but also DCs. Myeloid-derived DCs are the major subtype in the intestinal lamina propria and have been shown to form an extensive network beneath the intestinal epithelium [137]. Immature CD11c+ and CD11b+ DCs have been shown to produce IL-23 in response to TLR ligand binding [138]. And IL-23 contributes to the development of intestinal inflammation as shown by a murine model where depletion of IL-23 was associated with decreased proinflammatory responses [139]. Beside tissue adherent DCs, circulating macrophages migrate into the intestinal tissue and contribute to inflammation by producing proinflammatory cytokines like TNF-α and depletion of macrophages prevents the development of colitis in IL10$^{-/-}$ mice [140]. In general, homing of macrophages or other immune cells like DCs or neutrophils into mucosal tissue requires the expression of chemokines, cytokines and adhesion molecules.

The adaptive immune response in IBD is mainly characterized by mucosal B cells producing and secreting IgA and IgG, a mixture of T_H1, T_H17 and T_H2 cells and regulatory B and T cells (**Figure 3**) [141]. The activation and contribution of the single cell types is mediated by the presence or absence of certain cytokines. A predominant T_H1-driven inflammation is triggered by the presence of interferon-γ and IL-12p40 which communicates through signal transducers and activators of transcription (STAT) molecules. Inadequate STAT activation pattern was found in mononuclear cells from IBD patients [142], suggesting its importance. While STAT1 and STAT4 trigger T_H1 development, STAT6 is essential for T_H2 cell differentiation in response to IL-4 [143, 144]. In former times, CD was believed to be driven by predominant T_H1 cell response, while UC followed a T_H2 cell response [145, 146]. However, the detection of another CD4+ T cell lineage, T_H17, expressing and secreting several cytokines including IL-17, IL-21 and IL-22, revealed an additional layer of complexity. T_H17 development is promoted by IL-23 and suppressed by transcription factors required for T_H1 and T_H2 cell differentiation [147, 148]. The priming IL-23 is mainly produced by professional antigen presenting cells, like

DCs or macrophages [149, 150]. Additionally to T$_H$17 priming, IL-23 stimulates IL-1, IL-6 and TNFα secretion from DCs or macrophages in an autocrine manner, as both express the IL-23 receptor [148]. T$_H$17 cell cytokine IL-22 signaling drives the production of antimicrobial proteins and promotes epithelial regeneration and healing by activating the transcription factor STAT3 in IEC [151]. The IL-23 axis potentially contributes to IBD pathogenesis as the spontaneous development of colonic inflammation in IL-10$^{-/-}$ mice is prevented in IL-10XIL-23p19$^{-/-}$ double-knockout mice, pointing to the crucial role of IL-23 in the induction of colitis [152]. And T$_H$17 cells and T$_H$17 cytokines have been found to be enriched in the inflamed gastrointestinal mucosa of patients with IBD [153]. Factors that determine whether activated DCs will preferentially produce IL-23 or IL-12 are not clear, but endoplasmic reticulum (ER) stress and activation of an unfolded protein response can synergize with TLR signals to selectively increase IL-23 expression by DCs [154].

The fine balanced interaction of pro- and anti-inflammatory mechanisms is on the anti-inflammatory side mainly ensured by the cytokines Transforming Growth Factor-β (TGF-β) and IL-10 [155]. A crucial cell type for regulating intestinal homeostasis are the regulatory T (T$_{reg}$) cells [156]. These cells were found to act by TGF-β and IL-10 expression to inhibit proinflammatory T cell responses [157, 158]. In the absence of proinflammatory mediators, TGF-β promotes the development of forkhead box P3+ (FoxP3+) T$_{reg}$ cells which suppress inflammatory responses [159, 160]. Deletion of the TGF-β encoding gene *Tgfb1* in mice contributes to the development of IBD [161]. TGF-β is required for the differentiation of both, T$_{reg}$ cells and T$_H$17 cell populations. T cells that can not respond to TGF-β escape T$_{reg}$ cell-mediated control, like shown in T cells from IBD patients, which are more resistant to the anti-inflammatory actions of TGF-β through expression of the negative regulator of TGF-β signaling, SMAD7 [162].

In contrast, the presence of STAT3-mediated signals (such as IL-6 or IL-23) promotes T$_H$17 cells at the expense of FoxP3+ T$_{reg}$ cells [163]. Such a mechanism allows the inflammatory response to override T$_{reg}$ cell induction in the presence of proinflammatory stimuli, promoting intestinal effector T cell responses and host defence. Deletion or loss-of-function mutations in the gene encoding Foxp3 result in fatal inflammatory disease in mice and immune dys-regulation accompanied by intestinal inflammation in humans [164]. Notibly, T$_{reg}$ cell accumulation is reduced in colon from germfree mice, suggesting a role of microbiota in promoting intestinal T$_{reg}$ cell responses [165]. FoxP3+ T$_{reg}$ cells control oral tolerance to dietary and microbial stimuli and mediate control of intestinal homeostasis by competing with effector T cells. For example, mice with deletion in FoxP3+ T$_{reg}$ cells develop aggressive colitis owing to uncontrolled T$_H$17 responses [163]. In this context, the critical role of T$_{reg}$ cells in modulating the development of IBD has been described [166].

Additionally to T_{reg} cells, regulatory B (B_{reg}) and a subset of nature killer T cells were found to be involved in fine-tuning of inflammatory responses [167, 168]. IL-10-secreting B_{reg} cells inhibit T_H1 and T_H17 cell responses and instead favour T_{reg} and T_H2 cell responses [167]. The importance of IL-10 is reflected by IL-10$^{-/-}$ mice, which lack the hyperresponsiveness towards commensal bacteria and develop colitis, but despite this, IL-10$^{-/-}$ mice housed under germ-free conditions or treated with antibiotics do not show colitis [169]. In patients, mutations in the IL-10 receptor genes *IL10RA* and *IL10RB* seem to lead to severe early-onset of IBD [170].
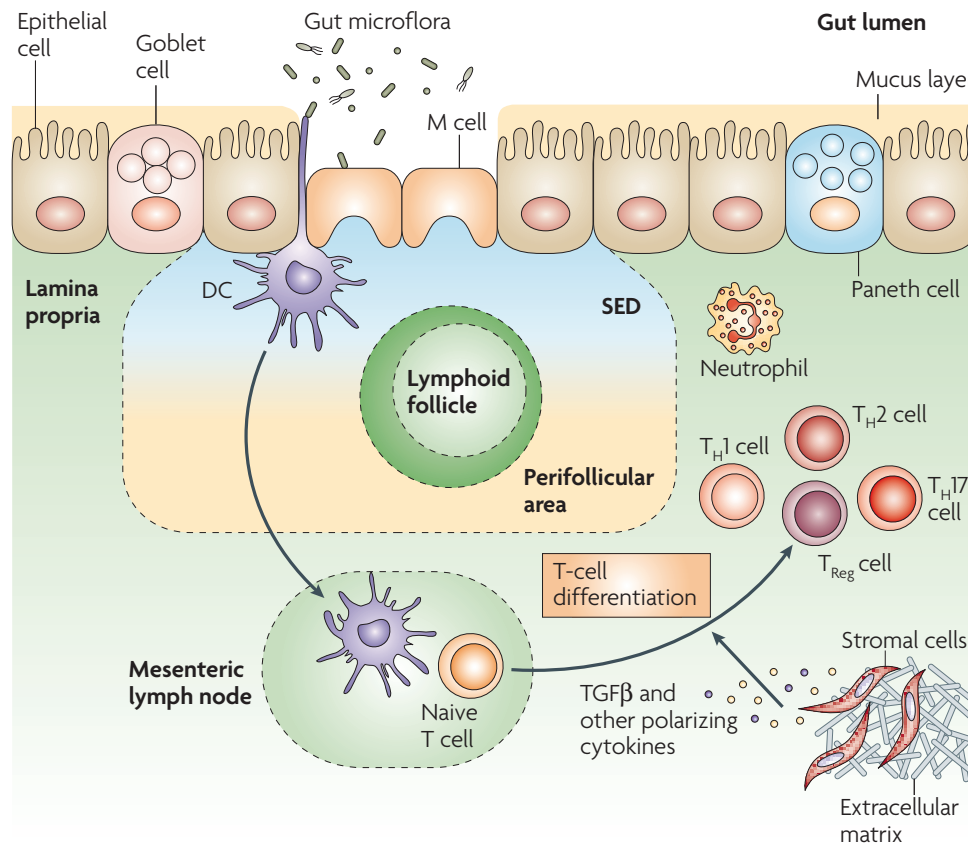
Figure 3. Key features of the intestinal epithelial barrier and the associated immune system. (Adopted from Cho JH 2008 [171]) The IEC monolayer seperates the luminal content from the underlying tissues. Several cell types form the IEC monolayer, like columnar IEC, goblet cells, Paneth cells and microfold cells (M cells). In case of a disrupted barrier or the presence of pathogenic bacteria, M cells or DCs become activated and migrate to the mesenteric lymph nodes to further activate T cells. T cells undergo differentiation and trigger the adaptive immune response.

1.9 Genetical predisposition to IBD

Genome-wide association studies (GWAS) revealed several IBD susceptibility loci. The first identified locus associated with IBD was in the *NOD2* gene [172, 173]. Individuals who carrier one of the identified germline variations of *NOD2* have an up to 40-fold increased likelihood of developing ileal CD. Experimental data confirmed the importance of NOD2, as mutations in the LRR domain of NOD2/CARD15 disable the signaling function of the protein and prevent MDP-induced NF-κB activity *in vitro* [174]. These findings clearly underline the importance of microbial-mucosal interaction in the

pathogenesis of IBD. Since *NOD2*, several additional susceptibility loci were identified. To date 71 distinct loci with genome-wide significant evidence for association with CD and 47 risk loci associated with UC were identified [175, 176]. Approximately 28 of them are shared between CD and UC, indicating that these diseases engage common pathways and may be part of a mechanistic continuum [177]. The pathways of the identified loci associated with increased IBD risk include intestinal homeostasis, including barrier function (e.g. *MUC19*, *HNF4A*), epithelial restitution (e.g. *REL*, *PTGER4*, *NKX2-3*), microbial defence (e.g. *XBP1*), innate immune regulation (*NOD2*, *CARD9*), reactive oxygen species (ROS) generation (e.g. *GPX4*, *UTS2*), autophagy (e.g. *ATG16L1*, *CUL2*), regulation of adaptive immunity (e.g. *IL-23R*, *JAK2*, *IL-12B*, *IL-23*, *IL-5*, *IL-10*), ER stress (e.g. *ORMDL3*, *CPEB4*) and metabolic pathways associated with cellular homeostasis (e.g. *SLC2A4RG*) [177]. Amongst the identified risk loci several genes encoding proteins of the SLC family have been identified. These included *SLC9A4*, *SLC22A5*, *SLC22A4*, *SLC9A3*, *SLC26A3* and *AQP12A/B*. However, no GWAS yet identified *Pept1* as a susceptibility gene for IBD. Nevertheless, one targeted analysis investigating the association of 12 *Pept1* gene polymorphisms in two scandinavian cohorts revealed one *Pept1* gene polymorphism (rs2297322) to be associated with IBD susceptibility [178].

1.10 PEPT1 contributes to the development of colonic inflammation

Beside one targeted search for potential *Pept1* polymorphisms associated with IBD, expression analysis in IBD patients and experimental data support a modulating role of PEPT1 in proinflammatory processes in IBD. The first potential connection was presented in 1998 by Merlin D et al., showing that PEPT1 has the ability to transport a bacterial tripeptide with a characteristic formylated amino group, *N*-formyl-methionyl-leucyl-phenylalanine (fMLP), known to act as a chemoattractant on neutrophils [27, 179]. An aberrant fMLP signaling was proposed to contribute to pathologies like CD, UC or pouchitis [180-183] and shown to induce inflammation when experimentally administered to mice and rats [182, 184]. Merlin D et al. showed *in vitro* on Caco2-BBE cells that fMLP is internalized. This internalization leads to intracellular acidification and could be inhibited by the dipeptide glycyl-proline but not by glycine. In addition, fMLP internalization into Caco2-BBE cells resulted in directed movement of neutrophils across the epithelial monolayer, while solutes that inhibit hPEPT1-mediated fMLP transport decreased neutrophil transmigration. So finally, Merlin D et al. conclude that these data define the importance of PEPT1 in mediating intestinal inflammation, raising the possibility that modulating PEPT1 activity could influence states of intestinal inflammation, and providing the first evidence of a link between active transepithelial transport and neutrophil–epithelial interactions [27]. Further data on the contribution of PEPT1-mediated fMLP transport to colonic inflammation was presented by Shi B et al., showing increased colonic

inflammation in rats after short bowel resection, another non-physiological condition under which PEPT1 might be up-regulated [185, 186]. In 2001 Merlin D et al. presented the first data about aberrant PEPT1 expression in the colon of IBD patients [50]. In addition, the group found enhanced major histocompatibility complex class I (MHCI) surface expression in Caco2-BBE cells after fMLP treatment. However, the report about colonic PEPT1 in IBD did not include any information about functional properties of aberrant expression of PEPT1, like it was the same case in another study showing up-regulated *Pept1* mRNA in colonic samples from IBD patients without information about the protein amount or other functional relevance [49]. But since 2001 Merlin D and colleagues have been intensively investigating the possible role and mechanisms that may lead to abnormal colonic PEPT1 expression and the consequences, providing till date most of the data on this issue. In a study published in 2002, the group also presented data from intestinal perfusion experiments with fMLP on the jejunum and colon of male Wistar rats. Perfusion with 1-10 μM for at least 4 h resulted in a significantly increased myeloperoxidase (MPO) activity and altered the architecture of the jejunal villi. In contrast, perfusion of the colon with 10 μM fMLP did not induce any inflammatory response [181]. Further expanding this to PEPT1 during intestinal inflammation, Buyse M et al. showed that the T_H1 cytokine Interferon-γ (IFN-γ) increases hPEPT1 function in Caco2-BBE cells [187]. IFN-γ was proposed to increase di-tripeptide uptake in dose- and time- dependent manner via PEPT1. However, IFN-γ does not affect the hPEPT1 expression at the mRNA and protein levels, but may increase the basal intracellular pH leading consequently to an enhanced electrochemical gradient across the apical plasma membrane, increasing PEPT1 mediated transport. Other cytokines were also tested for their ability to modulate PEPT1 expression. In 2006, a study by Vavricka SR et al. about IL-1β, IL-2, IL-8, IL-10, TNF-α and IFN-γ and their effects on PEPT1 regulation *in vitro* and *in vivo* after administration in C57BL/6 mice by a single intraperitoneal injection was published [12]. Here they described increased Gly-Sar uptake into Caco2-BBE cell monolayers and total and apical membrane protein expression of PEPT1 in mouse colon in response to TNF-α and IFN-γ. As no changes in *Pept1* mRNA were observed, a post-transcriptional regulation was proposed. Non of the other tested cytokines showed any effect on PEPT1 expression or function.

In addition to the neutrophile chemoattractant fMLP, PEPT1 was shown to transport NOD1 and NOD2-activating structures. One of those is muramyl dipeptide (MDP), which specifically interacts and activates NOD2 and is found in stool samples from normal humans in a range between 20-87 μmol/L but which is not detectable in duodenal fluids [28, 188, 189]. In Caco2-BBE cells it has been shown that PEPT1 is required for MDP uptake (K_m 4.3 mmol/L). Uptake rates for MDP were decreased in the presence of Gly-Sar

or after *Pept1* silencing using siRNA. In addition, MDP uptake in Caco2-BBE cells resulted in activated NF-κB signaling and increased IL-8 release, what led the authors conclude that PEPT1 may play an important role in promoting colonocyte participation in host defense and pathogen clearance through increased uptake of MDP [189]. Compatible with this assumption, the same group found that *in vitro* infection of HT29-Cl.19A cells with the enteropathogenic *Escherichia coli* (EPEC) induced PEPT1 expression and activity especially in cholesterol-enriched lipid rafts in these cells [69]. When PEPT1 was overexpressed in these cells, a markedly reduced adherence and attenuated EPEC-triggered proinflammatory responses has been shown [69]. This was speculated to originate from PEPT1-caused conformation changes in lipid rafts, which in turn may result in modified binding activities of EPEC to lipid rafts. As a conclusion, colonic PEPT1 expression might be protective for the host by modulating bacterial-epithelial interactions and immune responses.

Furthermore, *ex vivo* and *in vivo* experiments showed increased *Pept1* mRNA after *c. rodentium* (a murine pathogen [190]) infection in colon from wild-type mice. And humanized transgenic mice, overexpressing hPEPT1 under the control of the *villin* promotor (*villin*-hPEPT1) exhibited decreased *c. rodentium* colonization, neutrophil accumulation and proinflammatory cytokine expression (IL-1β, IL-6, IL-12, TNF-α and IFN-γ) in the colon [69]. The authors conclude that pathogenic colonization is required for colonic PEPT1 expression and reveal a novel role for PEPT1 in host defense via its capacity to modulate bacterial-epithelial interactions and host immune responses.

In addition to pathogenic bacteria, PEPT1 up-regulation was also shown by the short chain fatty acid butyrate, an end product of bacterial fermentation in the gut. Dalmasso G et al. showed that butyrate increases *Pept1* gene expression by butyrate-activated Cdx2 binding to the *Pept1* promotor in Caco2-BBE cells [68]. Furthermore, they hypothesized that the induced PEPT1 expression in inflammation could be explained by a dysfunction of butyrate metabolism in colonocytes. An altered butyrate metabolism with decreased butyrate oxidation was shown in IBD patients and during DSS colitis [191, 192]. And this oxidation default may induce an intracellular accumulation of butyrate in colonocytes, which in turn could be responsible for increased PEPT1 expression.

In addition, PEPT1 regulation was also shown in response to the presence of the harmless gram-positive aerotolerant lactic acid producing probiotic bacterium *Lactobacillus plantarum (LP). LP* attenuated immune-mediated colitis in IL-10$^{-/-}$ mice [51, 193]. Chen HQ et al. found that PEPT1 expression was significantly increased both at protein and mRNA levels in the colon of non-treated IL-10$^{-/-}$ mice, and *LP* treatment ameliorated colitis and prevented the increase in colonic PEPT1 expression. Furthermore, plasma levels of the cephalosporin antibiotic cephalexin, a PEPT1 substrate, were

increased in non-treated IL-10$^{-/-}$ as compared to *LP* treated IL-10$^{-/-}$ mice after colonic perfusion [51]. Notably, the PEPT1-mediated transepithelial pathway and the paracellular pathway by impairments in barrier function in the colon of IL-10$^{-/-}$ mice could result in movement of bacteria or bacteria-derived antigens across the intestinal epithelium. Thus both pathways could contribute to the epithelial barrier dysfunction and subsequent development of spontaneous colitis. In a further study which focused on the small intestine, Chen HQ et al. showed increased amino acids and cephalexin plasma concentrations in *LP* treated IL-10$^{-/-}$ mice as compared to non-treated IL-10$^{-/-}$ mice after in *situ* single-pass perfusion of the small intestine [194]. However, Western blot and quantitative PCR analysis revealed no significant differences in PEPT1 protein and mRNA expression levels between *LP* treated and untreated IL-10$^{-/-}$ mice. The enhanced PEPT1 function correlated with increased PKC activity in these mice suggesting that the enhanced PEPT1 function could result from an increased PEPT1 phosphorylation. It was finally concluded, that the *LP*-induced promotion of amino acid absorption by PEPT1 may lead to improvement of IBD in IL-10$^{-/-}$ mice [194].

Further evidence for a protective function of up-regulated PEPT1 in colonic IBD is given by the fact that PEPT1 might transport anti-inflammatory acting peptides, like the neuropeptide alpha-melanocyte-stimulating hormone (alpha-MSH)-derived tripeptide KPV. KPV was shown to have beneficial effects in two murine colitis models, DSS colitis and an adoptive T cell-transfer colitis model in Rag$^{-/-}$ mice and feeding the alpha-MSH-secreting *Lactobacillus casei* to mice showed significant anti-inflammatory effects [195, 196]. In fact, a study by the Merlin group showed that KPV was transported by PEPT1 *in vitro*, resulting in the reduction of proinflammatory cytokine production. Furthermore, oral KPV administration reduced the severity of DSS-, and 2,4,6-trinitrobenzene sulfonic acid (TNBS)-induced colitis, which led the authors to conclude that KPV is transported into cells by PEPT1 and might be a new therapeutic agent for IBD [30].

The list of bacterial structures which elicit an immune response after being transported by PEPT1 was growing further as the Merlin group published in 2010 that the proinflammatory tripeptide L-Ala-γ-D-Glu-*meso*-diamin-opimelic acid (Tri-DAP), which can be recognized by the LRR-domain of the intracellular PRR NOD1, is a PEPT1 substrate [29, 108, 197]. Dalmasso G et al. found that *in vitro* uptake of Tri-DAP into Caco2-BBE cells activate NF-κB and MAP kinases, consequently leading to production of the proinflammatory cytokine IL-8. This effect was abolished by *Pept1* silencing or in HT29-Cl.19A cells that do not express PEPT1. Finally they concluded that PEPT1 is highly expressed in the colon during inflammation and PEPT1-mediated Tri-DAP transport may occur more effectively during such conditions, further contributing to intestinal inflammation [29] (**Figure 4**). Beside the PEPT1-NOD1 pathway, the Merlin group showed

that the PEPT1-NOD2 connection aggravates intestinal inflammation by demonstrating increased susceptibility of humanized transgenic mice expressing the hPEPT1 protein under the control of the *actin* promotor (*actin*-hPEPT1) towards DSS- and TNBS-induced colitis. While humanized transgenic *villin*-hPEPT1 mice appeared only more susceptible to DSS- but not TNBS-induced colitis. And *NOD2*$^{-/-}$ or *actin*-hPEPT1 and *villin*-hPEPT1 with a deletion in *NOD2* had similar levels of susceptibility to DSS-induced colitis, indicating that hPEPT1 overexpression increased intestinal inflammation in a NOD2-dependent manner [198].
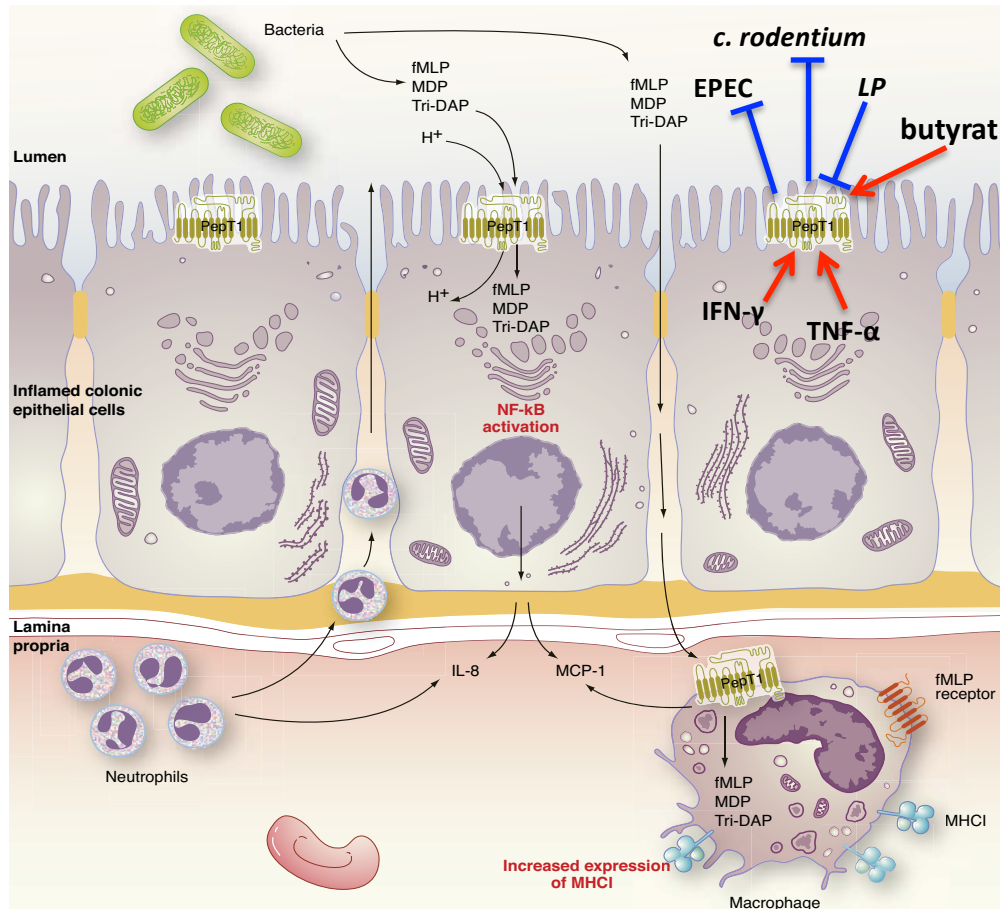
Figure 4. How PEPT1 triggers proinflammatory processes.
(Adopted from Ingersoll SA et al. [199]) Bacterial peptides internalized into IEC by PEPT1 activate the production of proinflammatory cytokines, in dependence of NF-κB. Intestinal barrier disruption may allow bacterial peptides to pass the epithelium by the paracellular pathway and to directly interact and activate (PEPT1 expressing) immune cells. Additionally, PEPT1 was shown to be regulated by cytokines, butyrate and LP, whereas to protein itself influences adhesion of bacteria.

1.11 Other intestinal transporters and exchangers connected to IBD

Beside PEPT1, several other apical membrane transporters have been linked with IBD. Amongst those are the organic cation transporters (OCTNs), OCTN1 and OCTN2. OCTN1 and OCTN2 have been shown to transport a number of endogenous substrates, like carnitine or choline, in either a Na$^+$- or pH-dependent manner [200-202]. OCTN1 is encoded by the *SLC22A4* gene and OCTN2 by the *SLC22A5* gene, both located within

the IBD5 susceptibility locus of CD [203]. The OCTN2 transporter has been shown to be up-regulated *in vitro* in Caco2-BBE cells and in mice, particularly in the colon, after treatment with IFN-γ and TNF-α. And, colonic epithelial OCTN2 expression was also found to be increased in humans in areas of active inflammation of both, CD and UC biopsy samples [204]. Another study investigating OCTN1 expression and carnitine transport in intestinal biopsies and resections from CD patients and controls found similar OCTN1 expression levels and carnitine transport rates in patients and controls. However, there was a trend towards higher carnitine transport in subjects with OCTN1 or OCTN2 IBD susceptibility mutations [205]. In contrast, another study conducted in UC patients found in a sample size of 100 individuals down-regulated OCTN1 and OCTN2 mRNA levels in active UC and even in remission as compared to healthy controls [206], confirming findings from other studies [49, 207]. OCTN2 expression and function was also found to be decreased in a rat model of TNBS-induced colitis [208]. The importance of adequate OCTN expression is further underlined by experimental findings in OCTN2$^{-/-}$ mice which show impaired small intestinal and colonic morphologies and develop spontaneously intestinal villous atrophy and inflammation with an intense macrophage infiltration, leading to a colitis-like phenotype [209]. And in a rat model of TNBS-induced colitis, D'Argenio G et al. found decreased OCTN2 expression and function in inflamed tissue samples [208]. Despite these contradictory results from human studies, the totality of the data suggests that OCTNs play a crucial role to maintain intestinal health.

Another study investigating mRNA levels of 15 SLC transporters in ileum and colon of IBD patients found significantly elevated mRNA levels of the serotonin transporter (*SLC6A4*), the equilibrative nucleoside transporter (ENT) 1 (*SLC29A1*), ENT2 (*SLC29A2*), and the organic anion-transporting polypeptide (OATP) 2B1 (*SLCO2B1*), whereas levels of the apical sodium-dependent bile acid transporter (ASBT, *SLC10A2*) and *OCTN2* were significantly lower. In colon, mRNA levels for *ENT1*, *ENT2*, the concentrative nucleoside transporter (CNT) 2 (*SLC28A2*), *OATP2B1*, and *OATP4A1* (*SLCO4A1*) were significantly up-regulated, whereas mRNA levels for *OCTN2* were significantly decreased. *OCTN1* mRNA expression levels were not affected by IBD neither in small intestine nor in colon [49].

A second peptide transporter, the peptide/histidine transporter 1 (PHT1), encoded by the *SLC15A4* gene, was very recently identified as a putative transporter for NOD1 ligands in early endosomes [210]. And as its expression was found to be significantly up-regulated in colonic tissue biopsies from IBD patients, it might play a potential role for the modulation of peptidoglycan access to the cytosol in IBD etiology [210]. Further experimental data revealed PHT1 to be expressed in antigen presenting cells, like DCs or macrophages [211]. And PHT1$^{-/-}$ mice showed an impaired production of IL-12, IL-15, and IL-18 by DCs

in response to unmethylated DNA (CpG-ODN), which can be recognized by TLR9. Additionally, PHT1$^{-/-}$ mice develop a less severe form of DSS-induced colitis caused by the disturbed endosomal TLR9 presence and NOD1-dependent innate immune response [212].

Another SLC family member, SLC9A3, particularly interesting in relation to PEPT1, is the NHE3 exchanger that maintains the driving proton force for adequate PEPT1 function. NHE3$^{-/-}$ mice were shown to have increased susceptibility to DSS-induced colitis with accelerated mortality, histological lesions and elevated levels of the proinflammatory cytokines IL-6, IL-1β, TNF-α. Additionally, NHE3$^{-/-}$ mice were predisposed to DSS-induced small intestinal injury [213].

2 MAIN AIMS OF THE STUDY

Although prominent PEPT1 expression in the small intestine is consistently found, data about its expression level in colonic tissues in health and disease conditions are controversial. Therefore, the main aims of this study are

1. to investigate and clarify in a systematical approach the expression pattern of *Pept1* mRNA and protein along the intestinal tract with high resolution and focus on the colon from mice, rats and humans to elucidate potential segmental and species differences. Especially for the high-quality detection of PEPT1 protein, specific custom-made antibodies against the human- and rat-PEPT1 protein were used. Furthermore, functional characterization of PEPT1 presence was carried out by transport studies using a radioactive PEPT1 tracer substrate. Tissue from *Pept1$^{-/-}$* mice were employed as an ultimate negative control for PEPT1 expression and function.

2. to investigate PEPT1 expression during intestinal inflammation in the small intestine and the colon from mice and humans. Therefore, several transgenic mouse models which mimic IBD-like inflammation, including TNF$^{\Delta ARE/WT}$, IL-10$^{-/-}$, IL-10XTLR2$^{-/-}$, and IL-10XTLR4$^{-/-}$, and Rag2$^{-/-}$ mice, as an adoptive T cell transfer model, were studied. So far, PEPT1 expression during intestinal inflammation has been solely studied in context with colonic inflammation. However, the study using TNF$^{\Delta ARE/WT}$ mice, as model of chronic ileitis, could provide first data on whether PEPT1 regulation might follow comparable pathways in the small intestine and colon. Finally, human specimens from IBD patients undergoing surgery were assessed for PEPT1 expression.

3. to test whether *Pept1$^{-/-}$* mice show an altered susceptibility to chemically induced DSS colitis in comparison to wild-type mice. Potential differences were assessed on the basis of clinical parameters like body weight, stool blood content, food and water intake, daily activity, and also post mortem diagnostics like colon length, MPO activity or histopathology.

3 MATERIALS AND METHODS

3.1 Materials

3.1.1 Chemicals

All chemicals were of highest quality available.

2-(N-Morpholino)-ethane sulphonic acid (MES)	Roth, Karlsruhe, Germany
2-Mercaptoethanol	Merck, Darmstadt, Germany
2-Propanol	Roth, Karlsruhe, Germany
4-Nitrophenyl phosphate disodium salt hexahydrate	Boehringer, Mannheim, Germany
6x DNA Loading Dye	Fermentas, St. Leon-Rot, Germany
Acetic acid	Roth, Karlsruhe, Germany
Agarose (Roti®garose) NEEO Ultra	Roth, Karlsruhe, Germany
Antibody Diluent, Background Reducing	Dako, Via Real, USA
Antipain	Sigma-Aldrich, Taufkirchen, Germany
Benzamidin	Roth, Karlsruhe, Germany
Bromphenol Blue sodium salt	Sigma-Aldrich, Taufkirchen, Germany
Calcium chloride dihydrate	Roth, Karlsruhe, Germany
Chloroform	Merck, Darmstadt, Germany
Citric acid monohydrate	Sigma-Aldrich, Taufkirchen, Germany
di-potassium hydrogen phosphate	Roth, Karlsruhe, Germany
di-sodium hydrogen phosphate anhydrous	Roth, Karlsruhe, Germany
D(-)-Mannitol	Roth, Karlsruhe, Germany
DEPC-treated water	Roth, Karlsruhe, Germany
Dextran Sodium Sulfate (DSS, MW: 36.000-50.000)	MP Biomedicals, Heidelberg, Germany
Diethanolamine	Merck, Darmstadt, Germany
Dimethyl sulfoxide (DMSO)	Roth, Karlsruhe, Germany
Dithiothreitol(DTT)	Roth, Karlsruhe, Germany
Endoglycosidase H (Endo H)	New England Biolabs, Frankfurt, Germany
Eosyn Y 0,2% alcoholic solution	Medite Group, Burgsdorf, Germany
Ethanol	Merck, Darmstadt, Germany
Ethidium bromide solution (1%, 10 mg/ml)	Roth, Karlsruhe, Germany
Ethylene glycol tetraacetic acid (EGTA)	Roth, Karlsruhe, Germany
Ethylenediamine-tetraaceticacid (EDTA)	Roth, Karlsruhe, Germany
Formaldehyde 37%	Roth, Karlsruhe, Germany
Glycyl-sarcosine (Gly-Sar)	Sigma-Aldrich, Taufkirchen, Germany
Glycerol	Roth, Karlsruhe, Germany

HEPES Pufferan®	Roth, Karlsruhe, Germany
Hexadecyltrimethylammonium bromide	Sigma-Aldrich, Taufkirchen, Germany
horseradish peroxidise (HRP)	Calbiochem, Darmstadt, Germany
Hydrochloric acid fuming 37%	Merck, Darmstadt, Germany
Hydrogen peroxide solution 30%	Merck, Darmstadt, Germany
Immersion oil acc. to ISO 8036	Merck, Darmstadt, Germany
Isoflurane	Baxter, Unterschleißheim, D
Isopropanol, 2-Propanol	Roth, Karlsruhe, Germany
Leupeptin	Sigma-Aldrich, Taufkirchen, Germany
Luminol sodium salt	Sigma-Aldrich, Taufkirchen, Germany
Magnesium chloride hexahydrate	Roth, Karlsruhe, Germany
Magnesium sulphate heptahydrate	Roth, Karlsruhe, Germany
Mayer's hemalum solution	Merck, Darmstadt, Germany
Mounting medium	Dako, Via Real, USA
N-linked-glycopeptide-(N-acetyl-beta-D-glucosaminyl)-L-asparagine amidohydrolase (PNGase F)	New England Biolabs, Frankfurt, Germany
nuclease-free water	Fermentas, St. Leon-Rot, Germany
o-Dianisidine dihydrochloride	Sigma-Aldrich, Taufkirchen, Germany
p-Coumaric acid	Sigma-Aldrich, Taufkirchen, Germany
Paraplast X-TRA®	Sigma-Aldrich, Taufkirchen, Germany
Pepstatin A	Sigma-Aldrich, Taufkirchen, Germany
PhastGel® Blue R	GE Healthcare Bio-Sciences, Uppsala, S
Phenylmethylsulfonyl fluoride (PMSF)	Sigma-Aldrich, Taufkirchen, Germany
Potassium chloride	Roth, Karlsruhe, Germany
Potassium dihydrogen phosphate	Merck, Darmstadt, Germany
RNase B	New England Biolabs, Frankfurt, Germany
RNase free water	QIAGEN, Hilden, Germany
RNaseZAP®	Sigma-Aldrich, Taufkirchen, Germany
Roti®-Liquid Barrier Marker	Roth, Karlsruhe, Germany
Roti®-Mount FluorCare mounting medium	Roth, Karlsruhe, Germany
Rotiszint® eco plus scintillation mixture	Roth, Karlsruhe, Germany
skimmed milk powder (frema reform)	primaVita GmbH, Lueneburg, Germany
Sodium chloride	Roth, Karlsruhe, Germany
sodium dihydrogen phosphate	Roth, Karlsruhe, Germany
Sodium dodecyl sulphate (SDS)	Roth, Karlsruhe, Germany
Sodium hydroxide	Roth, Karlsruhe, Germany
Sodium hydrogen carbonate	Roth, Karlsruhe, Germany

Sodium azide	Merck, Darmstadt, Germany
tri-Sodium Citrate 2-hydrate	Roth, Karlsruhe, Germany
Tris(hydroxymethyl)aminomethane	Sigma-Aldrich, Taufkirchen, Germany
Triton® X-100	Sigma-Aldrich, Taufkirchen, Germany
TRIzol® Reagent	Invitrogen, Darmstadt, Germany
TWEEN® 20	Sigma-Aldrich, Taufkirchen, Germany
Xylene	Roth, Karlsruhe, Germany

Radiolabeled Chemicals

[glycine-1-^{14}C]Glycylsarcosine ([^{14}C]Gly-Sar)	
Specific activity: 2.11GBq/mmol; 56mCi/mmol	GE Healthcare, Munich, Germany
Mannitol, D-[1-3H(N)] ([^{3}H]D-Mannitol)	
Specific activity: 20mCi/mmol	American Radiolabeled Chemicals, Inc., St Louis, MO, USA

Ladders

GeneRuler™ Low Range DNA Ladder	Fermentas, St. Leon-Rot, Germany
PageRuler™ Plus Prestained Protein Ladder	Fermentas, St. Leon-Rot, Germany

3.1.2 Instrumentation

Balances

PJ3000	Mettler-Toledo GmbH, Giessen, Deutschland
TB-215D	Denver Instrument GmbH, Goettingen, Germany
SPB52	Scaltec Instruments GmbH, Goettingen, Germany

Centrifuges

Allegra®64R centrifuge	Beckman Coulter GmbH, Krefeld, Germany
Centrifuge 5417R	Eppendorf AG, Hamburg, Germany
Centrifuge A14	Jouan, Saint Nazaire, France
MiniSpin® plus	Eppendorf AG, Hamburg, Germany
Sorvall Evolution RC Superspeed centrifuge with SS-34 rotor	Thermo Fisher Scientific Inc., Waltham, MA, USA
Savant SpeedVac®	Thermo Scientific, Karlsruhe, Germany

Electrophoresis systems

PerfectBlue™ Midi S gelelektrophoresis System	PEQLAB Biotechnologie, Erlangen, Deutschland
Minigel-Twin Electrophoresis System	Biometra, Goettingen, Germany

Fridges and freezers

-86ºC Ultra Low Freezer DF8517GL	Forma Scientific, Inc., Marietta, OH, USA
HERAfreeze®Chest freezer	Thermo Fisher Scientific Inc., Waltham, MA, USA
KT 1210 Economy Refrigerator	Liebherr, Kirchdorf an der Iller, Germany

Comfort freezer	Liebherr, Kirchdorf an der Iller, Germany

Microscopes

Confocal laser scanning microscope (SP2)	Leica Microsystems, Wetzlar, Germany
DMI4000B light and fluorescence microscope	Leica Microsystems, Wetzlar, Germany

Microwaves

Micromat 15 - Typ G715MA	AEG, Nuernberg, Germany
FH-Alaska – Typ KOR-6185	METRO Cash & Carry Deutschland GmbH, Duesseldorf, Deutschland

Power Supplies

PowerPac 200 (4 Agarosegele)	Bio-Rad Laboratories GmbH, Munich, Germany
Power Pack P25 (for SDS PAGE)	Biometra, Goettingen, Germany
PowerPac^{TM} HC (for Blotting)	Bio-Rad Laboratories GmbH, Munich, Germany

Vortexers

mini Vortexer	VWR International GmbH, Darmstadt, Germany
Vortex-Genie 2 (model G560E)	Scientific Industries, Inc., New York, USA

AP280 Embedding Center	Microm International GmbH, Walldorf, Germany
BioPhotometer	Eppendorf AG, Hamburg, Germany
Digital caliper	BGS technic KG, Wermelskirchen, Germany
Dounce like homogenizer (glass – glass)	Wheaton Science Products, Millville, NJ, USA
TProfessional Thermocycler	Biometra, Goettingen, Germany
SBH200 D/3 block heater	Bibby Scientific Limited, Staffordshire, UK
UV gel reader (Gel iX Imager)	Intas GmbH, Göttingen, Germany
FD23 drying oven	BINDER GmbH, Tuttlingen, Germany
Feeding-Drinking-Activity (FDA) device	TSE-Systems, Bad Homburg, Germany
LightCycler$^{®}$Carousel-based System	Roche Diagnostics GmbH, Mannheim, Germany
Liquid Scintillation Analyzer Tri-Carb 2810 TR	Perkin Elmer, Waltham, MA, USA
Magnetic stirring hotplate MR 3001	Heidolph, Schwabach, Germany
Microtome HM 3555 S	Microm International GmbH, Walldorf, Germany
Microwave Tender Cooker	Nordic Ware, Minneapolis, US
Mini Trans-Blot Cel	Bio-Rad Laboratories GmbH, Munich, Germany
Miniature Shaker KM 2	Edmund Bühler GmbH, Hechingen, Germany
Modular Flake-Ice Machine MF 36	Scotsman Ice Systems, Milano, Italy
Nanodrop ND-1000	PEQLAB Biotechnologie, Erlangen, Germany
Odyssey Infrared Imaging System	LI-COR, Bad Homburg, Germany
pHmeter pH 540 GLP	WTW GmbH, Weilheim, Germany
PIPETMAN$^{®}$ Pipettes (P2, P10, P20, P100, P200, P1000)	Gilson, Inc., Middleton, WI, USA

Shaking platform Incubator 1000	Heidolph, Schwabach, Germany
Tissue processor TP1020	Leica Microsystems, Wetzlar, Germany
Minigel-Twin PAGE system	Biometra, Goettingen, Germany
Ultrasonic Homogenizer UP200S	Hielscher Ultrasonics GmbH, Teltow, Germany
Varioscan multi-well plate reader	Thermo Fisher Scientific Inc., Waltham, MA, USA

3.1.3 Consumable Materials

1 ml Norm-Ject® plastic syringe	Henke-Sass, Wolf GmbH, Tuttlingen, Germany
0.2 ml reaction tube	Eppendorf AG, Hamburg, Germany
1.5 ml reaction tube	Eppendorf AG, Hamburg, Germany
2 ml reaction tube	Eppendorf AG, Hamburg, Germany
0.22 µm polystyrene filter	Corning B.V. Life Sciences, Amsterdam, The Netherlands
96 well plate	TPP, Trasadingen, Switzerland
Falcon Conical Centrifuge Tube 15 ml	BD Biosciences, Heidelberg, Germany
Falcon Conical Centrifuge Tube 50 ml	BD Biosciences, Heidelberg, Germany
Whatman Filter, Grade 595	Whatman Int. Ltd., Maidstone, UK
Blotting paper, pure cellulose (extra thick, 10+15 cm)	Sigma-Aldrich, Taufkirchen, Germany
Centrifuge Bottle 26.3 ml (Polycarbonate)	Beckman Coulter GmbH, Krefeld, Germany
Cover slips (24x50 mm)	Roth, Karlsruhe, Germany
Cuvettes REF 67.742	Sarstedt AG & Co, Nürnbrecht, Germany
Gentle Skin® grip gloves	Meditrade GmbH, Kiefersfelden, Germany
Glas slide 76 x 26 mm	Roth, Karlsruhe, Germany
Greiner® polypropylene 96 well plates	Greiner Bio-One, Kremsmünster, Austria
Histosette®II, M492 embedding cassette	VWR, Darmstadt, Germany
Microtome blade SEC 35	Microm International GmbH, Walldorf, Germany
Nitrocellulose membrane (Optiptran BA-S85 0.45µm)	Whatman Int. Ltd., Maidstone, UK
Pipette tips	Gilson, Inc., Middleton, WI, USA
SafeSkin PURPLE NITRILE® gloves	Kimberly-Clark Worldwide, Inc., Dallas, USA
Star thread	Wenco, Essen, Germany
Sterican 24G needle	B. Braun Melsungen AG, Melsungen, Germany
Superfrost ultraplus glas slides	Menzel GmbH&Co KG, Braunschweig, Germany

3.1.4 Antibodies (ABs)

Primary Antibodies

Table 1. List of primary antibodies used for IF staining and Western Blot analysis.

Antibody	Antigen	AB host/ type	Application, Dilution	Distributor
anti-human Actin	C-terminus of human Actin	goat, polyclonal affinity purified	WB, 1:1000	Santa Cruz, sc-1615, C-11
anti-CD36	recombinant CD36	mouse monoclonal	WB, 1:250	Abnova, MAB2325
Rat anti-mouse DC-SIGN	extracellular region of mouse DC-SIGN	rat purified	IF, 1:50	eBioscience, San Diego, CA, USA
anti-SLC26A3 (DRA)	aas 503-601 of human DRA	mouse monoclonal	WB, 1:200	Abnova, clone 2E3, Lot 09210-2E3
anti-DAT		rabbit polyclonal	WB, 1:100	Millipore, AB1591P
anti human GM130	aas 527-783 of human GOLGA2	mouse, polyclonal	IF, 1:100	Novus Biologicals,
Anti-rat MCT1	A 15-aa peptide of rat MCT1 C-terminus	chicken IgG, purified over antigen-agarose	IF, 1:500	Alpha Diagnostics International
Anti-rat NHE3	22-aa peptide of rat NHE3 C-terminus	purified rabbit IgG,	WB, 1:500	Alpha Diagnostics International
E-Cadherin M168	C-terminal region of mouse E-Cadherin	mouse monoclonal	WB, IF, 1:50	Abcam, Cambridge
anti-human Ghrelin	active human Ghrelin	chicken polyclonal	IF, 1:250	GeneTex®, Inc., Irvine, USA
anti-SLC22A5 (OCTN2)	aas 350-450 of human OCTN2	rabbit polyclonal	WB, 1:200	Abcam, Cambridge, AB79964
anti-SLC22A5 (OCTN2)	17-aa peptide from mouse OCTN2	rabbit polyclonal	WB, 1:200	Alpha Diagnostics International, OCTN21-S
anti-SLC36A1 (PAT1)		rabbit polyclonal	WB, 1:100	Atlas Antibodies, HPA035937
Anti-human PEPT1 (animal 1)	C-terminus of human PEPT1 NH2-CRLEKSNPYFMSGANSQKQM-COOH (20aas)	rabbit, polyclonal unpurified antiserum	IF, 1:1000; WB, 1:3000	Custom made (Pineda, Berlin, Germany)
Anti-rat PEPT1 (animal 1)	C-terminus of rat PEPT1 NH2-CVGKENPYSSLEPVSQTNM-COOH (19aas)	rabbit, polyclonal	IF, 1:1000; WB, 1:3000	Custom made (Pineda, Berlin, Germany)
Anti-Serotonin	Serotonin conjugated to BSA	monoclonal	IF, 1:200	Millipore, MAB 352
Anti-mouse SGLT-1	C-terminus of mouse SGLT-1	Affinity purified goat polyclonal	IF, 1:100	Santa Cruz, M-19
Anti-human Villin	C-terminus of human Villin	goat, polyclonal affinity purified	WB, 1:1000	Santa Cruz, sc-7672, C-19

Custom-made primary antibodies (ABs) against rat and human PEPT1

The rabbit polyclonal AB against rPEPT1 was directed against the 18 amino acids of the C-terminus of rPEPT1 (NH2-CVGKENPYSSLEPVSQTNM-COOH). And the anti-hPEPT1 was directed against the 19 amino acids of the C-terminus of hPEPT1 (NH2-CRLEKSNPYFMSGANSQKQM-COOH). Both PEPT1 antigen sequences started with an added cysteine in the N-terminal position of the antigen peptide. The aa sequences of rat and human PEPT1 C-terminus show only 35% identity. While the alignment of rat and mouse PEPT1 C-terminus share 94% amino acid sequence homology. Both custom-made ABs were produced by a company (Pineda, Berlin, Germany).

Secondary antibodies

AffiniPure donkey anti-rabbit IgG
Cy^{TM}5-conjugated   Jackson ImmunoResearch, Newmarket, UK

AffiniPure donkey anti-rabbit IgG fluorescein
isothiocyannate (FITC)-conjugated   Jackson ImmunoResearch, Newmarket, UK

AffiniPure donkey anti-rabbit IgG
DyLight^{TM}549-conjugated   Jackson ImmunoResearch, Newmarket, UK

AffiniPure donkey anti-mouse IgG
Cy^{TM}3-conjugated   Jackson ImmunoResearch, Newmarket, UK

AffiniPure donkey anti-goat IgG
Cy^{TM}3-conjugated   Jackson ImmunoResearch, Newmarket, UK

AffiniPure donkey anti-rat IgG
Cy^{TM}3-conjugated   Jackson ImmunoResearch, Newmarket, UK

anti-rabbit IgG (H+L) F(ab')2 fragment
Alexa Fluor$^®$ 488 conjugated   Cell Signaling Technology, Danvers, MA, USA

IRDye$^®$ 800CW donkey
anti-rabbit IgG (H+L)   LI-COR Biosciences, Lincoln, NE, USA

IRDye$^®$ 680 donkey
anti-goat IgG (H+L)   LI-COR Biosciences, Lincoln, NE, USA

Other dyes

4',6-diamidino-2-phenylindole,
dihydrochloride (DAPI)   Invitrogen, Darmstadt, Germany

DRAQ5   Cell Signaling Technology, Danvers, MA, USA

Lectin from *Ulex europaeus (UEA)*   Sigma-Aldrich, Taufkirchen, Germany

Propidium iodide (PI)   Sigma-Aldrich, Taufkirchen, Germany

3.1.5 qRT-PCR-Primer

Table 2. Primer sequences (fw, forward; rv, reverse) used for qRT-PCR.

Gene product	Accession no.	Primers, 5'-3'	Product size [bp]	Tm (forward, reverse) [°C]
PEPT1	NM_053079.2	fw: ACC CGT TGA GCA TCT TCT TC rv: GCG ATC AGA GCT CCA AGA AT	187	59.3, 59.5
beta-Actin	NM_007393	fw: GAA ATC GTG CGT GAC ATC AA rv: AAG GAA GGC TGG AAA AGA GC	179	60.7, 60.0
Villin	NM_009509.2	fw: CTC TCG ACG GA GAA ACA AG rv: GAA CAC ATC CTC CTC CTC CA	220	60.0, 60.0
GAPDH	NM_008084.2	fw: ACT CCA CTC ACG GCA AAT TC rv: TCT CCA TGG TGG TGA AGA CA	171	60.1, 60.1
AP-1	NM_010591	fw: AGA ACA CGC TTC CCA GTG TC rv: AGT TGC TGA GGT TGG CGT AG	156	60.3, 60.5
Cdx2	NM_007673	fw: AAA CCT GTG CGA GTG GAT G rv: CCA GCT CAC TTT TCC TCC TG	170	59.7, 60.0
CREB	NM_133828	fw: CTG ATT CCC AAA AAC GAA GG rv: TGT ACC CA TCC GTA CCA TT	250	59.5, 59.9
klf4	NM_010637	fw: TAT ACA TTC CGC CAC AGC AG rv: CGC CTC TTG CTT AAT CTT GG	212	59.7, 60.0
Mzf1	NM_145819	fw: CAG GAA TTG CCA CTG AAC CT rv: CGC TAT GAG GAG AGG TCT GG	169	60.1, 60.0
Nrf2	NM_010902	fw: GCT TTT GGC AGA GAC ATT CC rv: TCT GTC AGT GTG GCT CTC GG	279	59.8, 60.0
PPAR-α	NM_001113418	fw: AGG AAG CCG TTC TGT GAC AT rv: TTG AAG AGC TTG GGA AGA	243	59.7, 59.9
Sp1	NM_013672	fw: TGG GTA CTT CAG GGA TCC AG rv: TGA GGC TCT CCT CAC T GT	239	59.9, 60.0
VDR	NM_009504	fw: GTG GCA GCC AAG ACT ACA AA rv: TCA ACC AGC TTA GCA TCC TG	196	58.9, 59.0

3.1.6 Buffers and Solutions

All solutions were prepared with filtered (Milli-Q, Millipore, Schwalbach, Germany) water.

<u>10x Phosphate-Buffered Saline (PBS)</u>

          1.37 M sodium chloride
          27 mM potassium chloride
          100 mM di-sodium hydrogen phosphate anhydrous
          18 mM potassium dihydrogen phosphate
          15.4 mM sodium azide

<u>PBS-T</u>

          PBS + 0,05% (v/v) TWEEN® 20

<u>Antibody diluent</u>

          PBS-T + 0,1% sodium azide

<u>Modified Krebs bicarbonate buffer (KBB)</u>

          119 mM Sodium chloride
          4.7 mM Potassium chloride
          2.5 mM Calcium chloride dihydrate
          1.2 mM Magnesium sulfate heptahydrate

1.2 mM Potassium dihydrogen phosphate
25 mM Sodium hydrogen carbonate
→ aerate Buffer 1h before use with carbonate

pH 7.4

Incubation buffer
119 mM Sodium chloride
4.7 mM Potassium chloride
2.5 mM Calcium chloride dihydrate
1.2 mM Magnesium sulfate heptahydrate
1.2 mM Potassium dihydrogen phosphate
2.5 mM Sodium hydrogen carbonate
1.01 mM MES
→ aerate Buffer 1h before use with carbonate
pH 6.0

DivCatPrehomogenization buffer
270 mM Mannitol
12 mM Tris
16 mM HEPES
1 mM EGTA

1.006 mM Calcium chloride dihydrate
pH 7.4
40 ug/ml phenylmethylsulfonyl fluoride (PMSF)
20 µg/ml Leupeptin
20 µg/ml Pepstatin A
20 µg/ml Antipain
1 mM DTT
4 mM Benzamidin

DivCatPre resuspension buffer
20 mM Tris(hydroxymethyl)aminomethane
150 mM sodium chloride
pH 7.4
40 µg/ml PMSF
1 mM DTT
4 mM Benzamidin

Laemmli sample buffer (4x)
125 mM Tris, pH 6.8
8% SDS
20% Glycerol
20% 2-Mercaptoethanol
0,4% Bromphenol Blue sodium salt

1x Tris-Acetat-EDTA (TAE)electrophoresis buffer Buffer
40 mM Tris-Acetat
1 mM EDTA
pH 8.3

Citrate buffer
0.1 mM Citric acid monohydrate
0.12 mM tri-Sodium Citrate 2-hydrate

1x Towbin Blot Buffer
0,025 M Tris
0,192 M Glycine
20% Methanol

10x Electrophoresis Buffer
 250 mM Tris(hydroxymethyl)aminomethane
 2 M Glycine
 34.7 mM SDS
 pH 8.4

3.1.7 Gels

SDS-PAGE Resolving gel (9%)
 9% (w/v) acrylamide
 375mM Tris-HCl, pH 8.8
 0.1% (w/v) SDS
 0.1% (w/v) APS
 0.1% (v/v) TEMED

SDS-PAGE Stacking gel
 5% (w/v) acrylamide
 125 mM Tris-HCl, pH 6.8
 0.1% (w/v) SDS
 0.1% (w/v) APS
 0.1% (v/v) TEMED

Agarose gel
 3% (w/v) agarose
 0.037 µg/mL ethidium bromide
 in TAE electrophoresis buffer

3.1.8 Kits

RevertAid™ Premium First Strand cDNA synthesis kit
 RevertAid™ Premium Enzyme Mix
 Oligo (dT)$_{18}$ Primer
 Random Hexamer Primer
 10mM dNTP Mix
 5X RT Buffer   Fermentas, St. Leon-Rot, Germany

Maxima® SYBR Green/ROX qPCR Master Mix (2X)
 MaximaTM SYBR Green qPCR Master Mix (2X)
 ROX Solution, 50 µM
 Water, nuclease-free   Fermentas, St. Leon-Rot, Germany

PNGase
 PNGase F Enzyme (500,000 U/ml)
 10X Glycoprotein Denaturation Buffer
 10X Reaction Buffer
 10% NP-40   New England Biolabs, Frankfurt, Germany

Endo H
 Endo H Enzyme (500,000 U/ml)
 10X Glycoprotein Denaturing Buffer
 10X G5 Reaction Buffer   New England Biolabs, Frankfurt, Germany

3.2 Software

GraphPad PRISM 5   GraphPad Software, Inc., La Jolla, CA, USA

Odyssey Scanner Application
Software (Version 3.0)   LI-COR Biosciences, Lincoln, NE, USA

Leica Application Suite
Advanced Fluorescence Lite

Version 2.1.0 build 4316	Leica Microsystems CMS GmbH, Mannheim, Germany
Leica Confocal Software Version 2.5 build 1227	Leica Microsystems GmbH, Heidelberg, Germany
Leica Application Suite V3.0.0	Leica Microsystems, Wetzlar, Germany
LightCycler Software Version 3.5	Roche Molecular Biochemicals, Mannheim, Germany
NanoDrop software version 3.1.2.	PEQLAB Biotechnologie, Erlangen, Germany
Intas GDS imaging software	Intas GmbH, Göttingen, Germany

3.3 Methods

3.3.1 Ethics Statement

All animal experiments were conducted in compliance with the German animal welfare act and approved by the Regierung von Oberbayern (TVA AZ 55.2-1-54-2531-164-09). Samples from IBD patients were collected in accordance with the declaration of Helsinki.

3.3.2 Animal experiments

Three wild-type mouse strains of different genetic backgrounds (C57BL/6N, 129/Sv, BALB/c) were used. Furthermore, tissues of transgenic mice lacking PEPT1 ($Pept1^{-/-}$) [59], samples from germ-free C3H/HeOuJmice (German Institute of Human Nutrition, DIfE, Potsdam) and intestinal tissue samples from Wistar rats were studied. Mouse models of spontaneous chronic intestinal inflammation were represented by transgenic $TNF^{\Delta ARE/WT}$ (generous gift from Dr. Georg Kollias at the Biomedical Sciences Research Center "Al. Fleming", Greece), $IL\text{-}10^{-/-}$, $IL\text{-}10XTLR2^{-/-}$, $IL\text{-}10XTLR4^{-/-}$(129/SvJ//C57BL/10-ScSn background bred at animal facilities of the Charité-Universitätsmedizin Berlin at the "Forschungsinstitut für Experimentelle Medizin") and $Rag2^{-/-}$ mice and used to assess PEPT1 during intestinal inflammation.

3.3.3 Experimental design of DSS treatment

To study PEPT1 expression and the genotype-specific susceptibility to acute experimental colitis mice were treated with dextran sodium sulfate (DSS, 36-50 kDa, MP Biomedicals, Heidelberg, Germany) for 7 days. Female weight-matched wild-type ($Pept1^{+/+}$) and knockout ($Pept1^{-/-}$) mice on C57BL/6 genetic background were housed individually in type III Makrolon cages in a Feeding-Drinking-Activity (FDA) device (TSE-Systems, Bad Homburg, Germany) in a specific pathogen-free facility at the Technische Universität München at 22°C ambient temperature with 12 h light and dark cycles. Animals were fed standard rodent chow (sniff® M-Z autoclavable V1124-3, sniff Spezialdiäten GmbH, Soest, Germany) and water ad libitum. After at least 5 days of acclimation, mice at the age of 12 weeks received either normal drinking water (Ctrl) or water enriched with 2.5% (w/v) DSS for 7 days. The DSS test solution was filtered sterile using a 0.22 µm polystyrene filter

(Corning B.V. Life Sciences, Amsterdam, The Netherlands). Body weight, stool consistency, stool blood content and general appearance of the mice was recorded daily to calculate the disease activity index (DAI); modified from Cooper HS et al. as a marker for clinical manifestation caused by DSS [214]. Furthermore, food intake and physical activity was recorded throughout the study period assisted by the FDA device. After sacrifice the entire colon was removed and the length was measured using a digital caliper (BGS technic KG, Wermelskirchen, Germany).

3.3.4 Tissuepreparation and processing

After cervical dislocation, the mouse intestine was quickly removed and rinsed with ice cold phosphate buffered saline (PBS, pH 7.4) to remove intestinal contents.

Then, depending on the later use, the tissue was either cutted in cross direction into pieces of 3-6 mm for paraffin embedding or cut open longitudinally for mucosal scrapings to conducted Western Blot analysis or qRT-PCR. For the mucosa scrapings, the flange of a glass slide (Roth, Karlsruhe, Germany) was pulled under slight pressure in a 45° ankle over the tissue to remove the mucosa from the seromuscular layer. The scrapings were snap-frozen in liquid nitrogen and stored at -80°C until further processing.

For protein as well as RNA isolation the first step of tissue processing was the disruption of the cells. This was achieved by a Dounce homogenizer, which consists of a round glass pestle that is manually driven into a glass tube and thus cell or tissue suspensions are sheared by forcing them through a narrow space between the pestle and the tube surface. For paraffin embedding, the tissue was fixed for at least 4 h at room temperature in PBS containing 4% formaldehyde (Roth, Karlsruhe, Germany) and dehydrated in an ascending ethanol series using a vacuum tissue processor TP1020 (Leica Microsystems, Wetzlar, Germany). The tissues were embedded in Paraplast X-TRA® embedding media (Sigma-Aldrich, Taufkirchen, Germany) and mounted on a Histosette®II embedding cassette (VWR, Darmstadt, Germany using the AP280 Embedding Center (Microm International GmbH, Walldorf, Germany).

3.3.5 Immunofluorescence (IF) staining

Paraffin embedded tissue sections (7µm) were deparaffinized in xylene (2x 5 min) and rehydrated in graded descending alcohol series (100% ethanol, 2x 5 min; 100% ethanol, 1x 3 min; 96% ethanol, 2x 2 min, 80% ethanol, 1x 2 min) followed by rinsing in tap water for 3 min. Slides were boiled 25 min in 1 mM citrate buffer (pH 6.0) for antigen retrieval, allowed to cool down in the steamer for at least 7min, blocked with 5% skimmed milk in PBS for 30 min, washed and incubated with primary AB for 2.5 h at room temperature in a humidified chamber. Following primary ABs, diluted AB diluent, were used, custom made (Pineda, Berlin, Germany) whole rabbit serum (1:2.000) from animals immunized against the C-terminus of rat or human PEPT1, commercially available mouse polyclonal anti-

GM130 (1:50; Novus Biologicals, Littleton, USA), goat polyclonal anti-Villin (1:50; C-19, Santa Cruz Biotechnology, Santa Cruz, CA), mouse monoclonal anti-E-Cadherin (1:50; Abcam, Cambridge, UK) or chicken purified IgG anti-MCT-1 (1:50; Alpha Diagnostic Intl. In., San Antonio, USA). For double-labeling a cocktail of primary ABs at their appropriate dilutions were prepared. After incubation the slides were washed three times with PBS and incubated with appropriate fluorochrome-labeled secondary ABs and 4′,6-Diamidino-2-phenylindole dihydrochloride (DAPI; Sigma-Aldrich, Taufkirchen, Germany), Propidium iodide (PI; Sigma-Aldrich) or DRAQ5® (Cell Signaling Technology, Boston, USA) dye as nuclear counterstain for 1.5 h. After incubation slides were washed again three times and mounted with Fluorescent Mounting Medium (DakoCytomation, Stockholm, Sweden) and examined using confocal imaging with a Leica SP2 microscope (Leica Microsystems, Wetzlar, Germany). Each test included negative controls with omission of the primary ABs and specificity of custom made ABs was additionally tested by incubation with preimmune serum and staining of intestinal tissue from $Pept1^{-/-}$ mice.

3.3.6 HE staining

Paraffin embedded tissue sections (6 µm) were deparaffinized and rehydrated as described above. Tissues were stained in 50% aqueous Hemalum solution (Merck KGaA, Darmstadt, Germany) for 1 min followed by 3 min bluing in continuously flowing water and 30 sec in 96% ethanol. For subsequent Eosin staining Eosyn Y (0,5%) alcoholic solution with Phloxin (Sigma-Aldrich, Taufkirchen, Germany) was used. Slides were incubated 5 min and finally washed in 80% and 96% ethanol and mounted as described above. A DMI4000B light microscopy (Leica Microsystems) was used to examine the stainings.

3.3.7 Brush border membrane protein isolation

Apical membrane protein was prepared from mucosal scrapings by the divalent cation precipitation (DivCatPre) technique as previously described [215, 216], with modifications. The method in general is based on the observation that the addition of divalent cations (like Ca^{2+} or Mg^{2+}) leads to an aggregation of microsomal membranes. This was first described for liver tissue [217] and later for the purification of intestinal brush border membranes [215]. The addition of divalent cations leads to the selective precipitation of membranes other than the brush border membrane. Divalent cations form aggregates of membranes, but this is diminished in case of brush border membranes which have an increased negative surface charge which prevents aggregate formation. Ca^{2+} and Mg^{2+} ions can be used equally successful but Mg^{2+} is preferred as Ca^{2+} might cause side effects e.g. on enzyme activity. To prevent proteolytic activities, the protease inhibitors Leupeptin, Pepstatin A, Antipain, Benzamidin, and phenylmethylsulfonyl fluoride (PMSF) were added to the homogenization buffer. As PMFS is not stable in water, it was freshly added from a 1 M stock solution in DMSO before using the buffer.

First, mucosal scrapings were disintegrated using a Dounce like homogenizer (glas – glas) in homogenization buffer (270 mM Mannitol, 12 mM Tris, 16 mM HEPES, 1 mM EGTA, 1.006 mM $CaCl_2$, pH 7.4, 40 ug/ml PMSF, 20 µg/ml Leupeptin, 20 µg/ml Pepstatin A, 20 µg/ml Antipain, 1 mM DTT, 4 mM Benzamidin) and an aliquot was saved for alkaline phosphatase-enrichment assay. The homogenate was centrifuged at 2.000 g for 10 min, the resulting pellet containing debris was removed and the supernatant subjected to 1 M $MgCl_2$in a final concentration of 10 mM – the most relevant part of DivCatPre. After 15 min incubation on ice with occasionally mixing, the samples were centrifuged at 3.000 g for 15 min. The resulting supernatant was decanted into a fresh reaction tube and centrifuged at 30.000 g for 30 min. The final brush border pellet was resuspended using a 24-gauge needle in resuspension buffer (20 mM Tris-Cl, 150 mM NaCl, pH 7.4, 40 µg/ml PMSF, 1 mM DTT, 4 mM Benzamidin). All steps in the preparation of the membrane were performed on ice and centrifugation at 4°C. Membrane preparations showed a 12-14-fold enrichment in the specific activity of alkaline phosphatase.

3.3.8 Determination of protein concentration

The protein concentration of respective processed tissue samples was determined by a Protein Assay (Bio-Rad, Munich, Germany) which is based on the method of Bradford [218]. Therefore, 799 µl double distilled water, 200 µl Bio-Rad Protein Assay dye reagent concentrate (Bio-Rad Laboratories GmbH, Munich, Germany) and 1 µl processed tissue sample were pipetted into 1 ml cuvettes (Cuvettes REF 67.742, Sarstedt AG & Co, Nürnbrecht, Germany) and extinction was measured at a wavelength of 595 nm (BioPhotometer, Eppendorf, Hamburg, Germany).

3.3.9 Alkaline Phosphatase assay

To measure the successful enrichment of brush border membrane protein, we determined the enzymatic activity of alkaline phosphatase, a sufficient marker protein. The procedure was based on that of Bessey OA et al. [219] in which the rate of formation of the yellow color of p-nitrophenol produced by hydrolysis of p-nitrophenylphosphate in alkaline solution is measured spectrophotometrically at 405 nm using a Varioscan multi-well plate reader (Thermo Fisher Scientific, Inc.).

3.3.10   SDS-PAGE and Western Blotting

Membrane protein concentration of each sample was determined using a protein assay (Bio-Rad Laboratories GmbH, Munich, Germany) as described above (3.3.8). The membrane extracts were lysed in 4x Laemmli loading buffer (125 mM Tris, pH 6.8, 8% SDS, 20% Glycerol, 20% beta-mercaptoethanol, 0.4% bromphenol blue sodium salt) and heated 5 min at 65°C. Afterwards, 10 µg protein per sample were size fractionated on a 9.5% SDS polyacrylamide gels. The gels were electrophoresed at 15 mA/gel for 20 min (concentration in the stacking gel) followed by 25 mA/gel for 30 min (fractionating in the

resolving gel) using a Minigel-Twin PAGE system (Biometra, Goettingen, Germany). The PageRuler[TM] Plus Prestained Protein Ladder (Fermentas, St. Leon-Rot, Germany) was used to identify the MW region between 35 and 130 kDa. After electrophoresis, the gels were transferred onto nitrocellulose membranes (Whatman Int. Ltd., Maidstone, UK) using a Mini Trans-Blot Cel tank blotting apparatus (Bio-Rad Laboratories GmbH, Munich, Germany). Transfer was performed at 0.36 A for 15 min and the membranes were subsequently blocked with 5% skimmed milk (primaVita GmbH, Lueneburg, Germany) in PBS for 30 min. The blots were probed with ABs against PEPT1 (1:3.000, custom made), beta-Actin (1:1.000; C-11, Santa Cruz Biotechnology, Santa Cruz, CA) and Villin (1:1.000; C-19, Santa Cruz Biotechnology, Santa Cruz, CA) in PBS-T for 3 h slightly shaking at room temperature. The membranes were washed three times and incubated with appropriate IRDye®-labeled secondary ABs (1:10.000; LI-COR Biosciences GmbH, Bad Homburg, Germany) for 1.5 h. After washing another three times with PBS the proteins were visualized using an infrared scanner (Odyssey, LI-COR Biosciences GmbH, Bad Homburg, Germany) which can simultaneously detect fluorescent signals at two wavelengths, namely 700 and 800 nm. Band intensities were quantified using the Odyssey Application Software (V3.0) provided with the imager station. PEPT1 expression was normalized to the expression of the reference proteins Villin and beta-Actin.

3.3.11 Isolation of total RNA and cDNA synthesis

The TRIZOL® Reagent (Invitrogen, Darmstadt, Germany) was used for RNA isolation. Frozen tissue (30-100 mg) was disintegrated using a Dounce like homogenizer (glas – glas, 30 hits) in 1 ml TRIZOL® Reagent. The homogenate was transferred into a 2-ml Eppendorf tube and incubated for 5 min at room temperature. Afterwards, it was centrifuged 5 min at 12.000x g and 4°C to get rid of cellular debris. The supernatant was carried over in a fresh 2 ml reaction tube, 0.2 ml chloroform (Merck, Darmstadt, Germany) was added and the mixture was incubated 3 min at room temperature before centrifugation for 12 min at 12.000x g and 4°C to separates the solution into an upper colorless aqueous phase, a lower red organic phenol-chloroform phase, and a white interphase. The upper aqueous phase was gently carried over in a fresh 2-ml Eppendorf tube as RNA remains exclusively in that phase. Next, to precipitate the RNA, 0.5 ml Isopropanol (Roth, Karlsruhe, Germany) was added and the solution was allowed to incubate for 10 min at room temperature before centrifugation for 10 min at 12.000x g and 4°C. The supernatant was removed and the RNA pellet –which precipitated on the bottom- was washed by adding 1 ml of a 75%-ethanol solution in DEPC-treated water (Roth, Karlsruhe, Germany) and mixed by pipetting and vortexing. Afterwards, it was centrifuged for 5 min at 7.600 g and 4°C. The Ethanol was gently decanted and the RNA pellet dried for at least 15 min in a Savant SpeedVac® (Thermo Scientific, Karlsruhe,

Germany). RNA was resuspended in 10-40 µl RNase-free water (QIAGEN, Hilden, Germany) and snap-frozen in liquid nitrogen. RNA samples were stored at -20°C if they were used within one week after isolation otherwise at -80°C. RNA integrity and quantity were confirmed spectroscopically using a Nanodrop ND-1000 (PEQLAB Biotechnologie GmbH, Erlangen, Germany) device with the corresponding software version 3.1.2 and by gel electrophoresis before use. Prior to the Nanodrop measurements, the paddle was well polished with RNase-free water (Qiagen, Hilden, Germany). RNase-free water was also used as blank. For the measurements, 1.5 µl of the samples were used. RNA concentrations were adjusted to 2.5 µg/µl.

First-strand cDNA was synthesized from 2.5 µg isolated RNA using the RevertAid^{TM} Premium First Strand cDNA synthesis kit (Fermentas, St. Leon-Rot, Germany). All steps were carried out on ice. For cDNA synthesis sterile, RNase free tubes were used. First, 1 µl of isolated RNA (concentration = 2.5 µg/µl) was pipetted into the tube followed by 0.25 µl of oligo (dT)$_{18}$ (conc. 25 pmol) and 0.25 µl random hexamer primer (conc. 25 pmol) and 1 µl 10 mM dNTP Mix. To eliminate secondary structures, the mix was incubated in a block heater (SBH200 D/3, Bibby Scientific Limited, Staffordshire, UK) at 65°C for 5 min and afterwards briefly chilled on ice. To start the reverse transcription reaction 4 µl of 5X RT Buffer and 1 µl RevertAid^{TM} Premium Enzyme Mix was added to each tube and the tubes were placed on a TProfessional Thermocycler (Biometra, Goettingen, Germany). The whole mixture was then incubated for 10 min at 25°C followed by 30 min at 50°C. The reaction was terminated by heating at 85°C for 5 min and briefly cooling down afterwards to 4°C. The synthesized cDNA was if directly used stored on ice or frozen at -20°C.

3.3.12 Quantitative real-time RT-PCR (qRT-PCR)

qRT-PCR was performed on a LightCycler$^®$ (Roche Diagnostics GmbH, Mannheim, Germany) using 1 µL single stranded cDNA, 12.5 µL of Maxima^{TM} SYBR Green/ROX qPCR Master Mix (Fermentas, St. Leon-Rot, Germany), 800 nmol/L of each primer (primer sequences are listed in **Table 2**) and nuclease-free water (Fermentas, St. Leon-Rot, Germany) filled up to a final reaction volume of 25 µL. Target gene-specific qRT-PCR primers were designed using the UCSC web base to find out the Reference Sequences of the corresponding cDNAs. Primers were then picked by the Primer 3 web tool [220] with the settings primer length, product size, Melting temperature and an intronspanning region was manually marked. Testing for non-specific amplification and primer-dimer formation were done by analysis of melting curve and agarose gel verification of amplicon size.

The qRT-PCR cycling conditions were as follows: initial denaturation for 8 min at 95°C, followed by 35 cycles denaturation at 95°C for 15 s, annealing for 30 s at 60°C and elongation for 30 s at 72°C. Melting curve analysis was carried out from 60°C to 95°C with a temperature transition rate of 0.1°C/s. Results were calculated using Ct values obtained

from the reactions and quantified using the $2^{-\Delta\Delta Ct}$ method [221]. The calculation steps were as follows: ΔCt = Avg. *Pept1* Ct – Avg. housekeeping gene Ct; $\Delta\Delta Ct$ = Avg. $\Delta Ct_{,tissueX}$ – Avg. $\Delta Ct_{,Jejunum}$. Ct values represent the cycle number at which the fluorescence intensity exceeds a determined threshold.

Pept1 transcript levels are presented as fold differences normalized to the housekeeping genes *Villin*, *beta-Actin* and *Gapdh* and expressed relative to the expression in wild-type jejunum. In detail, fold changes were calculated by subtracting the average Ct values of the housekeeping genes from the average Ct value for *Pept1* (ΔCt). The relative mRNA levels were related to the expression in wild-type jejunum ($\Delta\Delta Ct$).

3.3.13 Agarose gel electrophoresis

Amplified PCR products were qualitatively analyzed by electrophoresis to determine the predicted amplicon length (**Table 2**, **Figure 15**, **Supplemental Figure 2**). Therefore 3% (w/v) agarose gels dissolved in TAE electrophoresis buffer containing 0.037 µg/mL ethidium bromide (Roth, Karlsruhe, Germany) were used. LightCycler capillaries were turned upside down in a 1.5 ml reaction tube and centrifuged for 1 min at 2.000x g and room temperature to transfer the whole capillary content into the reaction tube. Subsequently, 8 µl 6X DNA Loading Dye (Fermentas, St. Leon-Rot, Germany) was added to each reaction tube und mixed by pipetting up and down several times before the samples were loaded on an agarose gel. During electrophoresis for 20 min at 200 V the negatively charged DNA fragments migrate towards the anode in the electric field at a rate determined by the size. After electrophoresis the DNA was visualized on a UV light transilluminator (Gel iX Imager, Intas GmbH, Göttingen, Germany) and images were recorded by the Intas GDS imaging software.

3.3.14 PEPT1 transport studies

PEPT1 transport was measured using the *ex vivo* everted sacs method modified from Wilson TH et al. [222] on the proximal and distal colon and the jejunal part of the small intestine of wild-type, *Pept1*$^{-/-}$ and TNF$^{\Delta ARE/WT}$ mice. Individual 4-5 cm long intestinal segments were rinsed immediately after removal with saline (0.9% NaCl solution), fat and mesenteric attachments were removed carefully and the tissue segments everted using a metal rod.

The distal end was ligated using star thread (Wenco, Essen, Germany) and the sac was filled with Krebs bicarbonate buffer (KBB; 119 mM NaCl, 4.7 mM KCl, 2.5 mM CaCl$_2$, 1.2 mM MgSO$_4$, 1.2 mM KH$_2$PO$_4$, 25 mM NaHCO$_3$, pH 7.4) using a 3 ml plastic syringe (Henke-Sass, Wolf GmbH, Tuttlingen, Germany) with a blunted needle. Afterwards, the sac was closed by a knot over the proximal end and incubated for 20 min in 5 ml substrate-containing incubation buffer (119 mM NaCl, 4.7 mM KCl, 2.5 mM CaCl$_2$, 1.2 mM MgSO$_4$, 1.2 mM KH$_2$PO$_4$, 2.5 mM NaHCO$_3$, 1.01 mM MES, pH 6.0) continuously bubbled

with carbogen at 37°C on a tempered shaking platform (Incubator 1000, Heidolph, Schwabach, Germany). Radio-labeled [^{14}C]Gly-Sar (GE Healthcare, Munich, Germany) with a specific activity of 0.5 Ci/mmol was used as PEPT1 substrate. After incubation, the sacs were washed three times in KBB and carefully dried on filter paper to remove adhering [^{14}C]Gly-Sar sac surface, before the serosal fluid was collected and the tissue dried at 55°C in a drying oven (FD23, BINDER GmbH, Tuttlingen, Germany), lysated in 1 M NaOH (Roth, Karlsruhe, Germany) and decolorized with 1 M H$_2$O$_2$. Scintillation mixture (Rotiszint® eco plus, Roth, Germany) was added to each sample and radioactivity of a defined amount serosal fluid, gut homogenate, initial mucosal fluid and final mucosal fluid was measured using a liquid scintillation counter (Tri-Carb 2810 TR, PerkinElmer, Waltham, USA). The protein content of each tissues were determined by a Protein Assay (Bio-Rad, Munich, Germany) based on the method of Bradford [218] and the relative transport was expressed as nmol/mg protein*20 min. To characterize the transporter properties, we examined the competitive inhibiting effects of 50 mM non-radioactive Gly-Sar (Sigma-Aldrich, Taufkirchen, Germany) on the initial uptake rates of [^{14}C]Gly-Sar. The changes in non-specific passive permeability were examined with [^{3}H]D-Mannitol which has been used to assess intestinal permeability in rodents [223] and which serves as a marker of paracellular diffusion and for normalizing [^{14}C]Gly-Sar uptake.

3.3.15 Deglycosylation studies

Peptide: N-glycosidase F (PNGase F; New England Biolabs, Frankfurt am Main, Germany) or Endoglycosidase H (Endo H; New England Biolabs, Frankfurt am Main, Germany) enzymes were used to study the glycosylation status of isolated brush border membrane protein. Endo H cleaves the chitobiose (dimer of β-1,4-linked glucosamine units) core mainly of high mannose oligosacharides from N-linked glycoproteins [224] while PNGase F is known to cleave between the innermost GlcNAc and asparagine residues from N-linked glycoproteins (**Figure 5**) [225, 226].

The experimental procedure was as follows. First, 20 µg of isolated membrane protein from each sample was divided into two equal portions, one for deglycosylation and one as control incubated with buffer only. An amount of 1 µl 10X Glycoprotein Denaturing Buffer and H$_2$O to a final volume of 10 µl was added. For denaturation the protein was heated at 100°C for 10 min and afterwards 1 µl PNGase F (500 units) or Endo H, respectively, plus 2 µl 10X G7 Reaction buffer, 2 µl 10% NP40 and filled up to 20 µl total reaction volume was added. All prepared according to the manufacturer's recommendations. Samples were incubated at 37°C for different time periods (1-3 h). The reaction was terminated by cooling down on ice and adding 4x Laemmli loading buffer. Results were detected by Western Blot analysis as described before. Deglycosylation of RNase B served as positive control and reaction products were visualized by proteinstaining of the SDS gels after

PAGE. For this staining, PhastGel Blue R, a Coomassie R 350 dye, was used. One PhastGel® Blue R tablet (GE Healthcare Bio-Sciences, Uppsala, Sweden) was dissolved in 2 L of a 10% acetic acid solution (Roth, Karlsruhe, Germany) and undisolved particles were removed by filtration through a Whatman Filter, Grade 595 (Whatman Int. Ltd., Maidstone, UK). After staining of the gels in the PhastGel® Blue R solution for 20 min at 50°C, the gels were washed three times in 10% acetic acid. Finally, the gels were scanned and evaluated by the Odyssey Infrared Imaging System (LI-COR, Bad Homburg, Germany).
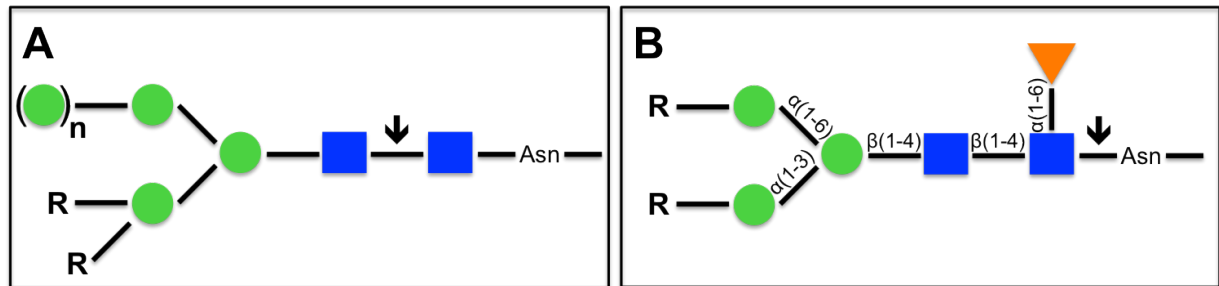

Figure 5. Glycosidase cleavage sites.
(Adapted from New England Biolabs glycosidase product informations) (A) EndoH cleaves (↓) within the core of high mannose and some hybrid oligosaccharides from N-linked glycoproteins. (B) PNGase F cleaves (↓) between the innermost GlcNAc and asparagine residues of high mannose, hybrid, and complex oligosaccharides from N-linked glycoproteins. ▼ - fucose, ■ -N-Acetyl-D-glucosamin (GlcNAc), ● - mannose

3.3.16 Myeloperoxidase Assay

The Myeloperoxidase (MPO) is a heme protein accounting for up to 5% of total cell protein in neutrophils and is released from their azurophilic granules [227]. It is the key constituent of the neutrophil's cytotoxic armament as it catalyzes the formation of hypochlorous acid, a potent oxidant with antibacterial activity. Furthermore, MPO activity modulates signaling pathways, like mitogen-activated proteinkinases-signaling or induces nuclear translocation of transcription factorsor modulates the activity of metalloproteinases [228-231]. To measure MPO activity, intestinal mucosa scrapings (10-20 mg) were homogenized by ultra sound (amplitude: 30%, cycle: 0,5, strokes: 15) in 500 µl 50 mM potassium phosphate (pH 6.0) containing hexadecyltrimethylammonium bromide (0,05%). The resulting homogenate was centrifuged 15 min at 15.000 g and 50 µl of the supernatant was used for MPO determination by mixing with 220 µl phosphate buffer (50 mM sodium dihydrogen phosphate, pH 6,0) containing 2 mg/ml o-dianisidine dihydrochloride and 30 µl hydrogen peroxide (30%) in a 96 well plate (TPP®; Trasadingen, Switzerland) to a total reaction volume of 300 µl. The plate was incubated 30 min in the dark and absorbance was recorded at a wavelength of 460 nm using a Varioskan Flash spectral scanning multimode reader (Thermo Electron GmbH; Karlsruhe, Germany). The measured values were converted to MPO activity per gram of scraped mucosa, determined with a standard curve (**Figure 6**) for which horseradish peroxidise (HRP; Calbiochem®; Darmstadt,

Germany) as reference enzyme was used. The amount that degraded 1 µmol peroxidase per minute was defined as one unit of MPO activity [232].
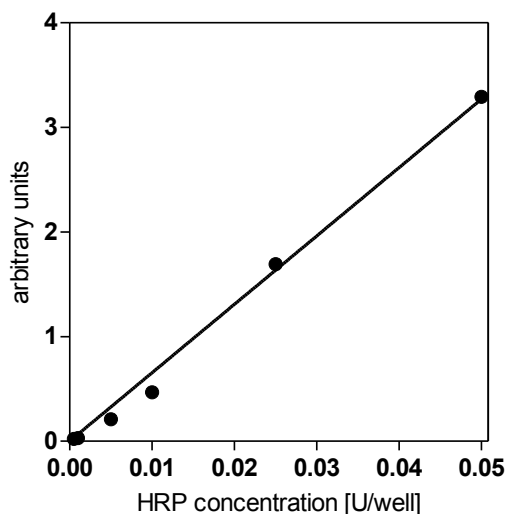

Figure 6. MPO standrad curve.
Different concentrations HRP ranging from 0.001 to 0.05 U/well were assessed in its concentration-dependent oxidation of o-dianisidine dihydrochloride in the presence ofhydrogen peroxide. The absorbance was recorded at 460 nm. The reactions were performed in triplicates and the means are depicted in the graph.

3.3.17   Fecal water content

Fecal samples were collected freshly excreted, weighted and dehydrated in a drying oven (BINDER GmbH, Tuttlingen, Germany) at 50°C over night. Fecal water content (%) was calculated as follows: ((fecal wet weight - fecal dry weight)/fecal wet weight) x 100.

3.3.18   Statistics

The results are expressed as means ± SEM. Statistical analysis were performed using GraphPad Prism 5.0 (GraphPad Software, San Diego, CA, USA). Statistical significant differences were defined as * $p < 0.05$, ** $p < 0.01$, and *** $p < 0.001$.

4 RESULTS

4.1 PEPT1 is expressed in healthy murine colon

To assess colonic PEPT1 expression in detail, colonic tissues of C57BL/6N, BALB/c and 129Sv wild-type mice were divided into 10 segments, starting very proximal next to the ceacum and ending distal near the rectum (**Figure 7**, upper panel). **Figure 7** A-B depict one representative IF staining from ileum and 5 representative IF stainings of colon from proximal to distal of C57BL/6N, BALB/c and 129Sv wild-type mice, respectively. For IF, paraffin embedded tissue sections were sliced with 6 µm thickness and transferred onto glass slides for staining. PEPT1 was detectable by immunofluorescence (IF) staining with high density in brush border membranes along the length of the entire villus of the small intestine from duodenum to ileum of C57BL/6N, BALB/c and 129Sv wild-type mice. In colon, PEPT1 showed a distinct pattern of distribution with marked differences between proximal and distal segments. No PEPT1 expression was detectable in the proximal colon but prominent expression was found from mid colon to rectum (**Figure 7**).
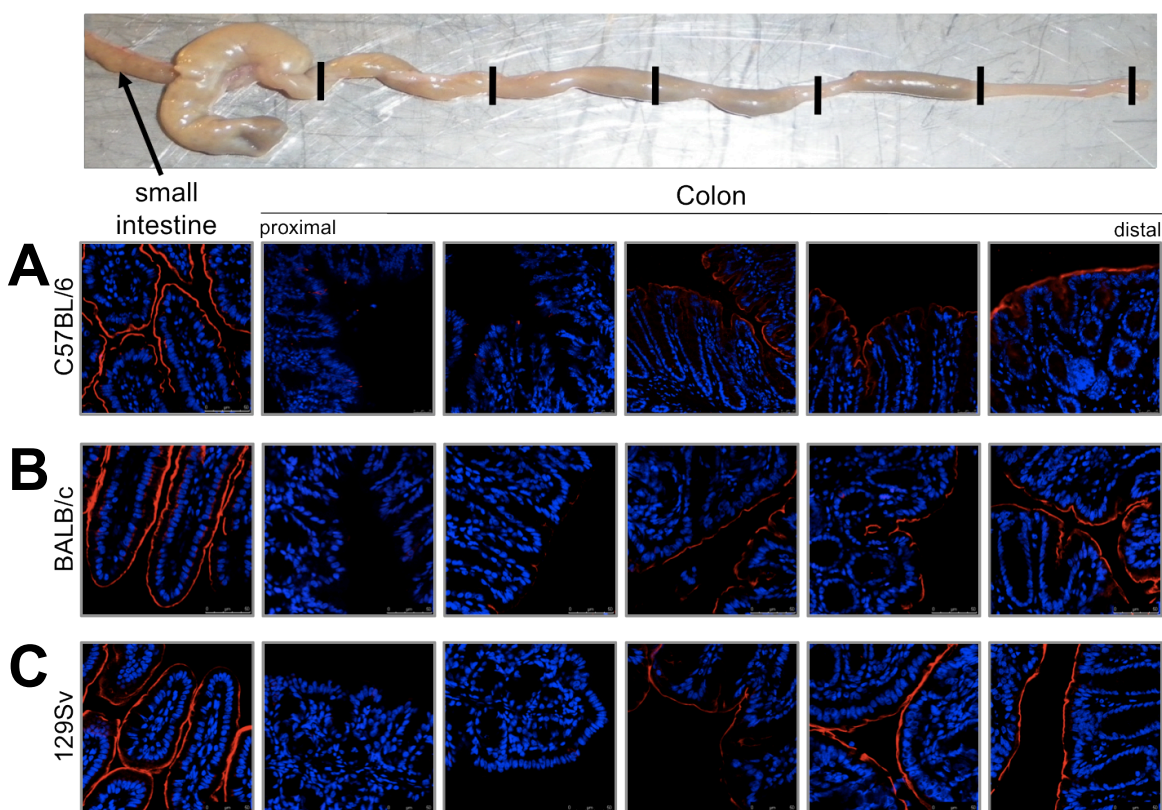

Figure 7. Assessment of PEPT1 expression along the small intestine and colon of mice.
Upper panel: Photograph of a mouse colon including cecum and terminal ileum (arrow). Black bars on the colon illustrate the defined sampling regions from proximal to distal of which IF stainings (lower panel) have been performed. (A) PEPT1 (red) is expressed on the apical membrane of the small intestinal epithelium. Whereas, PEPT1 is not detectable in proximal colon but notably, its immunoreactivity increased from mid colon towards the rectum of C57BL/6 mice. (B+C) Comparative sampling regions from the 129Sv and BALB/c wild-type strains show identical PEPT1 distribution along the intestine. DAPI or DRAQ5 were used as nuclear counterstain.

Identical PEPT1 expression patterns were observed in all three tested mouse strains. No PEPT1 signal was detectable in intestinal tissue of *Pept1$^{-/-}$* mice, which proofs the specificity and applicability of the AB for IF stainings (**Figure 8**).
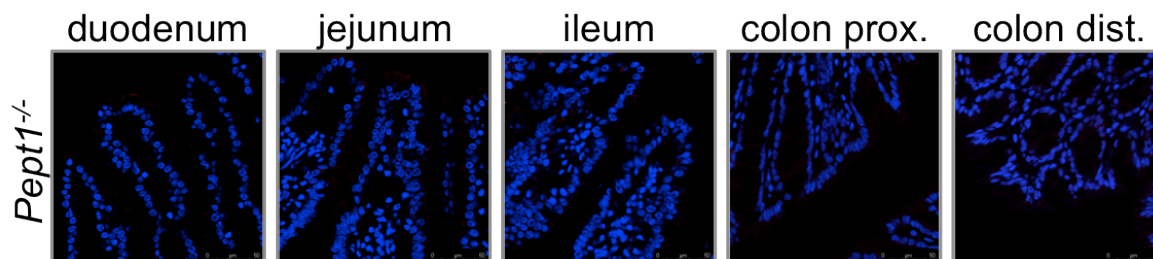

Figure 8. IF staining of a *Pept1$^{-/-}$* intestine.
A novel custom made primary AB against the C-terminus of rPEPT1 protein was tested for specificity. No PEPT1 immune reactivity was detectable in any intestinal segment from *Pept1$^{-/-}$* mice. DAPI was used as nuclear counterstain.

IF-based findings were confirmed by Western blot analysis of PEPT1 expression in duodenum, jejunum, ileum, the proximal and distal part of the colon from conventionally housed C57BL/6 wild-type mice (**Figure 9**). Western blots with the specific PEPT1 AB resulted in a predicted band with highest density and at a MW of approximately 95 kDa in all parts of the small intestine (**Figure 9 A**). In contrast, only a marginal staining was detectable in proximal colon whereas distal samples revealed again prominent staining. Notably, the MW of colonic PEPT1 differed from that found in small intestine at a MW of approximately 110 kDa (**Figure 9 A**, left panel). No PEPT1 band was found in any intestinal segment of *Pept1$^{-/-}$* mice, underlining the specificity of the used AB (**Figure 9 A**, right panel). For quantitative analysis the PEPT1 amount was normalized to the expression of beta-Actin or Villin. Beta-Actin as ubiquitous cytoskeleton protein is a well-known marker for general cell mass and loading control. Villin was chosen because it is specifically expressed in epithelial cells, and its use as reference protein was established previously [233, 234]. The densitometric quantification of PEPT1 revealed a reduced density of PEPT1 in distal colon as compared to small intestine with a 1.84-2.38-fold lower level. However, expression levels differed significantly ($p<0.05$) between proximal and distal colon with a mean 3.6-fold increased protein density in distal as compared to proximal colon (**Figure 9 B+C**).
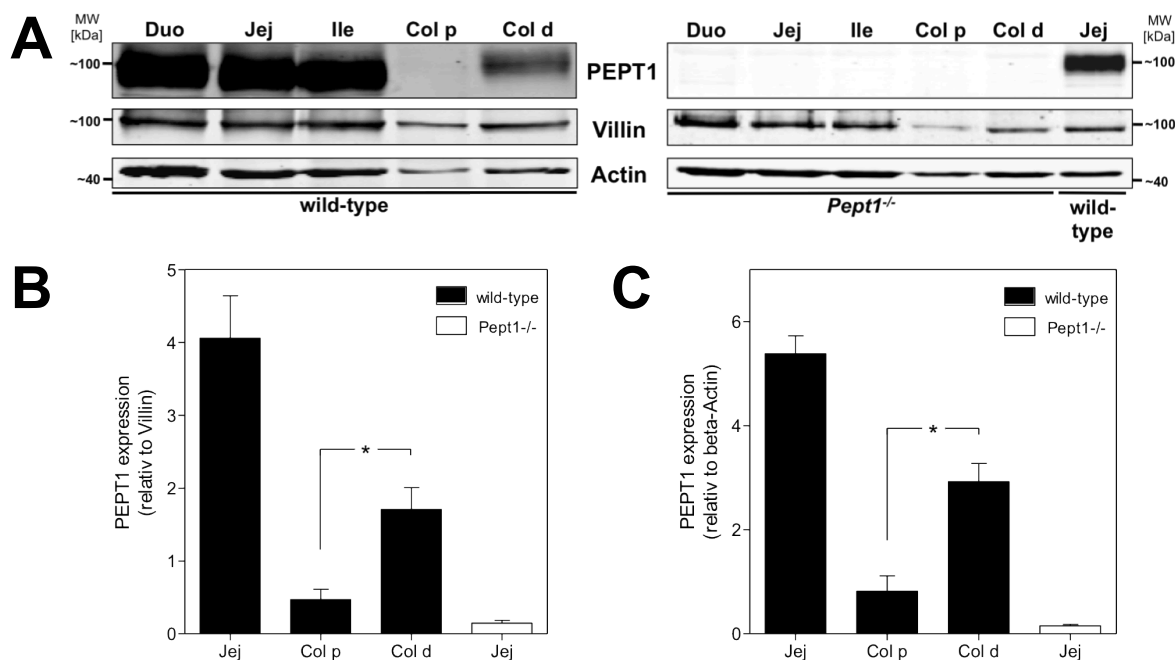
Figure 9. Western blot analysis of PEPT1 along the murine intestine.
(A) Representative Western Blot analysis of a wild-type (left) and a *Pept1*^{-/-} (right) mouse. The specific PEPT1 band appeared at ~95 kDa and was detectable in duodenum (Duo), jejunum (Jej), ileum (Ile) and a app. 10 kDa higher mass band in distal colon (Col d). Hardly any PEPT1 was detectable in proximal colon (Col p). Villin and beta-Actin were used as loading controls and for quantification. No PEPT1 band was detectable in any intestinal segment from *Pept1*^{-/-} mice (B+C). Densitometric quantification of PEPT1 Western blots. Villin (B) or beta-Actin (C) were used as reference proteins and densitometric quantification revealed distal colon to have around 40% of the amount of PEPT1 in small intestine and significantly lower PEPT1 expression in proximal as compared to the distal colon. Data are the means ± SEM of n=5-8 animals (*p<0.05).

Some individual cells in proximal mouse colon were found to stain PEPT1-positive. Staining of the proximal colon from *Pept1*^{-/-} mice also showed these single cells, indicating an unspecific binding of the anti-rPEPT1 AB (**Supplemental Figure 3**). In contrast, when the anti-hPEPT1 AB was used on proximal mouse colon, no signal was detectable. To define the cell type which stained positive with the anti-rPEPT1 in proximal colon, co-localization studies with *Ulex europaeus* (UEA) Lectin, DC-Specific Intercellular adhesion molecule-3-Grabbing Non-integrin (DC-SIGN), Ghrelin and Serotonin were conducted (**Supplemental Figure 4**). Unfortunately, none of the tested probes co-localized with PEPT1 in these individual cells.

PEPT1 expression along the intestine was also profiled in germfree mice to assess whether intestinal microbiota alter the expression. As demonstrated by IF, germfree animals revealed the same PEPT1 distribution including the differences in colonic PEPT1 expression as conventionally housed mice (**Figure 10**) suggesting that the microbiota does

not change colonic PEPT1 expression. Western Blot analysis and quantification of PEPT1 abundance revealed significant differences between PEPT1 in proximal colon as compared to the distal part (0.77 ± 0.17 vs. 2.17 ± 0.15, n=4, $p<0.001$). Moreover differences were also detectable in the small intestine with a significant increase of PEPT1 abundance from duodenum to ileum (2.08 ± 0.17 vs. 4.01 ± 0.19, n=4, $p<0.001$).
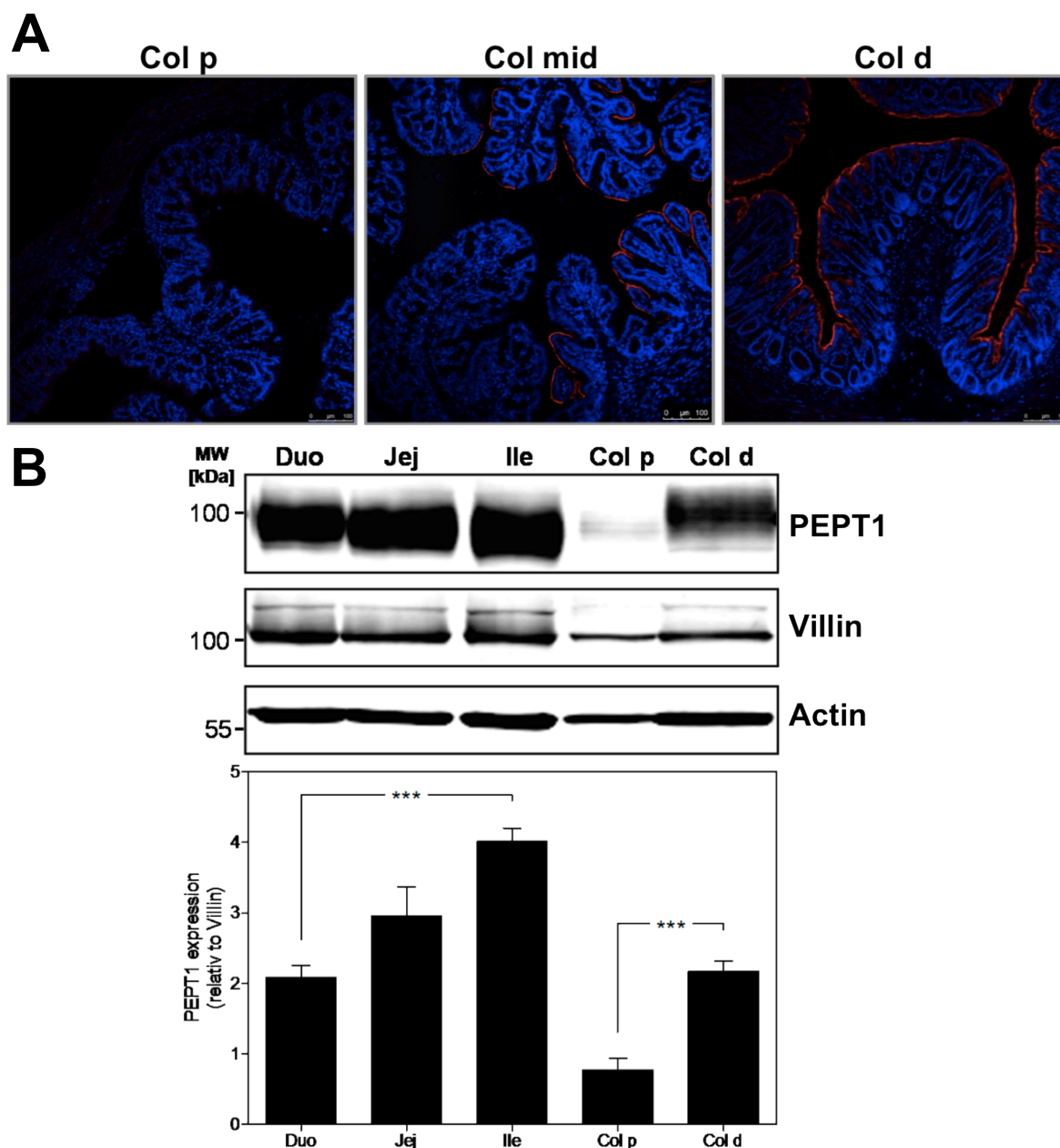

Figure 10. PEPT1 expression along the intestine of germfree mice.
(A) Representative IF stainings of PEPT1 (red) in proximal (Col p), mid (Col mid) and distal (Col d) colon from germfree mice. (B) Western Blot analysis of intestinal tissue from germfree mice. Upper panel: Representative Blots, lower panel: quantification of PEPT1 abundance. n=4, ***$p<0.001$.

4.2 Increased glycosylation pattern of colonic PEPT1

The differences in the apparent MW of small intestinal and colonic PEPT1 led us to studies on the protein glycosylation. PEPT1 has several putative N-glycosylation sites at

its large extracellular loop that comprises 203 amino acids. For deglycosylation, two enzymes well known to cleave N-linked glycan structures from asparagine residues, Endo H and PNGase F, were applied. First the activity of both enzymes on a positive control protein, namely RNase B was tested. RNase B is a glycoprotein equipped with N-linked high mannose structures. Both enzymes cleaved glycans from the RNase B, which resulted in a MW shift from approximately 18 kDa to approximately 15 kDa. Furthermore, the time-dependency of the reactions could be shown (**Figure 11**).
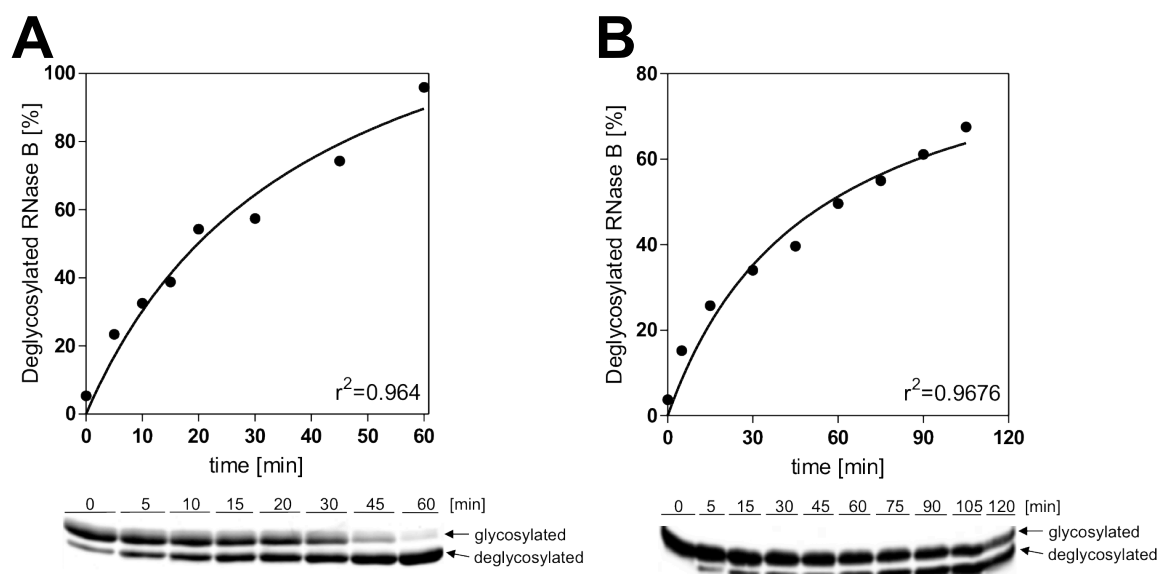

Figure 11. Time-dependent deglycosylation of RNase B.
Either Endo H (A) or PNGase F (B) were used for deglycosylation in an amount of 5 µg for Endo H or a concentration of500 Units for PNGase F. Lower panel: Coomassie Brilliant Blue stained 15% SDS-PAGE image depicts time-dependent Endo H (left) or PNGase F (right) mediated deglycosylation of the N-linked sugars from RNase B. The lower bands at ~15 kDa and upper bands at ~18 kDa represent the deglycosylated and intact (glycosylated) forms of RNase B, respectively. Deglycosylation of denatured RNase B was carried out at 37°C for respective time periods.

However, incubation of intestinal protein isolates with Endo H or PNGase F showed that only PNGase F is capable to succsessfully release glycans from the PEPT1 protein (**Figure 12**). Treatment with EndoH did not cause a MW shift (**Supplemental Figure 5**). PNGase F decreased the MW of the PEPT1 protein from around 95 kDa towards approximately 71 kDa corresponding to the proposed MW of the native non-glycosylated PEPT1 protein (3). And most remarkably, colonic PEPT1 was reduced in MW from around 110 kDa towards a band at the same MW of approximately 71 kDa, like the small intestinal protein. In addition, other Intestinal membrane proteins (CD36, DAT, DRA, OCTN2) were tested, whether they show similar glycosylation differences between different intestinal segments. But unfortunately among the tested proteins with the used ABs no specific signals could be detected (**Supplemental Figure 6**). Only NHE3 and PAT1 were detectable in jejunum by Western Blot (**Supplemental Figure 7**). NHE3 was

detectable in jejunum and colon with higher expression in proximal colon and lower expression in the distal colon. The MW of NHE3 appears at the same MW in both gut regions.
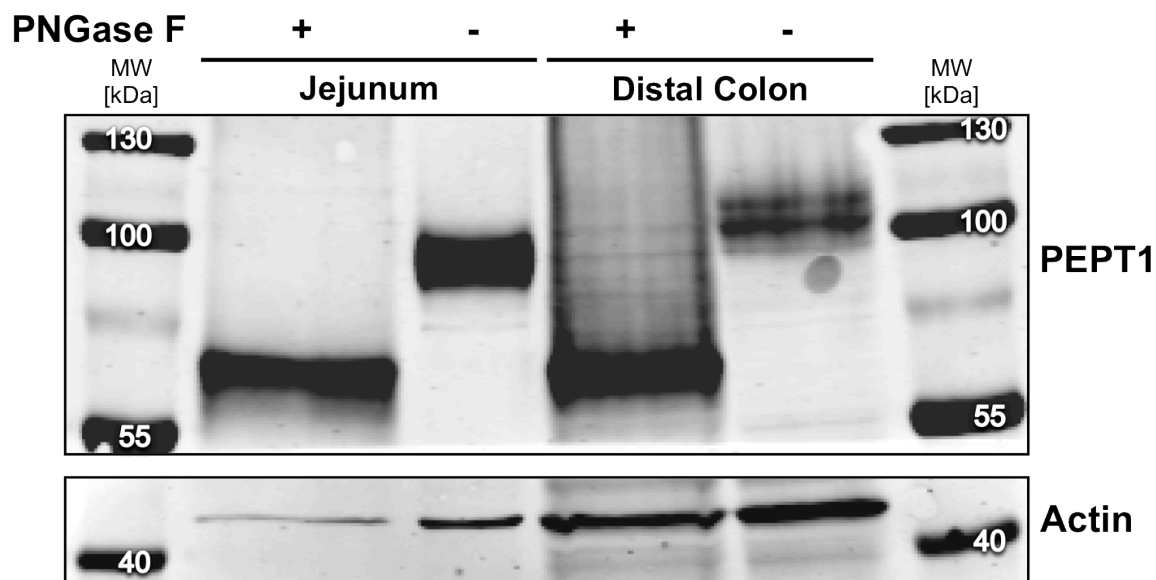

Figure 12. Deglycosylation of PEPT1 from wild-type mouse jejunum and distal colon.
Colonic PEPT1 when compared to the small intestinal protein is detected with a ~10 kDa higher MW. Deglycosylation with PNGase F (+) resulted in a MW shift from ~95 kDa (jejunum) or ~105 kDa (distal colon) to a band at ~71 kDa which corresponds to the proposed MW of the non-glycosylated PEPT1 protein. These findings establish that the PEPT1 glycan content varies between small intestine and colon.

4.3 Functional analysis of colonic PEPT1

Everted intestinal sacs were used to study PEPT1 transport function. Radiolabeled [^{14}C]Gly-Sar was applied as a specific PEPT1 substrate and highest uptake rates (19.76 nmol/20 min/mg protein) were observed in jejunal segments of the small intestine. Uptake by distal colon (1.71 ± 0.42 nmol/20 min/mg protein) was significantly (p<0.05) higher compared to proximal colon (0.30 ± 0.22 nmol/20 min/mg protein). Nevertheless, colon tissues showed generally lower transport rates than small intestine. Competitive inhibition studies were performed by adding 50 mM unlabeled Gly-Sar to the incubation solution, which led to a PEPT1-uptake inhibition by 88.4% in small intestine and 70.7% in distal colon. [^{14}C]Gly-Sar influx into tissues of *Pept1*$^{-/-}$ mice was only marginal, could not be inhibited and is therefore attributable to passive diffusion (**Figure 13**). These results proofed colonic PEPT1 to be functional.
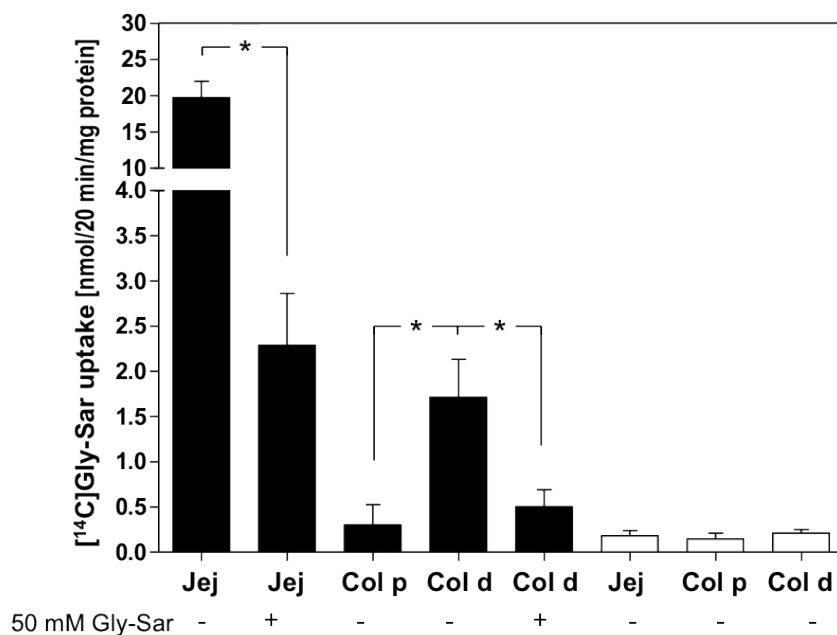
Figure 13. Functional activity of colonic PEPT1.
(A) Uptake studies in isolated intestinal tissue from wild-type and *Pept1*^{-/-} mice revealed highest uptake in jejunum from wild-type mice. The uptake could be significantly inhibited by addition of 50 mM non-labeled Gly-Sar (19.76 ± 2.24 vs. 2.29 ± 0.57 nmol/20 min/mg protein). The distal colon showed significantly higher PEPT1-mediated uptake compared to proximal colon (1.71 ± 0.42 vs. 0.30 ± 0.22 nmol/20 min/mg protein) and addition of 50 mM Gly-Sar led to a significant inhibition of [^{14}C]Gly-Sar uptake (1.71 ± 0.42 vs. 0.50 ± 0.19 nmol/20 min/mg protein) in distal colon. No active transport was measured in any intestinal segment of *Pept1*^{-/-} mice. n=5-8. Jej, jejunum, Col p, proximal colon, Col d, distal colon.

As a solute carrier, PEPT1 was shown to contribute to intestinal water transport [61] and therefore fecal water content was determined. Water content in feces of *Pept1*^{-/-} mice revealed significantly elevated levels ($67.9\pm3.0\%$ vs. $55.5\pm3.4\%$; $p<0.05$; **Figure 14**) as compared to feces from wild-type mice.

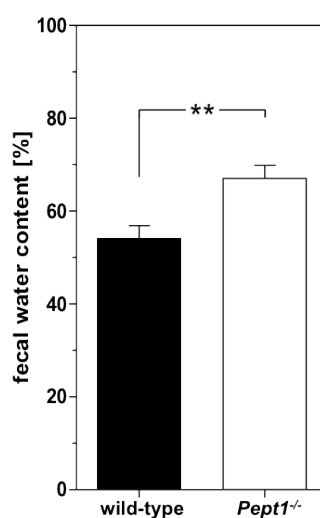**Figure 14. Fecal water content measured in wild-type and *Pept1*^{-/-} mice.**
Pept1^{-/-} mice showed significantly higher water amounts in feces as compared to wild-type mice ($67.93 \pm 2.99\%$ vs. $55.48202 \pm 3.42\%$). n=6-7, *$p<0.05$, ***$p<0.001$.

4.4 Pept1 mRNA shows high expression in distal colon

We further determined the spatial colonic PEPT1 expression on transcript level. For this, *Pept1* mRNA quantity was assessed by qRT-PCR in wild-type mice, and *Pept1$^{-/-}$* mice as negative control for primer specificity. Specific primers mapping a 187 bp sequence intron-spanning of the 3rd and 4th exon within the *Pept1* gene were used. These primers allowed distinguishing between WT and *Pept1$^{-/-}$* tissue as the protein coding region from bases +77 to +101 of exon 3 was target of deletion in *Pept1$^{-/-}$* mice [59].
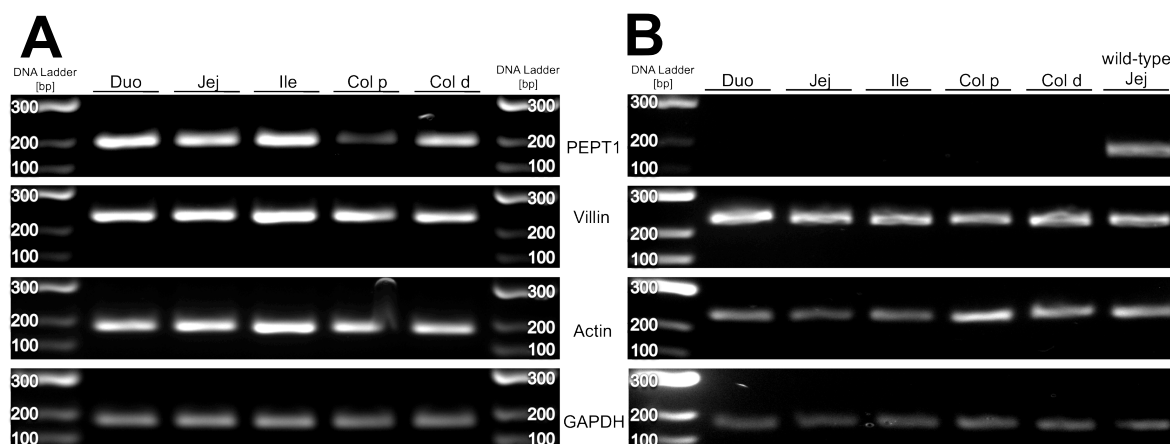

Figure 15 Representative agarose gels of qRT-PCR products.
qRT-PCR products were separated by agarose gel electrophoresis and stained with ethidium bromide. The expected and observed qRT-PCR amplicon sizes were for *Pept1* 187 bp, *Villin* 220 bp, *beta-Actin* 179 bp, and *Gapdh* 171 bp (A). All intestinal tissue segments from *Pept1$^{-/-}$* mice failed to deliver a *Pept1*-PCR amplicon (B).

Pept1 mRNA levels were normalized to the three housekeeping genes *Villin*, *beta-Actin* and *Gapdh* and are displayed as relative to the expression in jejunum. All housekeeping genes used have been shown before to be suitable as references genes, and especially *Villin* was tested to be useful as a reference gene for intestinal epithelium [235]. The expected and observed product sizes using agarose gel electrophoresis were *Pept1* 187 bp, *Villin* 220 bp, *beta-Actin* 179 bp, and *Gapdh* 171 bp. No signals for *Pept1* were detectable in intestinal segments from *Pept1$^{-/-}$* mice (**Figure 15**).

The *Pept1* mRNA levels in small intestine were found to decline from duodenum to ileum. In colon, substantial *Pept1* mRNA levels were detectable in distal regions, significant 5.2-fold higher (p<0.001) levels compared to those of proximal colon (**Figure 16**). These results revealed that PEPT1 protein levels crossly follow the mRNA levels in longitudinal distribution.
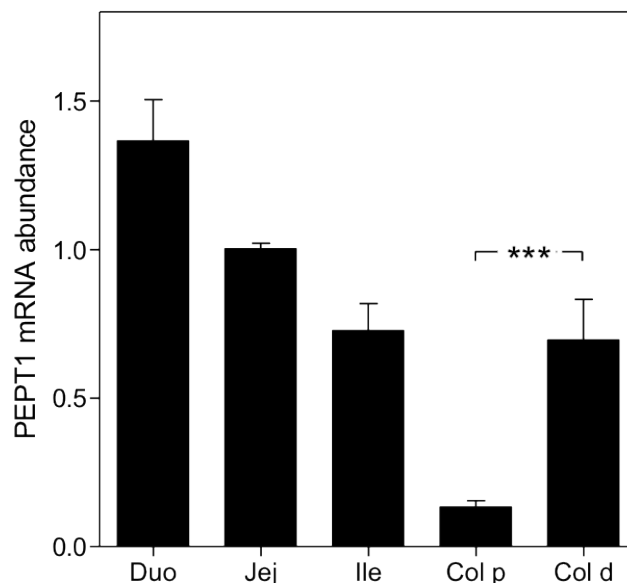
Figure 16. Quantification of *Pept1* mRNA.
Pept1 mRNA was normalized to the three housekeeping genes *Villin*, *beta-Actin* and *Gapdh* and related to the expression in wild-type jejunum. n=5-8, ***p<0.001.

4.5 Putative transcription factors regulating colonic *Pept1* expression

To test which transcription factor may influence the side-specific *Pept1* expression in colon, several proposed candidates were tested, whether they also show distinct longitudinal expression patterns. Among the proposed transcription factors involved in regulation of *Pept1* expression the following were tested: AP-1, Cdx2, CREB, klf4, Mzf1, Nrf2, PPAR-α, Sp1, VDR. The expression was recorded from jejunum, proximal colon and distal colon and quantified by the $2^{-\Delta\Delta Ct}$ method, as described earlier.

The transcription factors Cdx2 and CREB did not show marked different mRNA expression levels between jejunum, proximal colon and distal colon (Cdx2 1.01 ± 0.05, 1.21 ± 0.10, 0.81 ± 0.11; CREB 1.01 ± 0.04, 1.18 ± 0.09, 1.59 ± 0.26, n=7-8). Klf4 showed significantly higher expression levels in proximal (p<0.001) and distal (p<0.01) colon as compared to jejunum (4.12 ± 0.42/2.99 ± 0.51 vs. 1.01 ± 0.06, n=8). Similar expression profiles were observed for Mzf1 (5.64 ± 1.52/3.78 ± 1.15 vs. 1.04 ± 0.09, n=5-8, p<0.05/ p<0.01) and Nrf2 (4.29 ± 0.93/3.06 ± 0.77 vs. 1.04 ± 0.08, n=13, p<0.05/ p<0.01). PPAR-α and VDR showed significantly higher expression in proximal colon (p<0.001) in comparison to jejunum and distal colon (PPAR-α 3.59 ± 0.34 vs. 1.00 ± 0.04/0.84 ± 0.14; VDR 6.63 ± 0.62 vs. 1.00 ± 0.031/2.10 ± 0.32, n=8). And finally, the two transcription factors AP-1 (jejunum: 1.00 0± 0.02, proximal colon: 0.43 ± 0.03, distal colon: 1.11 ± 0.24) and Sp1 (jejunum: 1.00 ± 0.04, proximal colon: 0.46 ± 0.04, distal colon: 1.04 ± 0.16) showed significantly lower (p<0.001) expression in proximal colon as compared to

jejunum or distal colon (Figure 17 B); this represents a similar expression pattern as *Pept1* (jejunum: 1.00 ± 0.02, proximal colon: 0.04 ± 0.002, distal colon: 0.37 ± 0.04, n=10).

Thus, AP-1 and Sp1 may be the prime determinants controlling the spatial transcriptional regulation of *Pept1* expression. However, further analysis is warrant to clarify their exact role. In contrast, AP-1 and Sp-1 expression in intestinal tissue from *Pept1*^{-/-} mice showed altered expression as compared to the respective wild-type intestinal segments. (**Figure 17 C**). AP-1 showed a higher expression in proximal colon as compared to the distal colon (1.25 ± 0.20 vs. 0.32 ± 0.07, n=5, p<0.0001) and Sp-1 showed higher expression in proximal and distal colon as compared to jejunum (4.36 ± 0.77/ 3.95 ± 0.52 vs. 1.22 ± 0.18, n=5, p<0.0001).

The next steps to validate the detected transcription factors participating in *Pept1* regulation should first clearify whether the mRNA profile of the transcription factors translates into protein abundance. Second, the binding activity to *Pept1* promotor region should be validated by electrophoretic mobility shift assay (EMSA) or comparable detection methods. And third, additional putative regulating factors, includicng microRNA, should be considered.
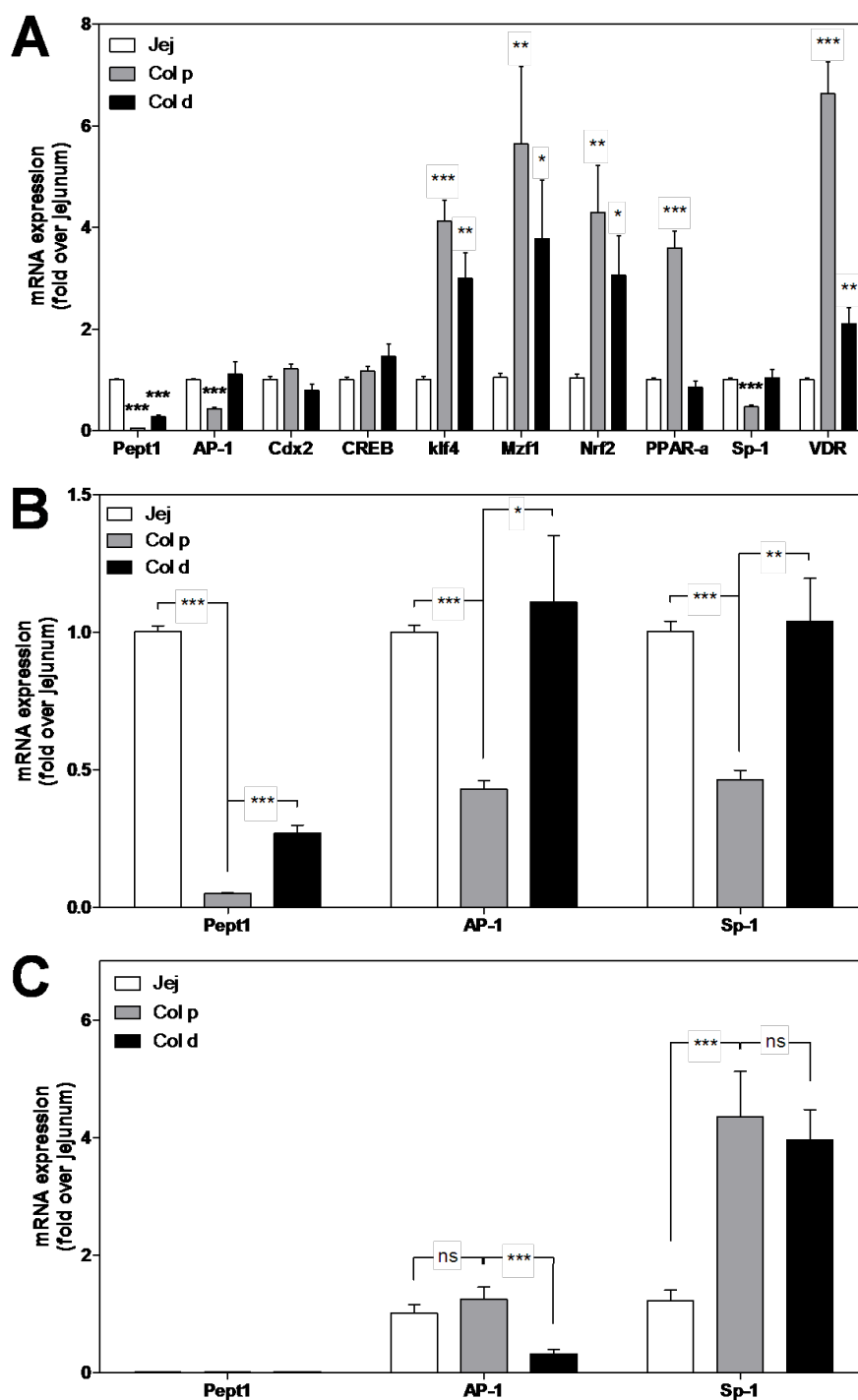
Figure 17. mRNA abundance of transcription factors postulated to be involved in basal Pept1 expression.
(A) QRT-PCR quantification of Pept1, AP-1, Cdx2, CREB, klf4, Mzf1, Nrf2, PPAR-α, Sp-1 and VDR expression in jejunum, proximal and distal colon from wild-type mice. Data are the means ± SEM compared to jejunum. (B) Detailed analysis of Pept1, AP-1 and Sp-1 comparing the expression between jejunum, distal colon and proximal colon. (C) QRT-PCR quantification of Pept1, AP-1 and Sp-1 expression in jejunum, proximal and distal colon from *Pept1^{-/-}* mice intestinal tissue. Data are the means ± SEM, n=5-10, *p<0.05, **p<0.001, ***p<0.0001.

4.6 PEPT1 in rat and human colon and intracellular localization

To proof that the spatial colonic PEPT1 expression is not restricted to mice, protein levels in rat (**Figure 18**) and human (**Figure 19**) intestine were assessed. IF stainings in both, rat and human small intestine showed similar expression profiles as found in mice. Furthermore, the absence of PEPT1 in proximal and its presence in distal colonic epithelium was comparable between the species. But by contrast, PEPT1 in distal colonic tissue from rats as well as humans revealed reduced apical membrane staining but increased labeling in intracellular compartments. The human intestinal tissue samples were histologically normal tissue derived from small intestine, colon ascendens and colon descendens obtained from patients undergoing surgery.

Immunofluorescene co-staining with GM130, a member of the golgin family of coiled-coil proteins, expressed on the *cis*-face of the Golgi apparatus [236], revealed colocalization with PEPT1 in distal colon (**Figure 19 B+C**) suggesting that in rats and humans more protein resides in the *cis*-Golgi as part of the posttranslational modification and trafficking machinery to the apical membrane.
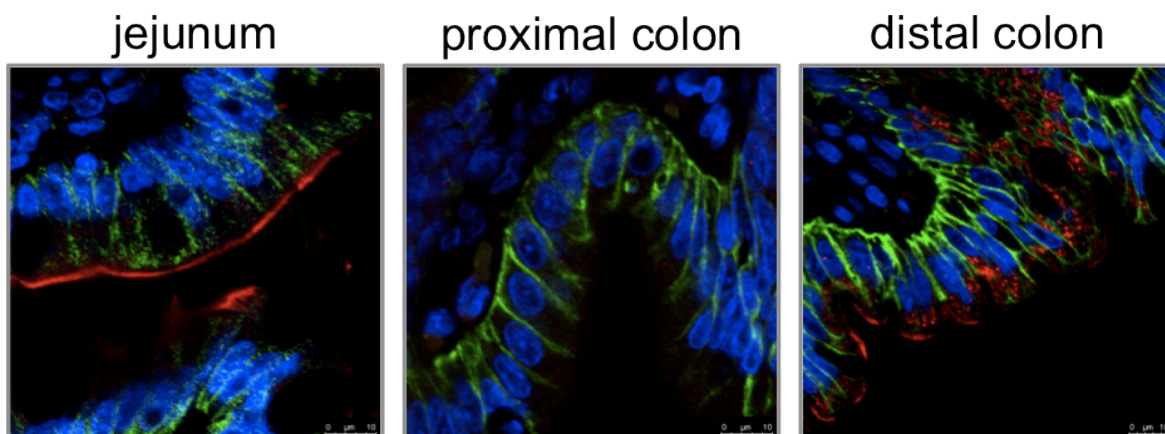
Figure 18. PEPT1 IF in rat intestine.
PEPT1 is expressed in the apical membrane of jejunum in rats. No PEPT1 expression is detectable in proximal colon but in distal colon. However, in distal colon the PEPT1 signal appears predominantly in intracellular compartments rather than in the apical membrane. MCT-1 (green) was used as marker of basolateral membranes to visualize the distribution and borders of enterocytes. DAPI was used as nuclear counterstain (blue).
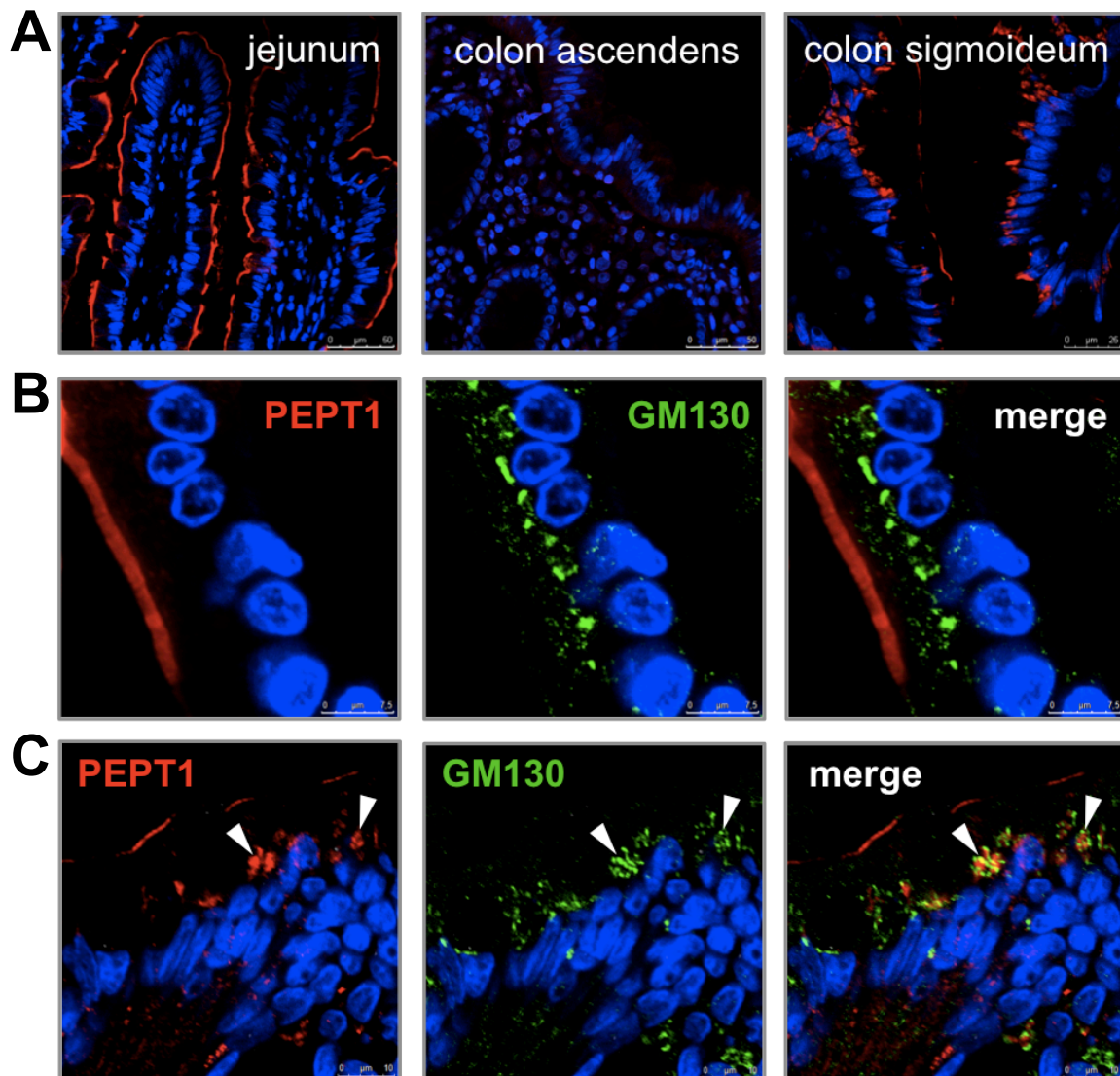
Figure 19. PEPT1 IF stainings in human small and large intestine.
(A) PEPT1 expression along the proximal-distal axis showed the presence in the apical jejunal membrane (left), no expression in colon ascendens (mid) and intracellular expression in colon sigmoideum (right) with only marginal presence in the apical membrane. (B-C) Co-localization of PEPT1 (red) and GM130 (green), a *cis*-Golgi marker, along the human intestine. (B) The small intestine shows PEPT1 expression on the apical surface (left) and intracellular GM130 labeling next to the nucleus (mid). The merged image reveals no colocalization of both (right). (C) PEPT1 expression in human colon sigmoideum in intracellular stores and only traces on the apical surface (left). GM130 as Golgi marker shows intracellular signal next to the nucleus (mid). The merged image (right) reveals PEPT1 colocalization with GM130 and thus, in Golgi structures. Nuclei are counterstained by DRAQ5 (blue).

PEPT1 expression during intestinal inflammation

4.7 PEPT1 expression in TNF$^{\Delta ARE/WT}$ mice

TNF$^{\Delta ARE/WT}$ mice represent a model of T$_H$1 cell-mediated Crohn's like ileitis, mainly located in the terminal ileum. These mice have a deletion of the AU-rich element (ARE) in the untranslated region of the TNF-α mRNA which is associated with increased constitutive levels of TNF-α production [237].
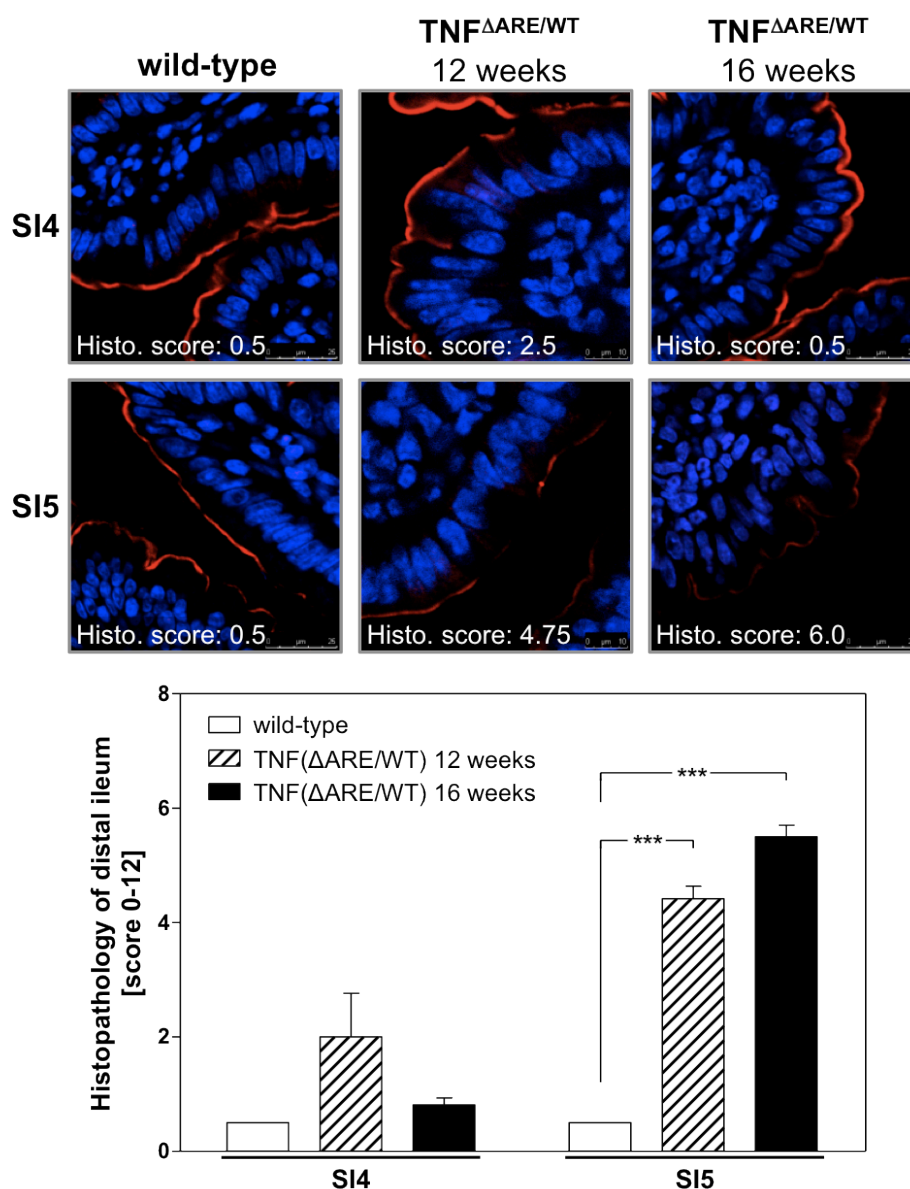
Figure 20. PEPT1 expression during intestinal inflammation in TNF$^{\Delta ARE/WT}$ mice.
The small intestine was divided into five segments from proximal (SI1) to the distal (SI5). (A) IF of PEPT1 in distal segments SI4 and SI5 from wild-type control and TNF$^{\Delta ARE/WT}$ mice, 12 and 16 weeks of age. PEPT1 expression declines with the progression of inflammation on week 12 and is hardly detectable on week 16 in segment SI5. No changes are detectable in any other segment at any other time point. (B) Histological scoring (0-12) of distal small intestinal segments SI4 and SI5 from TNF$^{\Delta ARE/WT}$ mice at 12 and 16 weeks of age and wild-type controls. Data are the means ± SEM of n=3-4 animals. (***p<0.001).

With increasing age, TNF$^{\Delta ARE/WT}$ mice develop progressively a severe inflammation. PEPT1 expression in these animals was assessed at the age of 12 and 16 weeks. The small intestine was divided into five segments from proximal to the distal (SI1-SI5). IF and Western blot analysis showed decreased PEPT1 levels in segment SI5 on week 12 and 16 compared to wild-type controls (**Figure 20**) and densitometric quantification confirmed significantly lower PEPT1 protein densities (p<0.01) on weeks 12 and 16 in distal segment SI5 (**Figure 21 B**). In parallel, histopathological scoring revealed significantly increased (p<0.001) severity of inflammation in the tissue segment SI5 of 12 and 16 week old TNF$^{\Delta ARE/WT}$ mice compared to wild-type mice (**Figure 20**, lower panel). No differences were observed at any time in any of the segments SI1 to SI4. Thus, PEPT1 expression is diminished during small intestinal inflammation in this animal model.
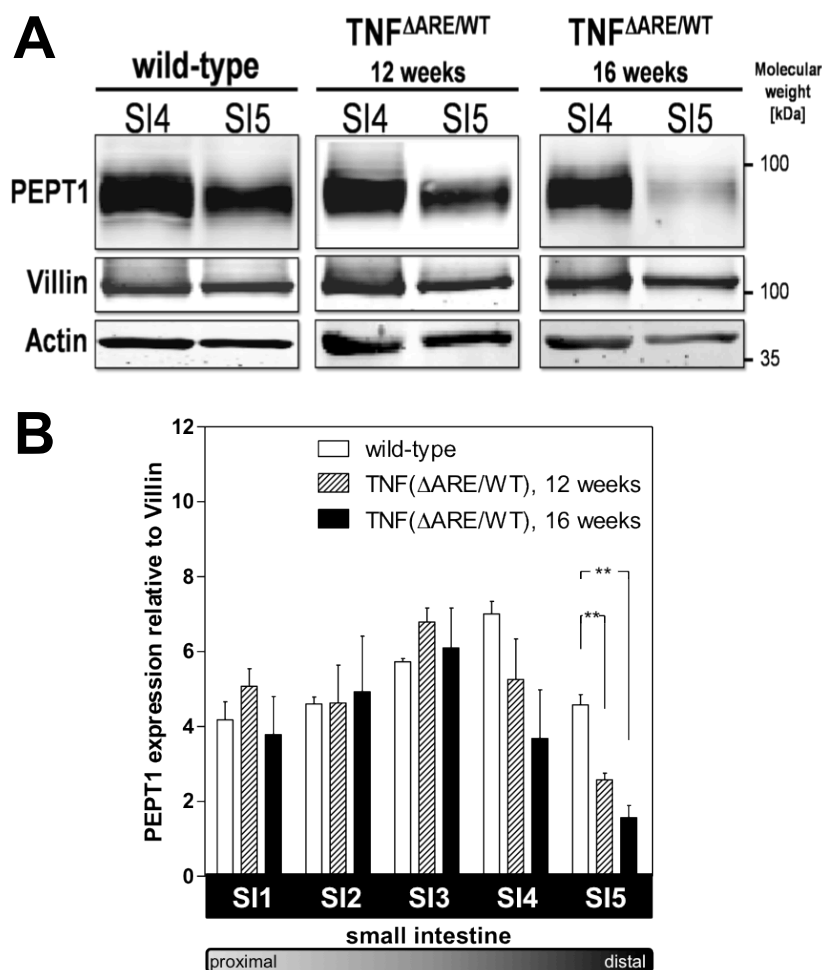
Figure 21. Western Blot analysis of PEPT1 expression in TNF$^{\Delta ARE/WT}$ mice.
Representative Western Blots (A) and quantification (B) shows significantly reduced PEPT1 levels in TNF$^{\Delta ARE/WT}$ mice on week 12 and 16 in segment SI5 compared to wild-type control. Data are the means ± SEM of n=5 animals (**p<0.01)

Uptake studies using [^{14}C]Gly-Sar in everted sacs from 16 week old TNF$^{\Delta ARE/WT}$ or wild-type control mice confirmed diminished PEPT1 expression on functional level. Transport rate in ileum of TNF$^{\Delta ARE/WT}$ was 2.84-fold lower compared to wild-type control mice

(9.86 ± 1.05 vs. 3.47 ± 0.49, n=3-8, p<0.001) with no differences in more proximal regions of the jejunum between wild-type and TNF$^{\Delta ARE/WT}$ mice (13.36 ± 0.91 vs. 11.05 ± 0.84, n=4-8, ns) (**Figure 22**). [^{3}H]D-mannitol was used as tracer to correct for paracellular flux.
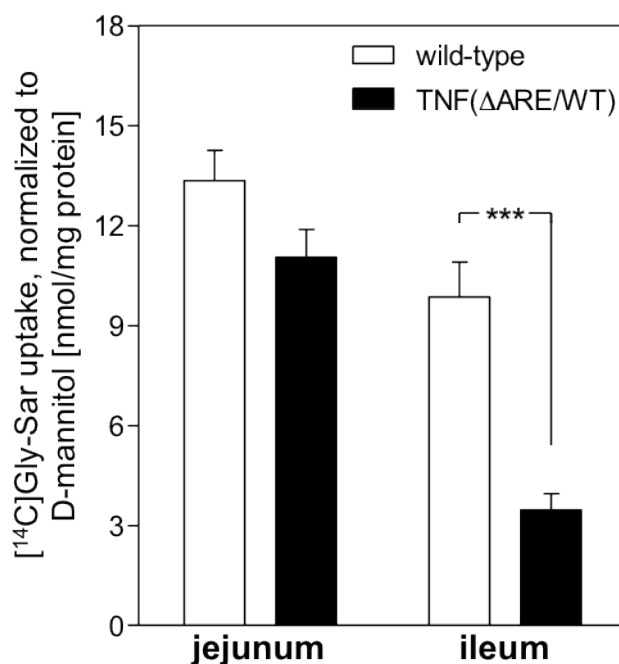
Figure 22. PEPT1 transport function in small intestine from TNF$^{\Delta ARE/WT}$ mice.
Functional analysis by [^{14}C]Gly-Sar uptake *ex vivo* on everted intestinal sacs showed decreased PEPT1 activity in the ileum from TNF$^{\Delta ARE/WT}$ mice compared to wild-type control. The values are normalized for paracellular D-mannitol-flux. n=4-8, ***p<0.001.

4.8 PEPT1 expression in IL-10$^{-/-}$, IL-10XTLR2$^{-/-}$ and IL-10XTLR4$^{-/-}$ mice

IL-10$^{-/-}$ mice develop spontaneously colitis when housed in conventional environments but not when housed under germfree conditions [238, 239], pointing to the crucial role of resident commensals in these mice. PEPT1 expression was assessed in germfree IL-10$^{-/-}$ and wild-type mice or mono-associated with the *E. faecalis* strain OG1RF. As it has been shown previously, OG1RF mono-association contribute to the development of intestinal inflammation [134]. IF and quantitative analysis (n=5) revealed significantly decreased PEPT1 levels after OG1RF mono-association in both genotypes, IL-10$^{-/-}$ and wild-type (p<0.05), but more pronounced in IL-10$^{-/-}$ mice (p<0.001) (**Figure 23**).
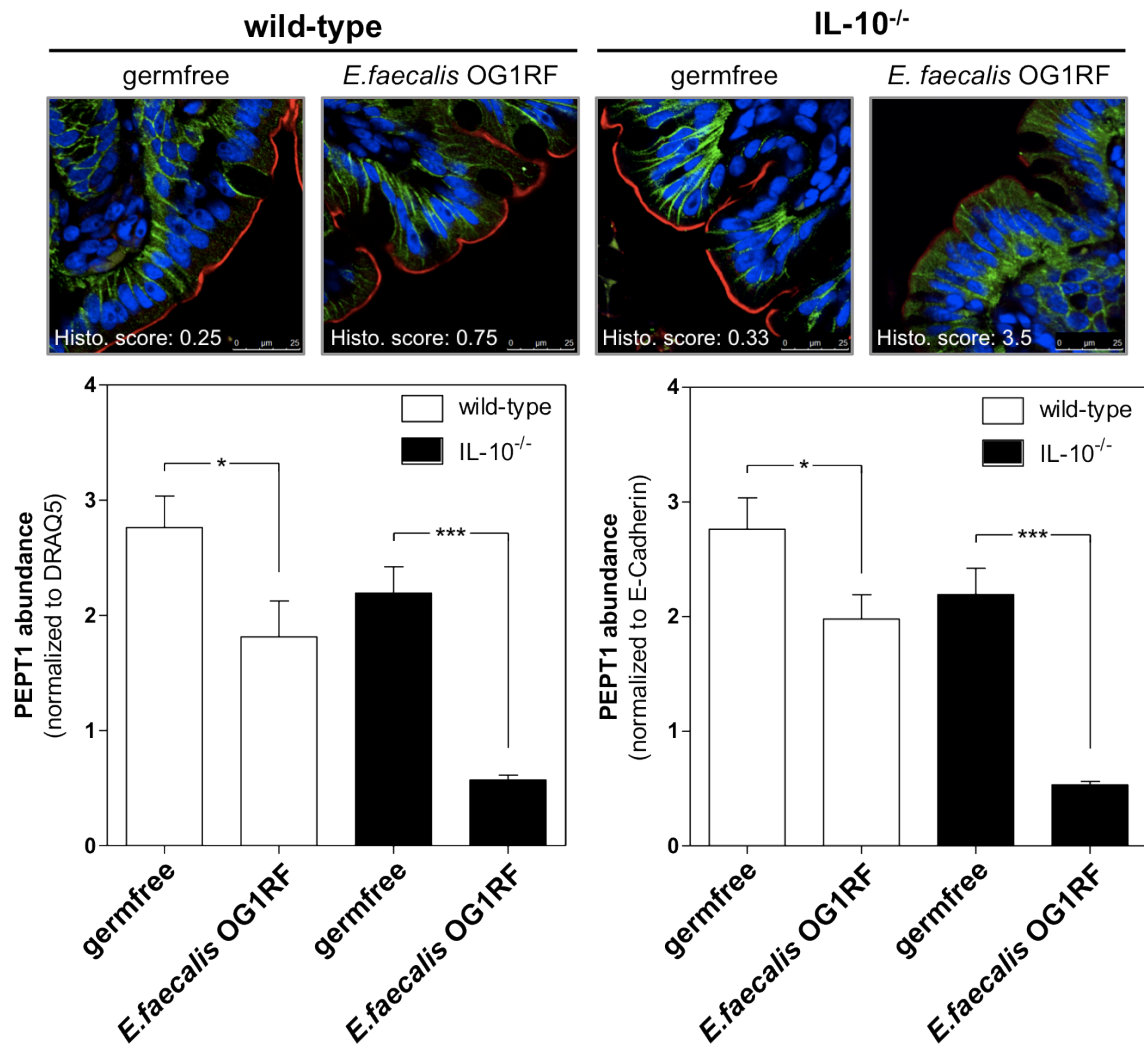
Figure 23. IF staining of PEPT1 in wild-type and IL-10$^{-/-}$ mice housed under germfree conditions or after mono-association with the *E.faecalis* strain OG1RF.
The histological score (Histo. score) ranged between 0 (noninflamed) and 4 (severe inflamed). Quantification of PEPT1 expression revealed significantly reduced PEPT1 levels in *E.faecalis* OG1RF monoassociated mice as compared to germfree controls. Data are the means ± SEM of n=3-5 animals (*$p<0.05$, ***$p<0.001$).

Furthermore, we assessed PEPT1 expression in IL-10$^{-/-}$, IL-10XTLR2$^{-/-}$ and IL-10XTLR4$^{-/-}$ mice at 1, 8 and 16 weeks of age. As demonstrated before before by Messlik A et al.[129], histopathological analysis of IL-10$^{-/-}$ mice revealed moderate colonic inflammation at the age of 8 and 16 weeks in these mice. This was also shown in IL-10XTLR2$^{-/-}$ double knock-out animals, whereas, IL-10XTLR4$^{-/-}$ mice were protected from inflammation with unaltered tissue pathology in colon.

With respect to PEPT1 expression, the protein was clearly detectable in all genotypes at week 1, indicating no genotype-specific influence on basal PEPT1 expression. However, at week 8 IL-10XTLR2$^{-/-}$ mice showed reduced PEPT1 levels while no changes where observed in IL-10$^{-/-}$ or IL-10XTLR4$^{-/-}$ mice the intermediate time point.

At week 16, PEPT1 was no more detectable in colonic tissues obtained from IL-10XTLR2$^{-/-}$ mice and only tiny amounts (significantly reduced by $p<0.001$) could be

found in IL-10$^{-/-}$ tissues. In the absence of tissue pathology, PEPT1 seemed unaltered in colonic tissues of IL-10XTLR4$^{-/-}$ mice as compared to wild-type controls (**Figure 24**). Our findings on inflammation states are in accordance with a previous report showing histologically a moderate inflammation in IL-10XTLR2$^{-/-}$ mice as compared to IL-10$^{-/-}$ mice and also that IL-10XTLR4$^{-/-}$ mice are protected from inflammation. Quantification of colonic PEPT1 abundance on week 16 revealed significantly reduced PEPT1 levels in IL-10$^{-/-}$ and IL-10XTLR2$^{-/-}$ mice as compared to germfree housed IL-10$^{-/-}$ mice (**Figure 24 B**).
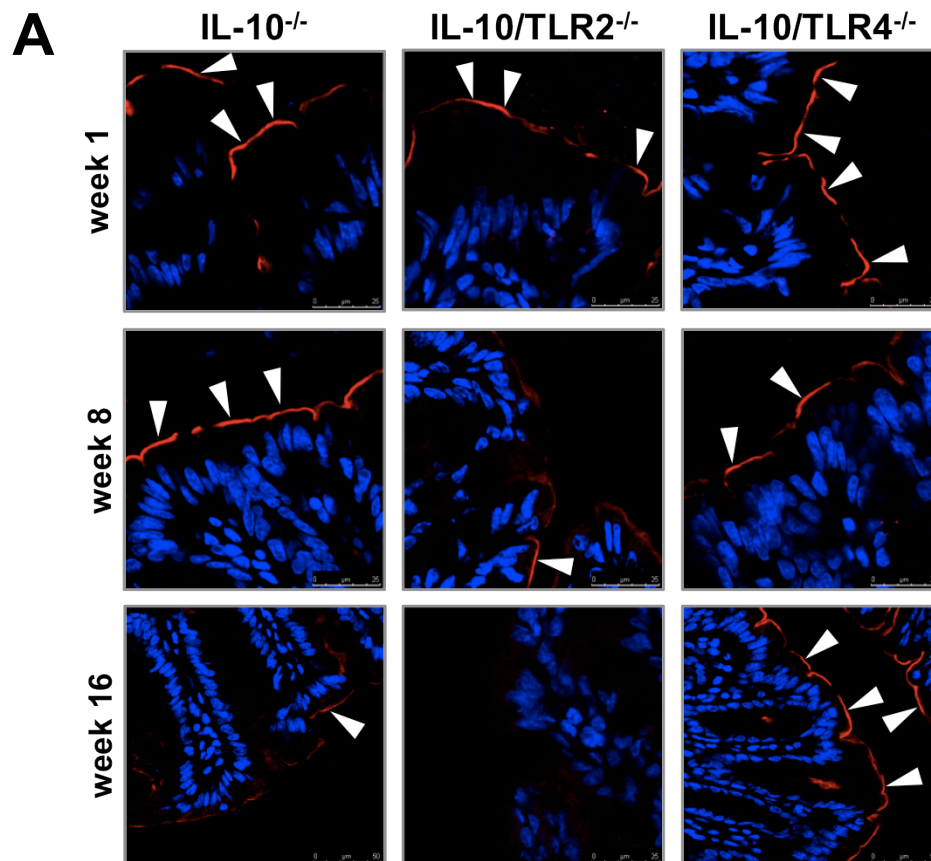
Figure 24. IF of PEPT1 in distal colon of IL-10$^{-/-}$, IL-10XTLR2$^{-/-}$ and IL-10XTLR4$^{-/-}$ mice.
(A) Immunofluorescence stainings of PEPT1 in IL-10$^{-/-}$, IL-10XTLR2$^{-/-}$ and IL-10XTLR4$^{-/-}$ mice at different ages (upper row, 1 week, middle row, 8 weeks and lower row, 1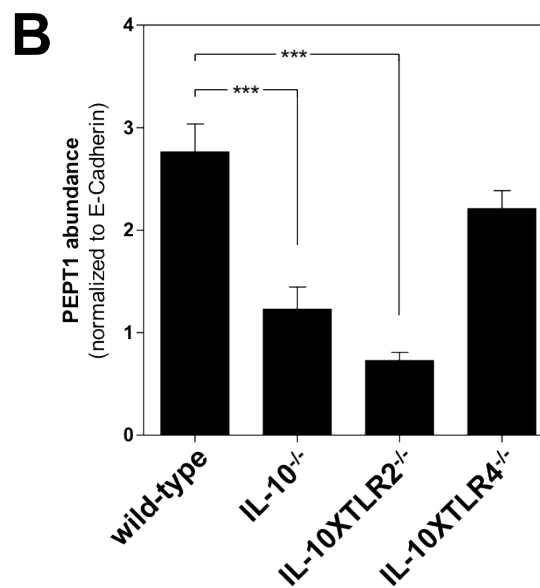6 weeks). PEPT1 is expressed in all genotypes at week one, slightly decreased in IL-10XTLR2$^{-/-}$ mice on week 8 but unchanged in IL10$^{-/-}$ or IL-10XTLR4$^{-/-}$ at that point of time. On week 16 no PEPT1 was detectable in colon from IL-10XTLR2$^{-/-}$ mice and only minimal levels in IL-10$^{-/-}$ mice. Whereas, colon from IL-10XTLR4$^{-/-}$ mice showed regular PEPT1 expression. DRAQ5 was used as nuclear counterstain.
(B) Quantification of PEPT1 expression revealed significantly reduced PEPT1 levels in IL-10$^{-/-}$ and IL-10XTLR2$^{-/-}$ mice at 16 weeks of age. n=5, **p<0.01.
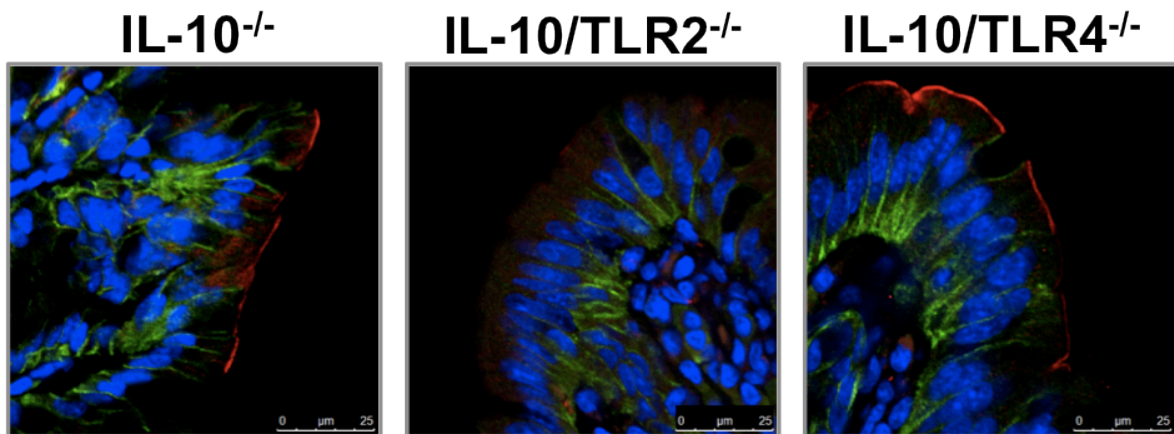
Figure 25. IF staining of distal colonic tissues of IL-10$^{-/-}$, IL-10/TLR2$^{-/-}$ and IL-10/TLR4$^{-/-}$ mice at the age of 16 weeks.
PEPT1 is stained in red, E-Cadherin is stained in green and nuclei blue. E-Cadherin expression remained obviously unaltered in all genotypes and was used for quantification.

4.9 PEPT1 expression in Rag2$^{-/-}$ mice

The Rag2$^{-/-}$ mice are a adoptive T cell transfer model. These mice lack the adaptive immune response caused by the knock-out of an essential B and T cell receptor. Colonic inflammation in Rag2$^{-/-}$ mice is induced by injecting naive CD4+ T cells intraperitoneally into the recipient Rag2$^{-/-}$ mice. The injected T cells travel to the gut where they experience the gut antigens and responde with activation and production of cytokines that initiate and promote intestinal inflammation.

Rag2$^{-/-}$ and Rag2$^{-/-}$XIL-10$^{-/-}$ double knock-out mice were tested for PEPT1 expression in distal colon after the mice received T cells from wild-type or IL-10$^{-/-}$ mice or just control injections. Rag2$^{-/-}$ mice develop intestinal inflammation as graded by histophological assessment and scoring. Control mice of both, Rag2$^{-/-}$ and Rag2$^{-/-}$XIL-10$^{-/-}$ genotypes did not show signs of inflammation as judged by the histopathology score (0-0.5). These mice show regular PEPT1 expression in distal colon. When Rag2$^{-/-}$ and Rag2$^{-/-}$XIL-10$^{-/-}$ mice were injected with wild-type or IL-10 T cells, the mice developed colonic inflammation and PEPT1 protein expression decreased (**Figure 26**).

The severity of inflammation after T cell injection increases within the following weeks, showing only mild signs of inflammation after one week but pronounced inflammation four

weeks after T cell injection. In Rag2$^{-/-}$ mice injected with wild-type T cells and Rag2$^{-/-}$XIL-10$^{-/-}$ mice injected with T cells from IL-10$^{-/-}$ mice colonic inflammation was most pronounced showing histological disease scorings of 3-4.5, and these mice show very low, if not completely absent, PEPT1 expression,
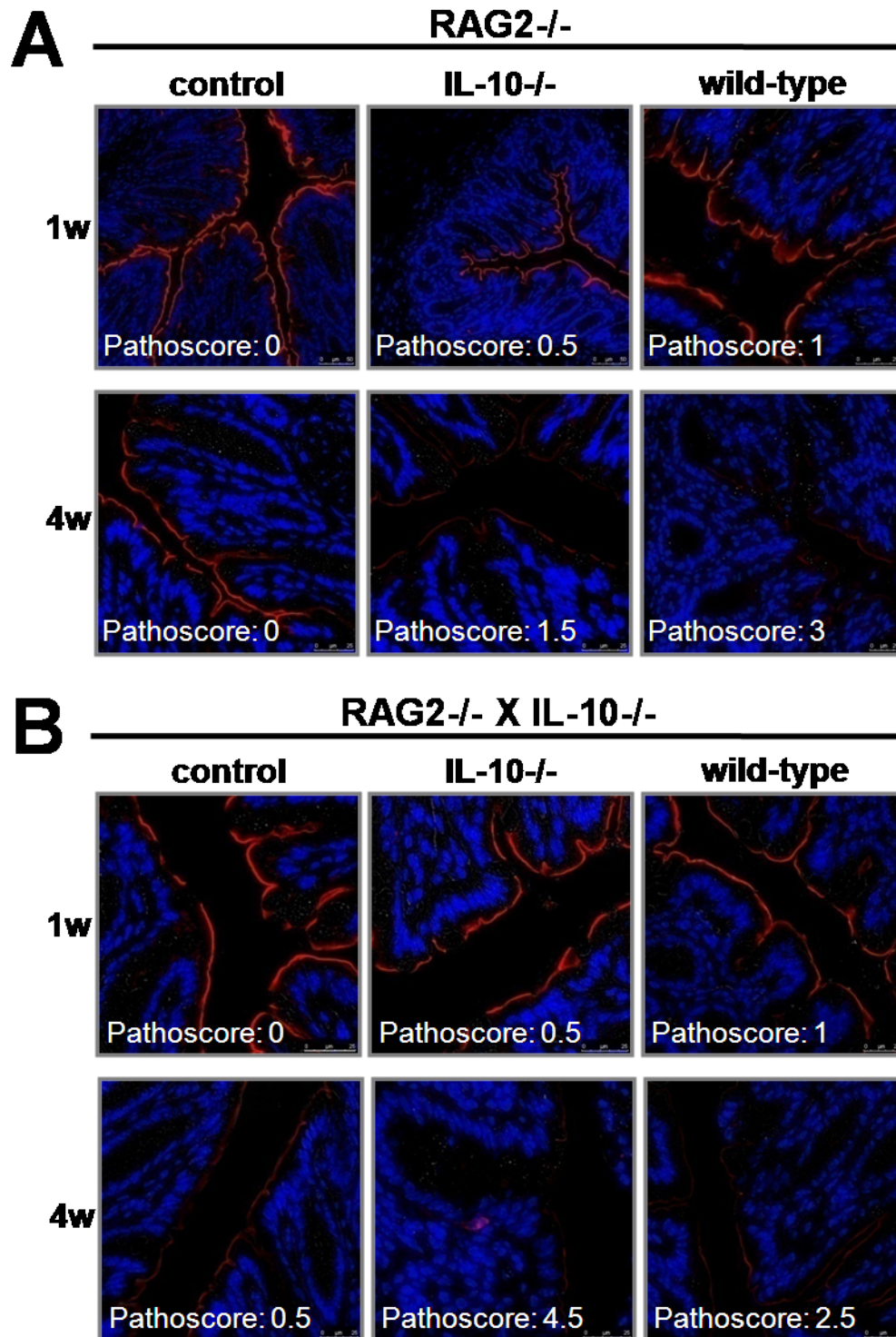
Figure 26. IF staining of distal colonic tissues from (A) Rag2$^{-/-}$ and (B) Rag2$^{-/-}$XIL-10$^{-/-}$ mice after adoptive T cell transfer.
PEPT1 (red) expression was determined one and four weeks after adoptive T cell transfer. DAPI was used as nuclear counterstain. The "Pathoscore" indicates the severity of histological tissue inflammation.

4.10 Susceptibility of *Pept1*^{-/-} mice to DSS-induced colitis

Histological assessement of colonic tissue

A model of chemical induced colitis was used on wild-type and *Pept1*^{-/-} mice to determine whether PEPT1 alters susceptibility or severity to DSS-induced epithelial injury.

Acute colitis was induced in wild-type and *Pept1*^{-/-} mice by adding 2.5% DSS to drinking water for 7 days. Histological analysis of H&E stainings of paraffin embedded tissue sections (6 µm) from proximal and distal colon of wild-type and *Pept1*^{-/-} mice showed a disrupted colonic architecture with crypt distortion, epithelial erosion, water infiltrates and intestinal wall swelling (**Figure 27**).
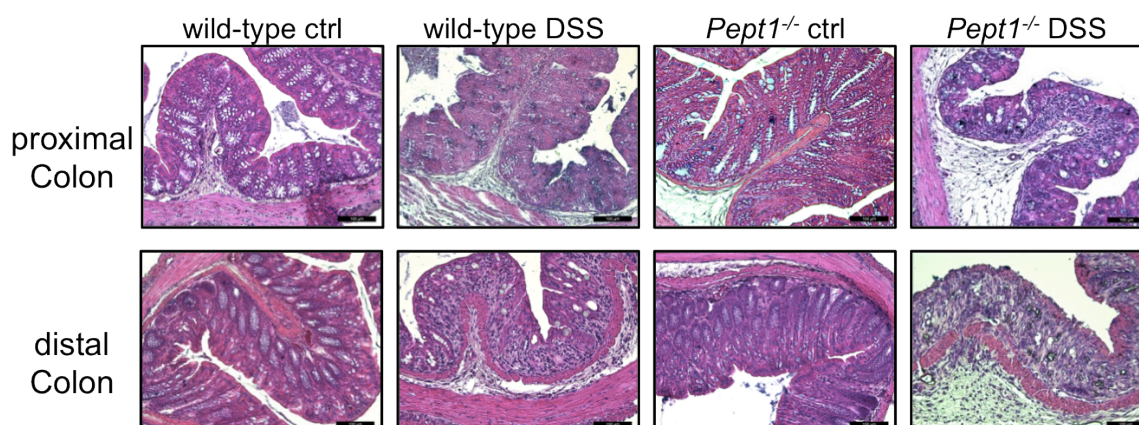
Figure 27. Representative H&E stainings of colonic segments of wild-type and *Pept1*^{-/-} mice. Mice were either treated for seven days with 2.5% DSS or without (ctrl) in drinking water. Histology of proximal (upper panel) and distal (lower panel) colonic tissue from DSS treated mice of both genotypes show disintegrated morphology with intestinal swelling, immune cell infiltration and water inclusions. Scale bars, 100µm.

Clinical parameters measured during DSS administration

In addition to the histological examination, clinical parameters were assessed daily throughout the DSS treatment period. Intestinal discomfort can reduce food and water intake which may also be a reaction to avoid these noxes. Therefore, the amount of food consumed by the mice before and during DSS treatment was recorded daily. At baseline, no differences between wild-type and *Pept1*^{-/-} mice were detectable (4.32 ± 0.26 g/d vs. 4.10 ± 0.17 g/d, n=13, p=0,4892). During DSS treatment the consumed food amount declined significantly in the wild-type (4.32 ± 0.26 g/d vs. 2.58 ± 0.16 g/d, n=8, p<0.0001) and *Pept1*^{-/-} (4.10 ± 0.17 g/d vs. 2.41 ± 0.12 g/d, n=8, p<0.0001) group, however no differences were detectable at any time point when comparing wild-type and *Pept1*^{-/-} groups in the DSS treatment arm or water control groups (**Figure 28**).
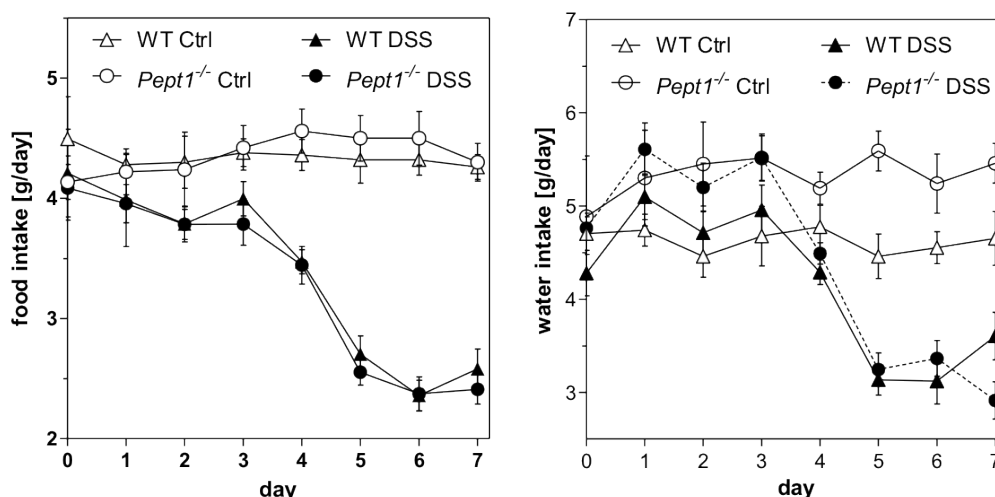
Figure 28. Changes in food (left) and water intake (right) during the DSS treatment period in control and DSS-treated mice.
Left panel: Decline in food intake from day 2 on till the end of the DSS treatment by 40.28% in wild-type and 41.33% in *Pept1*$^{-/-}$ mice. Right panel: Water consumption increased in both DSS treatment groups from baseline to day 3 by 18.94% in wild-type and 15.97% in *Pept1*$^{-/-}$ mice. From day 4 on water intake decreased and was at minimum 25.18% in the wild-type and 38.87% in the *Pept1*$^{-/-}$ group lower as the baseline amount. Means ± SEM are shown (n=3-8 per group).

With respect to water consumption, differences between wild-type and *Pept1*$^{-/-}$ mice were detectable right at the baseline. The wild-type control mice seem to drink less as compared to their *Pept1*$^{-/-}$ littermates. Quantification of the consumed water volumes revealed that the female *Pept1*$^{-/-}$ mice had a significantly higher absolute water intake (4.30 ± 0.10g/d vs. 5.11 ± 0.16g/d, n=20-23, p<0.0001) as compared to the female wild-type mice. The calculation of the water amount relative to the body weight of the mice showed the same significant differences between wild-type and *Pept1*$^{-/-}$ mice (0.188 ± 0.004 g/d vs. 0.216 ± 0.006 g/d, n=19-24, p<0.001) (**Supplemental Figure 8**).

The decreased food and energy intake was associated with the loss of body weight during DSS treatment. However, this may also be caused by energy wasting or by abolished intestinal nutrient absorption. The mean body weight was not different between the wild-type and *Pept1*$^{-/-}$ test groups at baseline (23.04 ± 0.34 g vs. 22.56 ± 0.47 g, n=8, p=0.418) and after 7 days DSS treatment (19.14 ± 0.85 g vs. 18.64 ± 0.47 g, n=5, p=0,613), respectively. The mean weight loss after 7 days DSS administration was 3.9 g in the wild-type and 3.92 g in the *Pept1*$^{-/-}$ group and this relates to nearly 20% weight loss from baseline in both treatment groups (**Figure 29 left**). Beside changes in body weight, stool consistency, stool blood content and general appearance of the mice were assessed daily to calculate the DAI depending on the values of the single parameters (**Figure 29 middle**). The DAI score slightly increased from day 2 on till day 7 with stronger increases from day
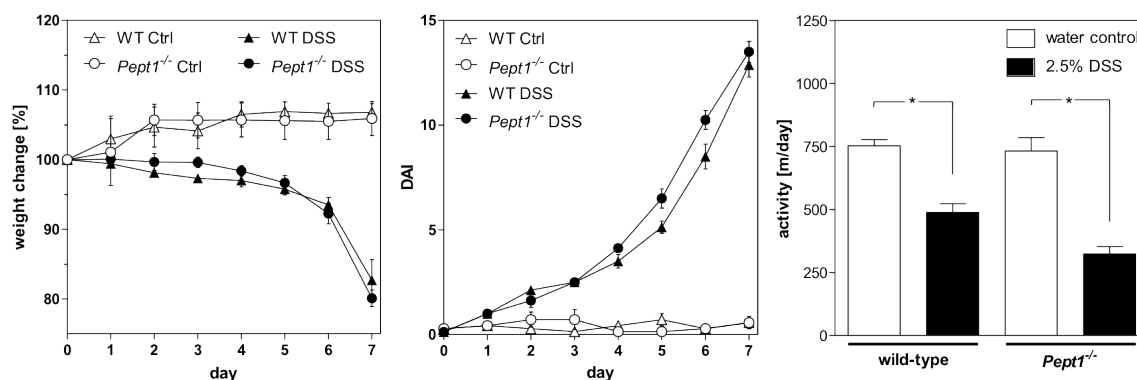
Figure 29. Evaluation of DSS-induced clinical activity.
Changes in body weight (left panel) were assessed daily and show a progressive decline in the DSS treated groups of both genotypes. Mid panel illustrates the clinical disease activity index (DAI) score over time. Four clinical parameters of disease were monitored including weight loss, stool consistency, stool blood content, and appearance to calculate a cumulative DAI score. The right panel depicts the daily activity on day 7 of DSS treatment with decreased activity by 35.11% in the wild-type and 55.74% in the *Pept1*^{-/-} test group both receiving 2.5% DSS as compared to the respective water control groups. No differences occur when comparing the wild-type and *Pept1*^{-/-} genetic background. Means ± SEM are shown (n=3-8 per group). *p<0.05.

5 on reflecting the slow manifestation of the DSS-induced injuries within the first days of treatment and progressive development of the disease during the last 2-4 days. As another parameter, which reflects behavioral changes during DSS treatment, the physical activity level of the mice was measured. At baseline no differences were detectable between wild-type and *Pept1*^{-/-} mice (752.92 ± 24.25 m/d vs. 732.07 ± 52.84 m/d, n=4, p= 0.726). After 7 days of DSS treatment the activity levels decreased significantly in both treatment groups (wild-type 752.92 ± 24.25 m/d vs. 488.58 ± 33.60 m/d, n=4, p<0.0001) and *Pept1*^{-/-} 732.07 ± 52.84 m/d vs. 323.99 ± 28.21 m/d, n=4, p<0.0001) (**Figure 29 right**). Directly after sacrifice, further parameters were assessed to further characterize the severity of DSS-induced injury. As such a marker the colon length of each mouse was measured directly after removal and the results showed significantly shorter colon samples in both DSS treatment groups as compared to the control groups; wild-type (7.41 ± 0.13 vs. 6.51 ± 0.35, n=5, p<0,05) and *Pept1*^{-/-} (7.15 ± 0.08 vs. 6.45 ± 0.20, n=4, p<0.05) (**Figure 30 left**). No differences were detectable when comparing the colon lengths after 7 days DSS treatment or water control between genotypes, wild-type vs. *Pept1*^{-/-} control (7.41 ± 0.13 vs. 7.15 ± 0.08, n=5, p=0.1712), wild-type vs. *Pept1*^{-/-} DSS (6.51 ± 0.35 vs. 6.45 ± 0.20, n=4, p= 0,8710). Another parameter was MPO activity in colonic mucosal scrapings from the test groups. MPO is an enzyme predominantly expressed in neutrophilic cells and is thus used as a surrogate marker for the activation of the innate immune system. The measured colonic MPO activities from DSS treated mice of both, wild-type and *Pept1*^{-/-} groups, were not different as compared to the values of the

corresponding water control groups; wild-type (0.81 ± 0.19 vs. 1.33 ± 0.82, p=0.597), *Pept1*^{-/-} (3.00 ± 1.26 vs. 3.84 ± 0.80, p=0.595) (**Figure 30 right**). However, significant differences could be found between the MPO activity in wild-type and *Pept1*^{-/-} mice after DSS treatment (0.81 ± 0.19 vs. 3.00 ± 1.26, n=4, p<0.05) and water control (1.33 ± 0.820 vs. 3.84 ± 0.80, n=4, p<0.05).
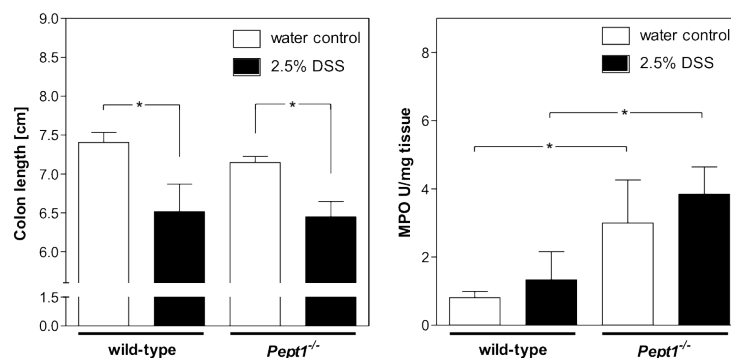
Figure 30. MPO activity and colon length were measured as parameters for inflammatory severity.
Colon length (left panel) as a marker for inflammatory severity showed significantly reduced values in both DSS treated groups compared to their controls. MPO activity (right panel) measured as marker for neutrophil infiltration showed a tendency to increased MPO activity caused by DSS, yet not significant. Unexpectedly, MPO activities were significantly different between the genotypes under control and DSS treated conditions. Means ± SEM are shown, n=3-8 per group, *p<0.05.

PEPT1 in colonic tissue of DSS-treated wild type mice

Distal colonic tissue of wild-type mice showed reduced PEPT1 levels after treatment with DSS. PEPT1 abundance correlates indirectly with disease severity as judged by the DAI (**Figure 31**).
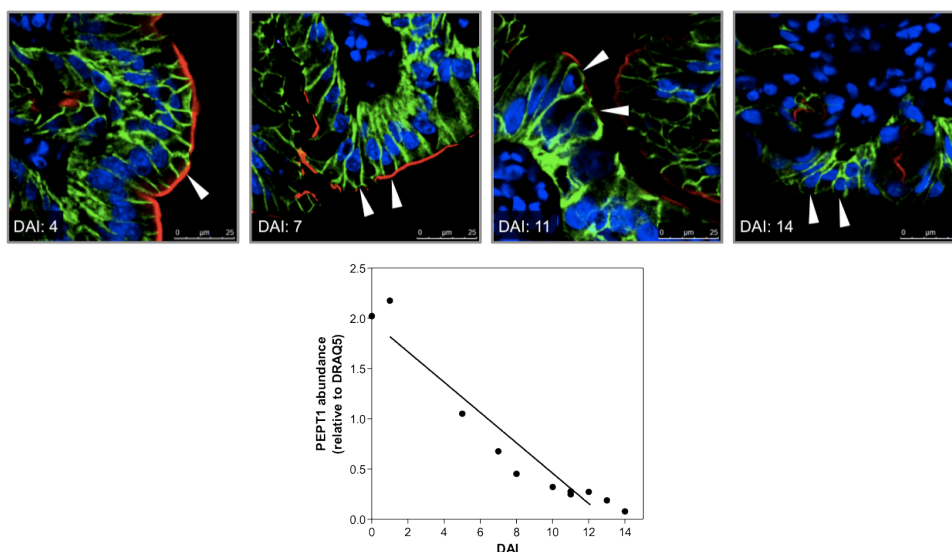
Figure 31. Decreased PEPT1 abundance with increasing DSS-induced disease activity.
Upper panel: IF shows decreased PEPT1 (red) expression with increasing DSS-induced colitis severity as indicated by DAI in wild-type mice. The four images are representative for distal colon of DSS treated mice with increasing DAI from left to right. DRAQ5 was used as nuclear counterstain. Lower panel: Indirect correlation between PEPT1 expression and the DAI, r^2=0.92.

65

Taken all findings together, *Pept1^{-/-}* mice did not show any altered susceptibility towards DSS-induced colitis. Additionally, in distal colonic tissue of wild-type mice, DSS-treatment resulted in reduced PEPT1 expression with increasing disease severity as judged by the DAI.

4.11   PEPT1 in human IBD

Changes in PEPT1 expression during inflammation were also assessed in paraffin embedded distal colon tissue samples obtained from CD and UC patients undergoing surgical resection. PEPT1 expression was markedly reduced in both, active CD and UC (**Figure 32**) and quantification of PEPT1 protein abundance relative to E-Cadherin or DRAQ5 revealed significantly reduced (p<0.001) PEPT1 levels with reduction by 71.48% in UC and 79.22% in CD, as compared to healthy descending colon (**Figure 32 B+C**). At the same time, E-Cadherin expression, used as reference marker, compared to nuclear staining remained unaffected (**Figure 32 D**).
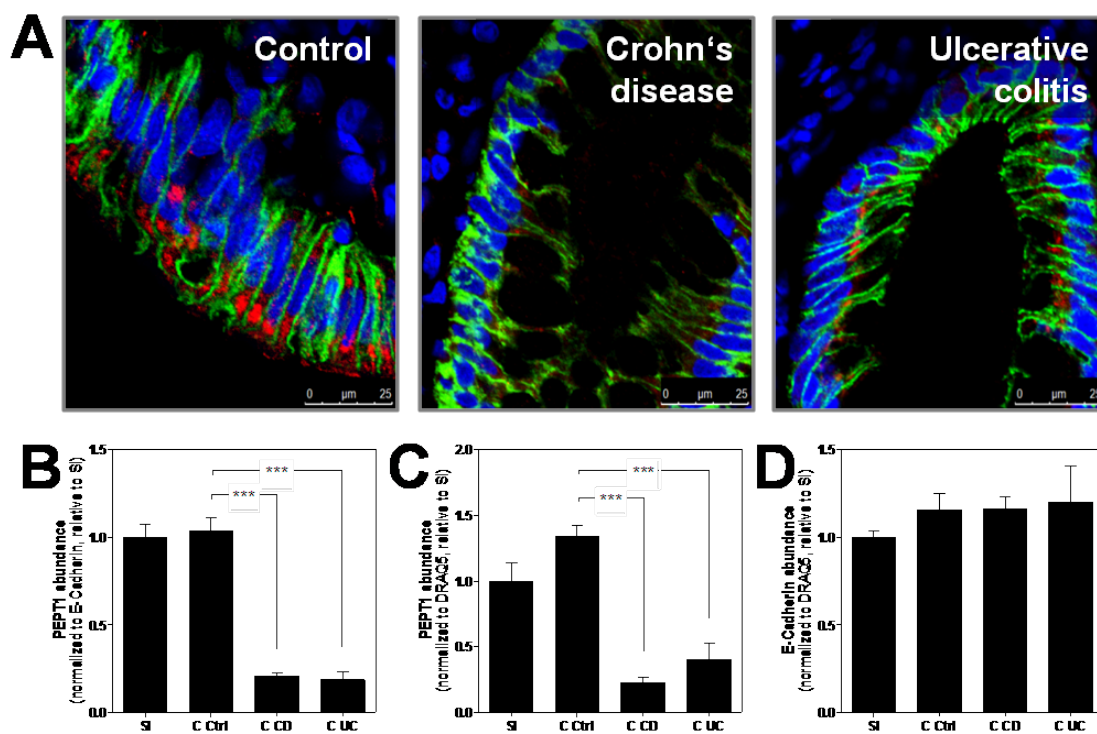
Figure 32. IF and relative PEPT1 abundance in tissue samples of descending colon from patients with active IBD.
(A) Representative IF stainings from colonic sections of a healthy control (left), a Crohn's patient (middle) and a patient with ulcerative colitis (right) demonstrating PEPT1 (red) presence in healthy but markedly reduced expression in tissues with CD or UC. (B-C) Quantification of PEPT1 protein abundance revealed significantly reduced levels in colonic tissues of CD or UC patients compared to healthy controls. E-Cadherin (green) or nuclei staining (blue) were used as references for normalization. (D) No differences in E-Cadherin expression were found between any condition when compared to nuclear staining. SI, small intestine, C, colon, Ctrl, control, CD, Crohn's disease, UC, Ulcerative colitis. Data are the means ± SEM of n=3-8 samples per group (***p<0.001).

5 DISCUSSION

The objective of the present study was to systematically assess the expression profile of the peptide transporter PEPT1 in rodent and human intestine in healthy and inflamed states to better define its proposed role in IBD.

5.1 Colonic PEPT1 expression, glycosylation and possible consequences

The data confirmed that PEPT1 is most abundantly expressed in small intestine with highest protein densities and consequnetly also highest transport rates in duodenum and jejunum but lower levels in ileum [2, 45]. Furthermore, a marked crypt-villus gradient was observed for PEPT1, which is also in accordance with previous reports [46, 240]. However, unexpectedly, PEPT1 expression was also detected in healthy colon from mice, rats and humans in distal but not proximal segments. PEPT1 is merely present in the proximal colon but shows fairly high levels in distal colon and rectum. The apparent MW of colonic PEPT1 is higher than in small intestine and this is due to a higher glycan content. Although several other transporter proteins were found to be expressed in small intestine as well as colon, like SGLT1, GLUT1, NHE3 and DRA, for none were different MWs in different intestinal regions reported [53, 54].

Glycosylation is one important co- and post-translational modification of proteins, whereby glycans (sugars) are covalently attached to specific amino acid residues of proteins. All cells, from bacteria to human, are covered by glycans. Glycosylation takes place on nascent protein chains when they are passing through the ER and the Golgi complex and it is necessary for correct translational processing, accurate protein folding and stability, exact sorting and trafficking of membrane proteins [241]. Glycans can be attached on N-, O- and C-residues. N-glycosylation takes place at asparagine residues where core glycans consisting of 14 sugars are co-translationally attached to newly synthesized polypeptides in the lumen of the ER. The attached glycan tree becomes modified subsequently in the Golgi apparatus by enzymatic modification, the so called trimming, which yields a wide diversity of glycan structures [242]. The main glycan structures are composed of N-acetyl-D-glucosamine (GlcNAc), D-mannose, D-galactose, L-fucose and sialic acid also known as neuraminic acid (N-acetylneuraminic acid) [243]. In epithelial cells the glycocalix forms an approximately 0.3 μm thick layer on the surface, represented by an array of highly diverse glycoproteins and glycolipids. These glycosylated structural elements may serve as receptors and form the primary site for bacterial adhesion. For example, the carcinoembryonic antigen-related cell adhesion molecule 6 (CEACAM6), found on the apical surface of ileal epithelial cells serves as a receptor for adherent-invasive *Escherichia coli* in CD [244]. For colonisation and invasion into the epithelium, bacteria commonly interact with glycan structures of the host glycocalyx [245]. This

attachment occurs through binding of bacterial lectins to the corresponding glycosylated proteins on the host cells [86]. However, the adherence of commensals or probiotic bacteria to IEC has yet not been characterised for a large number of bacterial species. Nevertheless, selected probiotic *Lactobacillus* species, that have the ability to adhere to IEC, have been shown to directly communicate with the epithelium and rapidly induce production of mucins and thereby may prevent the adherence of enteropathogens like EPEC and/or render the susceptibility to IBD [246]. In this context it is interesting to note that the adherence of EPEC was also shown to be markedly reduced *in vitro* in PEPT1 expressing cells as compared to non-PEPT1 expressing cells [69].

Amongst the glycoprotein structures in the intestine, mucins are the most dominant entities. They are highly glycosylated and have the ability to form mesh-like gels and are part of a physical – yet permeable gel layer that prevent direct contact of noxious entities but allowing the exchange of gases and nutrients with the underlying epithelium. Thereby mucins play a pivotal role in the maintanance of an intact intestinal epithelial barrier [247]. Mucins can be subdivided into secretory and membrane-bound forms. Secreted mucins are known to contribute to the formation of the mucus gel, whereas the function of membrane bound mucins is not well understood [248]. In the context of IBD, the mucus layer in UC patients was found to be thinner than that in healthy controls and this seems to be related to impaired synthesis and secretion of MUC2 in the active stage of UC. This reduction in MUC2 secretion makes the colonic mucus barrier less protective [249]. By modifying glycosation, the gut microbiota can further influence this barrier against pathogens, as shown in germ-free rodents in which the mucus layer is reduced by half, is less stable, and has an altered glycosylation profile as compared to a conventionally kept host [250, 251].

With the demonstration of an altered glycosylation pattern of the colonic PEPT1 protein, the PEPT1 related glycan structures may determine the ability for selected bacteria to interact with the mucosal surface. As some studies suggested PEPT1 to be responsible for allowing or preventing the adhesion of certain bacteria, the distinct presence or absence of particular glycan structures may modulate – beside other conditions – bacterial colonization in different regions of the intestine along the colon from proximal to rectal [252, 253]. Studies on the glycocalix composition in health and disease could therefore be a rewarding new science field.

Despite the known primary function of small intestinal PEPT1 in peptide uptake for amino acid delivery, colonic PEPT1 appears to play a different role and that could relate to interaction with commensal or pathogenic bacteria.

In this context, the differential colonization with bacteria along the colon may need to be considered. Certain metabolites, including phenolic compounds or products of

degradation of aromatic amino acids as fermentation products were found in colon in change in concentrations from proximal to distal. For example, concentrations of phenolic compounds were more than fourfold higher in the distal colon as compared to the proximal colon [254]. Additionally, saccharolytic activity was found to be higher in proximal colon as compared to distal colon whereas towards the distal colon proteolytic activity increases [252]. As shown by Macfarlane GT et al., products of protein fermentation, such as ammonia or branched-chain fatty acids, progressively increase from ascending to descending colon [252]. The fecal pH increases in similar fashion from ascending to descending colon, likely due to the accumulation of SCFA or other bacterial metabolites. As PEPT1 requires a proton gradient, its occurrence in the more acidic milieu of distal colon offers optimal conditions for PEPT1 transport function. In this context, PEPT1 might also serve as a sensor of luminal pH. Furthermore, the pH differences along the colon are likely to have a direct influence on the bacterial colonization. Here, PEPT1 might be involved – beside modulating bacterial attachment – in pH regulation and might therefore be one major factor to regulate bacterial colonization via a second route. Surprisingly, the NHE3 exchanger was found to be expressed in the colon but in inverted fashion from PEPT1. So colonic PEPT1 function seems not like in the small intestine be coupled to NHE3 [17, 18]. The distinct expression of NHE3 in proximal but not in distal colon has been linked to the greatest capacity for Na^+ and water absorption in this area, and much of this is probably associated with SCFA absorption [53, 255]. The mucosal pH in proximal colon from rats and mice was found to be lower as compared to the distal colon [256]. That might be linked to the absence of PEPT1 and the presence of NHE3 in proximal colon and the other way round in distal colon. The more acidic milieu of the proximal colon could be utilized to sustain SCFA absorption via both, apical $SCFA/HCO_3$ exchange and nonionic diffusion of SCFAs [257].

In addition to SCFA absorption, the perpetuation of stool acidity along the proximal colon would tend to favour or curtail growth and fermentative activities of certain bacterial species in this segment [253]. And bacterial colonization was shown to be not only altered by pH but as well by peptide availability, as tested *in vitro* using casein hydrolysate and peptone water [253]. Differences in PEPT1 expression between proximal and distal colon might therefore be interesting to study further the interplay between host and commensal bacteria.

5.2 Detection of PEPT1 by Western Blots

Beside the detected differences in the MW of PEPT1 between small intestine and colon based on different glycosylation states, several studies using different ABs, in different species have detected PEPT1 in different MW ranges. Initially, Fei YJ et al. detected the rabbit PEPT1 protein expressed in *Xenopus laevis* oocytes by WB at a MW of

approximately 71 kDa [2]. And rPEPT1 expressed *in vitro* in the rabbit reticulocyte system showed a band at approximately 75 kDa [5]. In contrast, isolated BBMV preparations from rat intestine and kidney yield bands of 90-95 kDa, when anti-rPEPT1-specific ABs were used [33, 62]. In another study on endoscopic tissue samples from humans, WBs showed a PEPT1 at approximately 95 kDa, when a commercially hPEPT1 AB was used [258]. Similar to that, the ABs used in the current study, directed against rPEPT1 and hPEPT1, both yielded bands for small intestinal PEPT1 at a MW of approximately 95 kDa. In contrast, other ABs against hPEPT1 directed against the 20 amino acids of the C-terminus of hPEPT1 have been described by Merlin D et al. and Ziegler TR [48, 50]. But both ABs were shown to yield a band at a MW of 80–85 kDa. However, no WB from any tissue sample so far has been published which would allow the exact MW to be obtained with a reference to a MW ladder. Despite this lack of information from tissues, the anti-hPEPT1 AB used by the group of Merlin D et al. revealed a band at approximately 100 kDa when applied to Caco2-BBE cells [29]. In addition, with the same AB, Dalmasso G et al. could not detect a PEPT1 band when the anti-hPEPT1 AB was used on intestinal tissue from wild-type mice, while PEPT1 could be detected in colonic tissue from transgenic *villin*-hPEPT1 mice [198]. The anti-hPEPT1 AB used for the WBs in this study was raised against the carboxyterminal 20 amino acids of the hPEPT1 protein [50], its ability to detect also mPEPT1 has never been demonstrated and seems to be limited as the 20 amino acids of the C-terminal sequence of mPEPT1 share only 30% similarity with the C-terminus of hPEPT1 (**Figure 33 B**). The AB specificity may therefore be a prime reason for the controversial findings on PEPT1 expression.

Another described rabbit anti-hPEPT1 AB against the amino acids 366–600 of hPEPT1 is proposed to recognize mouse and rat PEPT1 [12]. However, comparison of the mouse and rat PEPT1 amino acid sequences with the human sequence (for the amino acids 366-600) revealed only 72% sequence identity in comparison to the mPEPT1 sequence and 73% identity to the rPEPT1. As appropriate negative controls are not presented and none of the presented WBs depicts a MW marker, the specificity of the used AB remains questionable.

The AB used here for mouse samples was generated against the 19 amino acids of the C-terminus of rPEPT1. As both C-termini – that of rat and that of mouse – share 94% amino acid sequence homology (**Figure 33 A**) and no PEPT1 reactivity was found in intestinal samples from *Pept1$^{-/-}$* mice, our AB has been proved to be specific for detection of mPEPT1. This mouse-specific PEPT1 AB applied to human samples resulted in no specific staining. Therefore, a second custom-made AB for the specific detection of hPEPT1 protein was obtained. This AB targets the 19 amino acids of the hPEPT1 C-terminus and yields a MW band at approximately 95 kDa in human small intestine.

A
Rat vs. mouse C-terminus

```
Score = 58.7 bits (131), Expect = 1e-14
Identities = 17/18 (94%), Positives = 18/18 (100%), Gaps = 0/18 (0%)
Query    1       VGKENPYSSLEPVSQTNM 18 ——— rat sequence
                 +GKENPYSSLEPVSQTNM
Sbjct    692     IGKENPYSSLEPVSQTNM 709 ——— mouse sequence
```

B
Human vs. mouse C-terminus

```
Score = 12.5 bits (22), Expect = 255
Identities = 7/20 (35%), Positives = 7/20 (35%), Gaps = 8/20 (40%)
Query    5       KSNPYFMSGAN----SQKQM 20 ——— human sequence
                 K NPY        SQ  M
Sbjct 692        KENPY----SSLEPVSQTNM 707 ——— mouse sequence
```

Figure 33. Comparison of the amino acid homology of PEPT1 AB epitopes between different species.
(A) The PEPT1 AB used here is directed against the C-terminus of rPEPT1 but can also be used for detection of mPEPT1. The targeted epitop shows 94% similarity between the species. (B) The PEPT1 AB used by Merlin D et al. is directed against human C-terminus but is also used for detection of mouse PEPT1. The targeted epitop shows 35% similarity between the species.

5.3 Relevance and regulation of colonic PEPT1 expression in health and IBD

Although peptides are constantly produced by protein degradation and may also be present in larger quantities in the contents of the large intestine, the physiological importance of PEPT1 in distal colon and rectum in handling of di- and tripeptides remains to be determined. PEPT1 was recently shown to contribute to electrolyte and water transport in the small intestine [61] and this role was also demonstrated here with an increased water content in feces of $Pept1^{-/-}$ mice. Regardless of this function, peptides presented to PEPT1 in the large intestine may also include the proteolytic products of peptidoglycans such as MDP, fMLP and triDAP that were reported to utilize PEPT1 for uptake [29, 181, 189]. Moreover, the demonstrated effects of these peptides on NOD1, NOD2 and neutrophil activation suggest that PEPT1 could act as an amplifier of inflammation by delivery of these proinflammatory compounds to tissues and even more so, when PEPT1 expression is increased in IBD. In Caco-2 cells expressing PEPT1 it has been shown that exposure to interferon-γ and TNF can increase PEPT1 expression levels (6). As intestinal inflammation is generally associated with elevated levels of a variety of cytokines and chemokines it is reasonable to assume that their action increases PEPT1 tissue levels. However, in TNF$^{\Delta ARE/WT}$ mice which display constitutively increased TNF levels [237] we did not find any evidence for increased colonic PEPT1 levels. As the most surprising finding and contradicting other reports [50, 52] all of our three animal models reminiscent of human CD and UC with different disease severities and different sites of

lesions (30, 33, 36) revealed in all cases a reduced PEPT1 expression. Protein levels in distal colon decreased significantly in association with the severity of the disease based on histological scoring. Despite conservation of tissue structural integrity as judged by normal villin immunostaining, PEPT1 protein levels were either markedly reduced or immunoreactivity was completely absent. Since tissues from patients with active UC or CD were reported to possess elevated levels of PEPT1 mRNA (14) or protein (15), we also investigated colonic samples of clinically and histologically phenotyped patients with active CD and UC. PEPT1 expression profiled by Western blot analysis and IF staining revealed in all cases decreased levels compared to reference proteins and healthy control tissues.

Since we consistently observed reduced PEPT1 levels or even its absence in apical membranes of colonic samples from the murine IBD models or human IBD samples, the question arises how these contradictory findings can be explained. It needs to be emphasized that increased PEPT1 protein expression levels in IBD samples has only been reported once by immunohistochemical staining for human PEPT1 in one UC and one CD sample without specification of the origin (site of collection) of the samples [50]. In a second study on IBD biopsies, *Pept1* was only assessed on the mRNA level [49]. So far, both reports have never been confirmed or followed up on larger and more representative cohorts of IBD patients. As in both studies information on the exact site of sampling of the colonic biopsies is missing, it is difficult to judge what the data published really mean taken into account that we observed striking differences in PEPT1 expression level in proximal and distal colon in animals and humans.

In the study by Wojtal KA et al. not only *Pept1* but also other intestinal transporters like *ENT1*, *OATP4A1* or *OCTN2* were reported to be up-regulated during inflammation [49]. So maybe the results follow another undiscovered algorithm possibly implemented by the tissue inflammation or just due to methodological weekness by using only *Villin* as single references gene, which might be differentially expressed in health and inflammation. In the study by Wojtal KA et al. *Pept1* was not only measured in colonic IBD samples but also in small intestinal samples during inflammation. And here, no significant changes in *Pept1* levels from CD patients were observed [49].

Of whether PEPT1 is involved in colonic inflammation is currently hard to judge. Although its ability to transport bacterial peptides has been shown in several studies [27, 29, 189], the functional consequences *in vivo* and its role in the development of intestinal inflammation, has therefore to be clarified.

Whether PEPT1 has indeed some immune-modulatory functions in small intestine and colon is also uncertain. PEPT1 was shown to be up-regulated *in vitro* by EPEC and the presence of PEPT1 resulted in significantly decreased EPEC adherence suggesting that

the protein may contribute to host defense responses to EPEC infection [69]. In light of our current findings of a basal PEPT1 expression in distal colon one could speculate that PEPT1 may contribute to host colonization by pathogens. In this context it is interesting to note that it was shown in *in vivo* studies that an infection by the murine pathogen *c. rodentium* induced colonic PEPT1 expression and that transgenic *villin*-hPEPT1 mice exhibited a decreased *c. rodentium* colonization, neutrophil accumulation and proinflammatory cytokine expression (IL-1β, IL-6, IL-12, TNF-α and IFN-γ) in the colon [69]. As differences in the response to *c. rodentium* infection occured between wild-type and transgenic *villin*-hPEPT1 mice, different PEPT1 isoforms seem to have differential effects during *c. rodentium* infection, but the molecular mechanisms leading to these differences are still unknown. But, PEPT1 presence seems to protect the host against pathogenic colonization. PEPT1 regulation was also shown in response to the presence of the harmless probiotic bacterium *LP*, which can attenuate colitis in IL-10$^{-/-}$ mice [51, 193]. But despite an upregulation, *LP* prevented the increase in colonic PEPT1 expression [51]. From the present findings that PEPT1 is expressed in IL-10$^{-/-}$ mice and decreases with increasing colitis severity, and the rather poor quality of the WB and IF data provided by Chen HQ et al. interpreting these findings is essentially impossible.

Microorganisms are of course not only present in colon, but also in the small intestine. Although the small intestinal microbial biomass ranges between 10^3 cells/ml in duodenum to 10^8 cells/ml in terminal small intestine and is thus at least thousand times lower as compared to the 10^{11} cells/ml in the colon [259], bacterial products like fMLP or MDP should be present in considerable amounts also in the small intestine to elicit a host response that could be mediated by PEPT1. In this context it is important to note that it was shown *in vitro* that fMLP has antiinflammatory properties in physiological doses of 10-100 nM [260]. As shown by Carlson RM et al., fMLP mediated, by a mechanism involving the physiological expression of heat-shock protein 27 and TNF-α, a desensitation of NF-κB and subsequent decreased expression of proinflammatory cytokines [260]. As PEPT1 is expressed at high levels in small intestine, PEPT1 might play as a regulator of small intestinal homeostasis.

An interesting question is, what factors control PEPT1 expression and in turn control its function in relation to bacteria interaction. For example, PEPT1 upregulation was shown by the SCFA butyrate [68]. Dalmasso G et al. demonstrated that treatment of human intestinal epithelial Caco2-BBE cells for 24 h with 5 mM butyrate, increased PEPT1 mRNA and protein expressions and activity significantly. The same effects were found *in vivo* when mice were supplemented with 5 mM butyrate in drinking water. From these data it was concluded that butyrate enhances PEPT1 expression and function in mouse colon. However whether any supplemented butyrate will reach the colon to elicit these effects is

questionable. Butyrate is absorbed by anion exchange mechanisms and by non-ionic diffusion and this will take place in the small intestine [257, 261-263]. Whatever can reach the colon will most likely not change signifcantly the SCFAs levels with butyrate concentrations ranging between 10 and 15 mM [264, 265]. SCFAs including butyrate are of course produced by bacterial fermentation of non-digestable carbohydrates. And, if butyrate would be crucial for controlling colonic PEPT1 expression, the absence of intestinal bacteria in germfree animals should demonstrate that the lack of buytrate alters PEPT1 expression. The findings collected here from germfree mice revealed PEPT1 surface expression levels not significantly different to conventional animals serving as controls. Thus, a butyrate-effect on basal colonic PEPT1 expression might only be – if at all existing – marginal. However, Dalmasso G et al. linked the butyrate–induced PEPT1 expression with inflammation. As butyrate metabolism is impaired in colonocytes during intestinal inflammation leading to butyrate accumulation [191], they proposed that this could be responsible for increased PEPT1 expression during colonic inflammation.

Other factors that may regulate colonic PEPT1 expression, are proinflammatory cytokines like TNF-α or IFN-γ. In 2003 Buyse M et al. described that IFN-γ increases hPEPT1 functions in Caco2-BBE cells [187]. IFN-γ increased peptide uptake by PEPT1 in a dose- and time-dependent manner. However, IFN-γ seemed not to affect hPEPT1 expression at the mRNA and protein levels, but seemed to affect intracellular pH leading to an enhanced electrochemical gradient across the apical plasma membrane which is the driving force for PEPT1 transport. In 2006 the Merlin group published data about increased Gly-Sar uptake in Caco2-BBE cell monolayers with increased total and apical membrane protein expression of PEPT1 in response to TNF-α and IFN-γ treatment. This of course contradicted their own previous findings [12]. Their explanation of the observed differences was that a 10-fold higher IFN-γ concentration was used in the second study, to get a response on protein level. In our animal study with the TNF$^{\Delta ARE/WT}$ mice which have increased TNF-α levels, we did not find any evidence for differences in PEPT1 expression in colon. TNF$^{\Delta ARE/WT}$ mice were studied at different ages, as the severity of inflammation develops progressively. As PEPT1 was reported to be upregulated by TNF-α, TNF$^{\Delta ARE/WT}$ mice should not only show constitutive high TNF-α levels but also constitutive high PEPT1 levels. That was not found at any observed timepoint in any part of the TNF$^{\Delta ARE/WT}$ mice intestine. Beside the TNF$^{\Delta ARE/WT}$ mice with constitutive high levels of the proinflammatory cytokine TNF-α, IL-10$^{-/-}$ mice with a lack of the anti-inflammatory cytokine IL-10 were investigated. IL-10$^{-/-}$ mice are a model of human colitis, as these mice spontaneously develop a severe enterocolitis in the presence of microflora but not when housed under germfree conditions [238]. However, PEPT1 expression was found to be not different in germfree IL-10$^{-/-}$ as compared to germfree wild-type or conventionally housed wild-type

controls. And during inflammation, PEPT1 was down-regulated in IL-10$^{-/-}$ mice. PEPT1 down-regulation was also found in inflamed distal colon of IL-10XTLR2$^{-/-}$ double-knockout mice. PEPT1 was also studied in a T cell transfer model of colitis, the Rag2$^{-/-}$ mice. These mice are a specific model of T cell-based colitis pathogenesis, but do not show any differences with respect to decreased PEPT1 expression in distal colon during inflammation. Finally, the DSS-induced colitis model was applied on wild-type and *Pept1$^{-/-}$* mice to study whether intestinal barrier disruption by DSS causes different effects on inflammation severity in these mice. But no differences were found between wild-type and *Pept1$^{-/-}$* mice.

It should also be addressed that the Merlin group reported recently that colonic hPEPT1 expression in *villin*-hPEPT1 and *actin*-hPEPT1 mice leads not to colonic inflammation under basal conditions. Our findings in addition also suggest that colonic PEPT1 seems not to be a strong factor in promoting inflammatory processes.

5.4 Species differences of colonic PEPT1 expression

As a surprising finding, we observed striking differences in PEPT1 expression respectively its distribution in colonocytes between apical membrane and intracellular compartments. Samples from human and rat colon displayed scattered apical staining but prominent intracellular *cis*-Golgi associated immunoreactivity whereas small intestinal samples only revealed brush border membrane staining for PEPT1. In the three mouse strains we studied, PEPT1 was only found in the apical membrane in colon. Although it cannot *a priori* be excluded that differences in the microbiota contribute to those species-differences, germ-free mice revealed the same staining (in intensity and localization) as seen in conventionally housed mice suggesting that species rather than the gut microbiota defines the differences. In this respect, our data suggest that rats rather than mice may be closer to humans and may be more useful in assessing colonic functions of PEPT1 and its role in IBD. Further studies are needed to define these species-dependent differences in PEPT1 trafficking and localization. In *rab8* gene KO mice [266] it was shown that this small GTP-binding protein controls PEPT1 apical membrane localization that also involves protein-protein interactions via PDZK1 [267]. PEPT1 can form protein complexes important for trafficking but also for functional coupling, as proposed in case of NHE3 [17]. Trafficking of PEPT1 within the Golgi and to the plasma membrane could therefore be regulated differently in mice and humans. Whether this contributes to different disease susceptibility in IBD needs to be defined.

In summary, we here demonstrate that PEPT1 is expressed at considerable levels in healthy distal but not proximal colon in mice, rats and humans. We did not find any evidence for increased PEPT1 protein levels in intestinal inflammation as previously proposed, neither in different murine models of intestinal inflammation nor in tissues of

humans with active CD and UC. In contrary, PEPT1 protein levels were consistently decreased or the protein was even no more detectable under conditions of intestinal inflammation. The totality of our data obtained from healthy and diseased tissues of rodents and humans question whether PEPT1 contributes significantly to the genesis or progression of IBD.

5.5 Alternative uptake routes for bacterial peptides

Beside the proposed role of PEPT1 in transport of bacteria-derived peptides, *in vitro* studies demonstrate that bacterial peptide structures including MDP or Tri-DAP can be internalized by endocytosis. In HEK293T cells, MDP and Tri-DAP were shown to be internalized by the dynamin-dependent pathway via clathrin-coated pits. Internalization of NOD1 ligands was shown to be pH-dependent with an optimal pH ranging from 5.5 to 6 and required the processing by endosomal enzymes. In case of MDP, the internalization pathway was similar; optimal pH for internalization here ranged from 5.5 to 6.5. Moreover, a sterically gated endosomal transporter for NOD1 ligands was identified as the SLC15A4 (PHT1) protein, an oligopeptide transporter, expressed in early endosomes. A connection between SLC15A4 and aberrant immune response in inflammatory bowel disease was also demonstrated in colonic biopsies obtained from IBD patients that revealed increased SLC15A4 expression levels [210].

Further data on the involvement of SLC15A4 was presented by Sasawatari S et al., showing that SLC15A4$^{-/-}$ mice had impaired TLR9 and NOD1-dependent immune responses with a less severe T_H1-response in DSS colitis. Moreover, the SLC15A4$^{-/-}$ mice displayed impaired responses to a Tri-DAP induced NOD1 activation and subsequent IL-1β and TNF-α production. It was therefore concluded that SLC15A4 may promote colitis through Toll-like receptor 9 and NOD1-dependent innate immune responses [212].

5.6 Role of PEPT1 in chemical-induced colitis

In the transgenic *villin*-hPEPT1 and *actin*-hPEPT1 mice, Dalmasso G et al. recently showed that the sole existence of colonic hPEPT1 is not sufficient to induce intestinal inflammation [198]. These observations clearly contradict their previous findings on the role of colonic PEPT1 in intestinal inflammation based on transport of bacteria-derived peptides [27, 29, 50]. DSS administration in these humanized transgenic *villin*-hPEPT1 and *actin*-hPEPT1 mice for induction of colitis however resulted in an aggravation of inflammation in both humanized mouse strains as compared to wild-type controls, suggesting that the human protein expressed in addition to the moue protein in colonic cells can exacerbate colitis [198]. From another study investigating DSS colitis in rats, colonic PEPT1 expression was reported to increase in response to DSS. But the increased PEPT1 levels did not occur in inflamed colonic tissue but in regenerative

hyperplasia segments of the distal colon [52].

In the studies of Dalmasso G et al. a second colitis model with the use of TNBS was employed. TNBS did only affect the *actin*-hPEPT1 mice with a worsening of intestinal inflammation, but not the *villin*-hPEPT1 mice. These results could indicate that when bacteria-derived peptides get access to immune cells (when those express hPEPT1) in the *actin*-hPEPT1 mice, but not in *villin*-hPEPT1 transgenic mice, inflammation is affected [198]. Previous studies by the same group offer some data on PEPT1 expression in monocytes [36]. However, the explanation that additional expression of hPEPT1 in already PEPT1 expressing immune cells is again contrasting their own previous findings. In our current studies, we could not observe any PEPT1-immunoreactivity in intestinal monocytes, but previously demonstrated that the high affinity peptide transporter PEPT2 resides in glia cells and macrophages of the intestine [37]. In addition, it was recently shown that MDP-dependent NOD2 activation in macrophages does not require PEPT1 [268]. This suggest that other transport or signaling processes are involved in modulating the immune response in the models of chemically induced colitis.

According to all these previous findings, our $Pept1^{-/-}$ mice should have been protected or at least show less severe responses to DSS in colitis induction. To test this, we also employed DSS as a colitis model and compared the effects of treatment in wild-type and $Pept1^{-/-}$ mice. Based on the clinical symptoms and the DAI we did not observe any significant differences between the genotypes but detected reduced PEPT1 protein levels in inflamed tissues of distal colon of wild-type mice when treated with DSS.

5.7 Colonic PEPT1 in Short Bowel Syndrom

An upregulation of colonic PEPT1 expression has also been reported in patients with short bowel syndrome (SBS). However, there are also contradictory data, as some studies found up-regulated colonic PEPT1 but others did not. In general, SBS is characterized by clinical signs like diarrhea, dehydration, malabsorption of macronutrients, vitamins, trace elements and weight loss [269, 270]. One study demonstrated adaptive colonic mucosal changes with increased PEPT1 expression in the remaining colon [48]. Colonic tissue samples came from SBS patients with a postduodenal remnant jejunum <150 cm and with normal colonoscopy of the remaining colon in the absence of any treatment with steroids or immunosuppressive compounds in the 4 months preceding the study. This study clearly suggests that colonic PEPT1 in SBS does not coincide with colonic inflammation, as all patients did not show any signs of colonic inflammation and were not treated with anti-inflammatory drugs. Thus, these results also clearly contradict the findings by Merlin D et al. [50] proposing a proinflammatory role of colonic PEPT1.

In a second prospective case-control study, Joly F et al. described morphological colonic adaptation in patients undergoing massive surgical reduction of the small bowel [258]. The adaptive changes in the remaining tissue included increases in crypt depth and number of cells per crypt and an overall increased absorptive surface. Whereas, cell proliferation rates remained largely unchanged, also transcript and protein levels of PEPT1, NHE-2 and NHE-3 remained unaffected [258]. This is in accordance with a recently published study suggesting that ileal adaptation in a rat model occurs through cellular hyperplasia and not through an upregulation of transport proteins [271]. Another study investigated the intestinal adaptation for peptide absorption after massive mid-small intestinal resection in rats. Here it was found that villus height and peptide uptake increased in the remnant small intestine. However, PEPT1 mRNA and protein were decreased during the adaptation period at week 1 and week 4 after resection in the small intestine. In the colon, *Pept1* gene expression, peptide uptake, and histomorphology were completely unchanged at any given time point [272]. Although PEPT1 expression data from SBS studies are partially contradictory Shi B et al. proposed that abnormal expression of PEPT1 in the colon of rats undergoing a 80% small bowel resection could again via transport of bacterial fMLP contribute to immune activation, as increased MPO activity [185] was observed. This finding was essentially published twice at the same time with the same authors in the same year and same month [186].

5.8 *Pept1* as a susceptibility gene in IBD

A recent study investigating the association of 12 *Pept1* gene polymorphisms in two scandinavian cohorts [178] revealed one *Pept1* gene polymorphism as to be associated with IBD susceptibility. Most surprisingly, a Ser117Asn exchange in the protein coding region appeared to be protective against CD in the cohort from Finland, whereas the same single nucleotide polymorphism in the Swedish cohort was associated with an increased susceptibility to CD. Despite the fact that different genetic and ethnic backgrounds may result in such seemingly contradictory findings, the functional relevance of the rs2297322 SNP was demonstrated in HEK cells transfected with the *Pept1* variants coupled to a NOD2-mediated NFκB activation (21). Exposure of these cells to MDP caused in case of the Asn117 variant an around 35% higher activation of the reporter system. However, various GWAS on susceptibility genes for IBD did so far not detect *Pept1* as associated with increased IBD risk [273]. Nevertheless, the IBD incidence may by influenced by rare genetic variants in the *Pept1* gene and possible interactions between genes, which are not well captured by GWAS [177].

5.9 PEPT1 as potential therapeutic target for anti-inflammatory treatment

The last decade since PEPT1 is proposed to be up-regulated during colonic inflammation it was shown to transport the anti-inflammatory tripeptide KPV [30]. A distinct expression of PEPT1 in inflamed tissue would raise the promising opportunity to use PEPT1 as tool for anti-inflammatory therapy in colonic inflammation [30, 51, 198, 274]. Suprisingly, so far no data on this issue has been published. And the current findings with decreased PEPT1 expression during intestinal inflammation questions if targeting PEPT1 would be a promising therapy approach. In addition to the proposed up-regulated PEPT1 expression during colonic inflammation, PEPT1 has been shown to transport the anti-inflammatory tripeptide KPV. In a study by Dalmasso G et al. KPV transport *in vitro* resulted in the reduction of proinflammatory cytokine production. Furthermore, oral KPV administration reduced the severity of DSS-, and TNBS-induced colitis, which led the authors to the assumption that KPV is transported into cells by PEPT1 and might be a new therapeutic agent for IBD [30]. However, direct uptake of KPV in inflamed colon from mice and beneficial effects in humans has never been reported. Therefore, alternative transport or signaling routes can not be ruled out and are likely, as the inflammed intestinal tissue has been shown to display increased permeability [275].

5.10   Conclusion and future perspective

The intestinal peptide transporter PEPT1 has been linked to IBD by its capability to transport bacteria-derived immune-modulating short chain peptides and by the prime, yet questionable observation, that PEPT1 is not expressed in healthy colon but appears at increased levels in colonic inflammation. Our current study presents for the first time a systematic screen of PEPT1 expression and localization in normal and seemingly healthy colonic tissues of mice, rats and humans. The totality of our data unequivocally demonstrates that PEPT1 is expressed in normal healthy colon from mice, rats and humans. Moreover, in all models of small intestinal and colonic inflammation of the corresponding mouse models and in the human IBD samples we were unable to detect increased PEPT1 levels but clearly and consistently observed reduced transporter protein levels. These observations of course contradict all previous findings on PEPT1 and its role in colon in health and disease states.

Our data demonstrate that colonic PEPT1 expression in mammals occurs in a strict region-specific manner. No expression is found in proximal colon whereas distal colon shows prominent expression, which seems to be independent of the presence or the absence of the microbiota. We also demonstrate that colonic PEPT1 is functional and contributes to adequate water absorption from colon. We also collected some interesting data that together with findings from literature suggest that colonic PEPT1 might contribute to bacterial colonization in colon. It is very intriguing that we observed

differences in the extracellular glycan structures of PEPT1 in small intestine and colon which raises the question of the cell biology underlying this observation and what the consequences are. This requests for further studies and may include other brush border membrane proteins that constitute the glycocalix of epithelial cells in small and large intestine which form the contact sites by which bacteria (commensals and pathogenic) interact with the host.

6 APPENDIX

6.1 Supplemental Figures

A **solute carrier family 15 member 1 [Mus musculus]**

NCBI Reference Sequence: NP_444309.2

```
  1  mgmsksrgcf gyplsiffiv vnefcerfsy ygmrallvly frnflgwddn lstaiyhtfv
 61  alcyltpilg aliadswlgk fktivslsiv ytigqavisv ssindltdhd hngspdslpv
121  hvalsmvgla lialgtggik pcvsafggdq feegqekqrn rffsifylai nggsllstii
181  tpilrvqqcg ihsqqacypl afgvpaalma valivfvlgs gmykkfqpqg nimgkvakci
241  gfaiknrfrh rskaypkreh wldwakekyd erlisqikmv tkvmflyipl pmfwalfdqq
301  gsrwtlqatt mngkigaiei qpdqmqtvna ilivimvpiv davvypliak cgfnftslkk
361  mtvgmflasm afvvaaivqv eidktlpvfp ggnqvqikvl nignnnmtvh fpgnsvtlaq
421  msqtdtfmtf didkltsini sssgspgvtt vahdfeqghr htllvwnpsq yrvvkdglnq
481  kpekgengir fvntlnemvt ikmsgkvyen vtshnasgyq ffpsgekqyt inttavaptc
541  ltdfkssnld fgsaytyvir rasdgclevk efedippntv nmalqipqyf lltcgevvfs
601  vtglefsysq apsnmksvlq agwlltvavg niivlivaga ghfpkqwaey ilfaslllvv
661  cvifaimarf ytyinpaeie aqfdedekkk gigkenpyss lepvsqtnm
```

B **solute carrier family 15 member 1 [Rattus norvegicus]**

NCBI Reference Sequence: NP_476462.1

```
  1  mgmsksrgcf gyplsiffiv vnefcerfsy ygmrallvly frnflgwddd lstaiyhtfv
 61  alcyltpilg aliadswlgk fktivslsiv ytigqavisv ssindltdhd hdgspnnlpl
121  hvalsmigla lialgtggik pcvsafggdq feegqekqrn rffsifylai nagsllstii
181  tpilrvqqcg ihsqqacypl afgvpaalma valivfvlgs gmykkfqpqg nimgkvakci
241  rfaiknrfrh rskafpkrnh wldwakekyd erlisqikim tkvmflyipl pmfwalfdqq
301  gsrwtlqatt mtgkigtiei qpdqmqtvna ilivimvpiv davvypliak cgfnftslkk
361  mtvgmflasm afvvaaivqv eidktlpvfp sgnqvqikvl nignndmavy fpgknvtvaq
421  msqtdtfmtf dvdqltsinv sspgspgvtt vahefepghr htllvwgpnl yrvvkdglnq
481  kpekgengir fvstlnemit ikmsgkvyen vtshsasnyq ffpsgqkdyt intteiapnc
541  ssdfkssnld fgsaytyvir srasdgclev kefedippnt vnmalqipqy flltcgevvf
601  svtglefsys qapsnmksvl qagwlltvai gniivlivae aghfdkqwae yvlfaslllv
661  vciifaimar fytyinpaei eaqfdedekk kgvgkenpys slepvsqtnm
```

C **solute carrier family 15 member 1 [Homo sapiens]**

NCBI Reference Sequence: NP_005064.1

```
  1  mgmskshsff gyplsiffiv vnefcerfsy ygmrailily ftnfiswddn lstaiyhtfv
 61  alcyltpilg aliadswlgk fktivslsiv ytigqavtsv ssindltdhn hdgtpdslpv
121  hvvlsligla lialgtggik pcvsafggdq feegqekqrn rffsifylai nagsllstii
181  tpmlrvqqcg ihskqacypl afgvpaalma valivfvlgs gmykkfkpqg nimgkvakci
241  gfaiknrfrh rskafpkreh wldwakekyd erlisqikmv trvmflyipl pmfwalfdqq
301  gsrwtlqatt msgkigalei qpdqmqtvna ilivimvpif davlypliak cgfnftslkk
361  mavgmvlasm afvvaaivqv eidktlpvfp kgnevqikvl nignntmnis lpgemvtlgp
421  msqtnafmtf dvnkltrini sspgspvtav tddfkqgqrh tllvwapnhy qvvkdglnqk
481  pekgengirf vntfneliti tmsgkvyani ssynastyqf fpsgikgfti ssteippqcq
541  pnfntfylef gsaytyivqr kndscpevkv fedisantvn malqipqyfl ltcgevvfsv
601  tglefsysqa psnmksvlqa gwlltvavgn iivlivagag qfskqwaeyi lfaalllvvc
661  vifaimarfy tyinpaeiea qfdedekknr leksnpyfms gansqkqm
```

Supplemental Figure 1. Amino acid sequences of mouse, rat and human PEPT1 protein including the target regions of our custom-made ABs.
(A) Mouse PEPT1 amino acid sequence consisting of 709 amino acids. (B) Rat PEPT1 amino acid sequence consisting of 710 amino acids. (C) Human PEPT1 amino acid sequence consisting of 708 amino acids. The blue underlined part indicates the amino acids sequence against which the AB used by Merlin D et al. is directed. The green line indicates the epitop sequence of the AB used in our studies.

Supplemental Figure 2. Representative agarose gels of qRT-PCR products.
qRT-PCR products were separated by agarose gel electrophoresis and stained with ethidium bromide. The expected and observed qRT-PCR amplicon sizes were for *AP-1* 156 bp, Cdx2 170 bp, CREB 250 bp, klf4 212 bp, Mzf1 169 bp, Nrf2 279 bp, PPAR-alpha 243 bp, Sp1 239 bp, and VDR 196 bp.
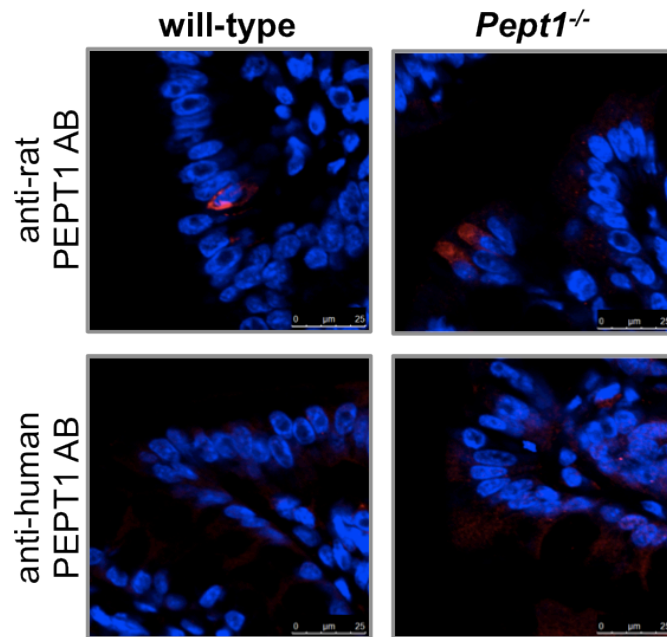
Supplemental Figure 3. IF staining of PEPT1 in proximal colon from wild-type and *Pept1$^{-/-}$* mice.

The ABs used were directed against rat-PEPT1 (upper panel) or human-PEPT1 (lower panel). Single PEPT1-positive cells (red) were detected in wild-type and *Pept1$^{-/-}$* mice using the anti-rat PEPT1 AB. No specific signal was detectable when the anti-human PEPT1 AB was used. DRAQ5 was used as nuclear counterstain.
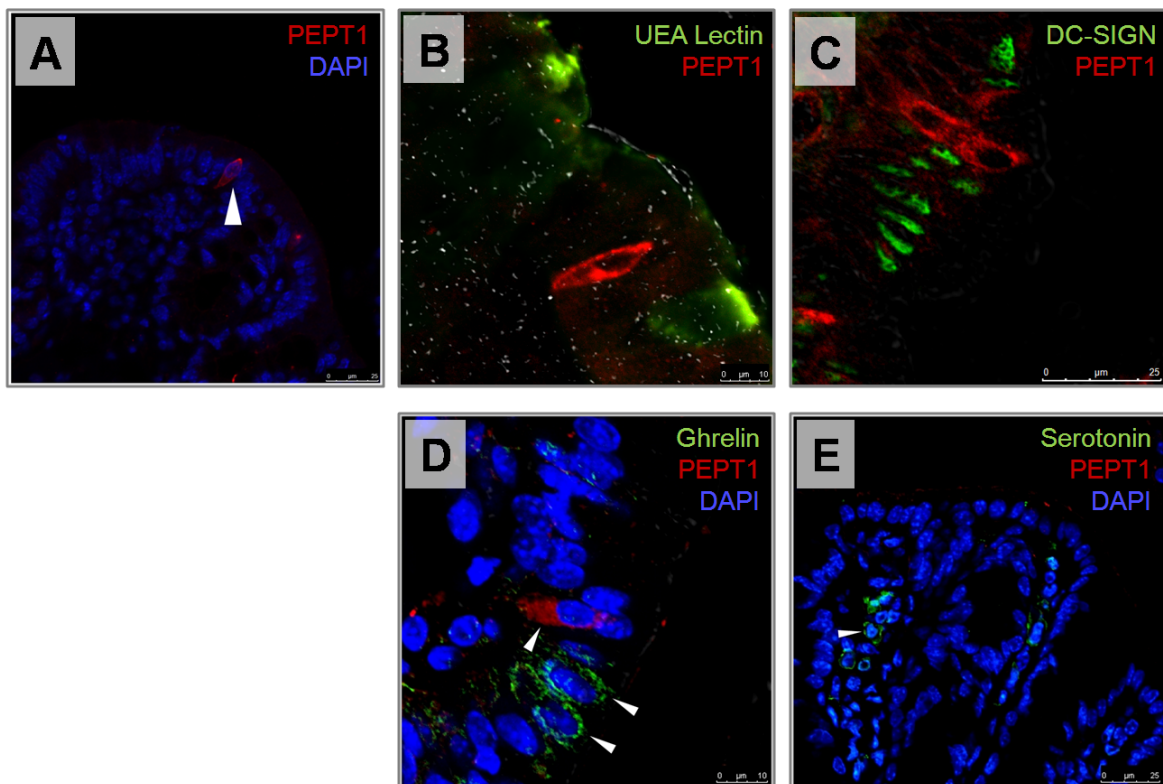
Supplemental Figure 4. IF staining of PEPT1, UEA Lectin, DC-SIGN, Ghrelin and Serotonin in proximal colon from wild-type mice.

PEPT1 is expressed sporadically in single cells (red, A-E). None of the tested targets shows colocalization with PEPT1 positive cells. DAPI was used as nuclear counterstain.
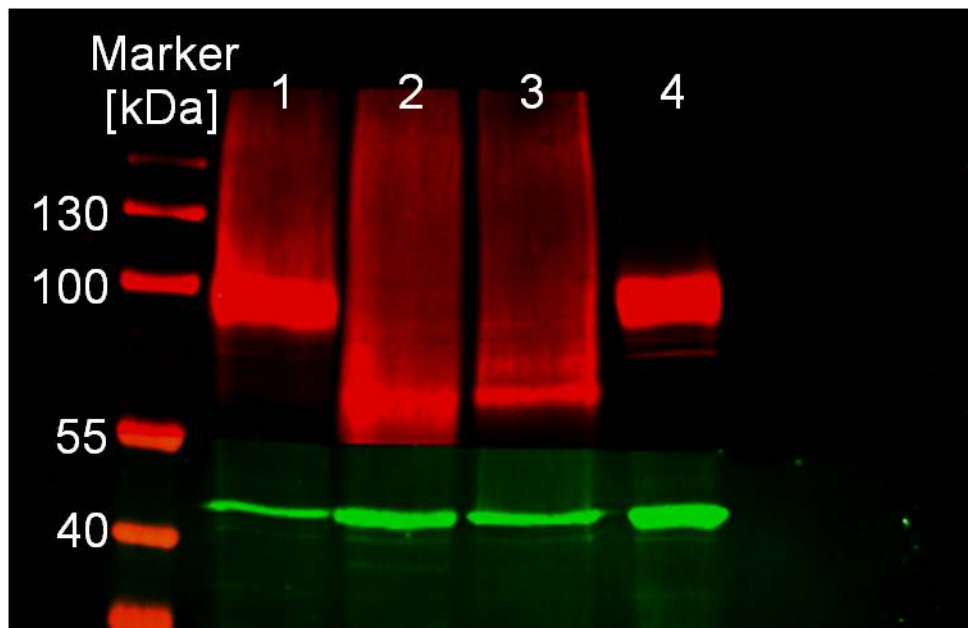
Supplemental Figure 5. PEPT1 deglycosylation studies on wild-type mouse jejunal tissue using Endo H and PNGase F.
Deglycosylation with Endo H resulted in a PEPT1 band at ~95 kDa, whereas addition of PNGase F (lane 2) or Endo H + PNGase F in combination resulted in a MW shift from ~95 kDa to a band at ~71 kDa, as compared to control, without glycosidase (lane 4)
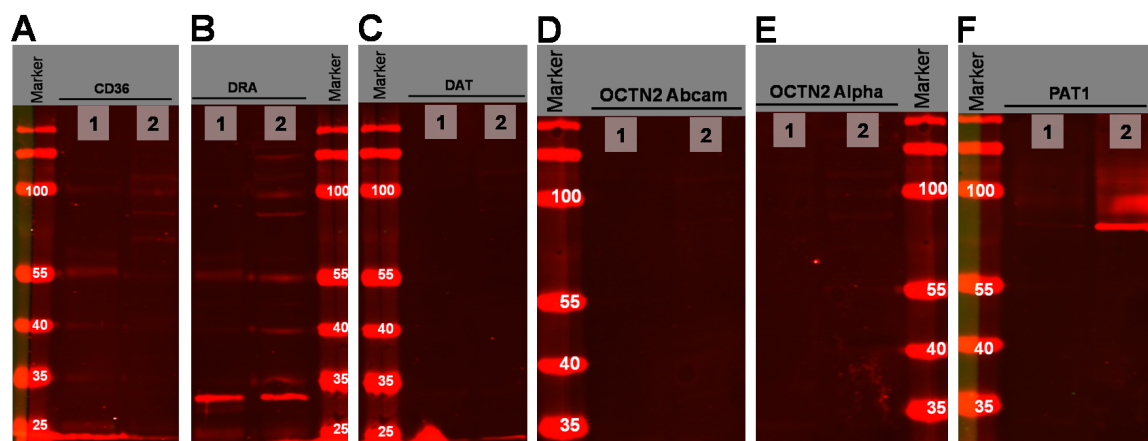
Supplemental Figure 6. Western Blot AB test of putative intestinal membrane proteins CD36, DRA, DAT, OCTN2 and PAT1.
Lane 1 shows wild-type jejunum protein, isolated by asimplified method without divalent cation precipitation. Lane 2 shows wild-type jejunum protein, isolated by divalent cation precipitation. Test of (A) a monoclonal mouse CD36 AB (dilution: 1:250; clone D-2712, MAB2325) from Abnova (Taipei City, Taiwan), (B) a anti-SLC26A3 (DRA) AB (dilution: 1:200; clone 2E3, Lot 09210-2E3) from Abnova (Taipei City, Taiwan), (C) a rabbit polyclonal anti-DAT AB (dilution: 1:100, AB1591P) from Millipore (Temecula, CA, USA), (D) a rabbit polyclonal anti-SLC22A5 (OCTN2) AB (dilution AB79964) from Abcam (Cambridge, UK), (E) a second polyclonal rabbit anti mouse OCTN2 AB (dilution: 1:200, Cat. OCTN21-S) from Alpha Diagnostic Intl. Inc., San Antonio, TX, USA) and a rabbit anti-SLC36A1 (PAT1) AB (dilution: 1:100, Lot R33538).
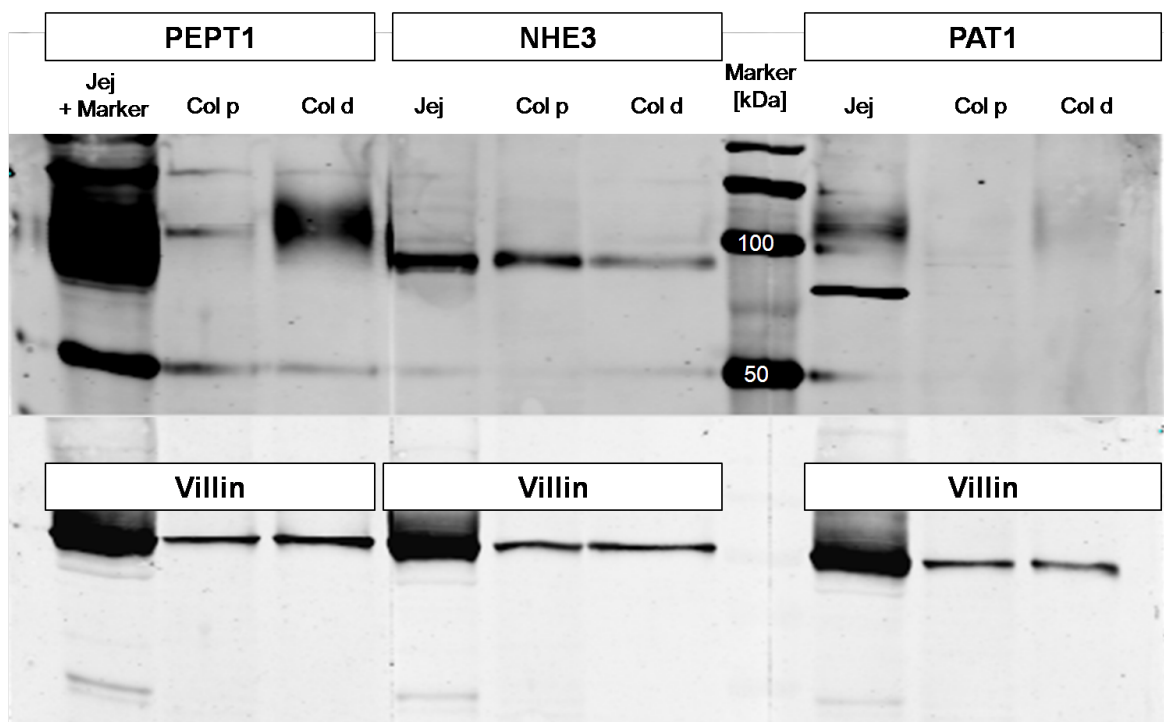
Supplemental Figure 7. Western Blot analysis of PEPT1, NHE-3 and PAT1 in jejunum (Jej), proximal colon (Col p) and distal colon (Col d) from a wild-type mouse.
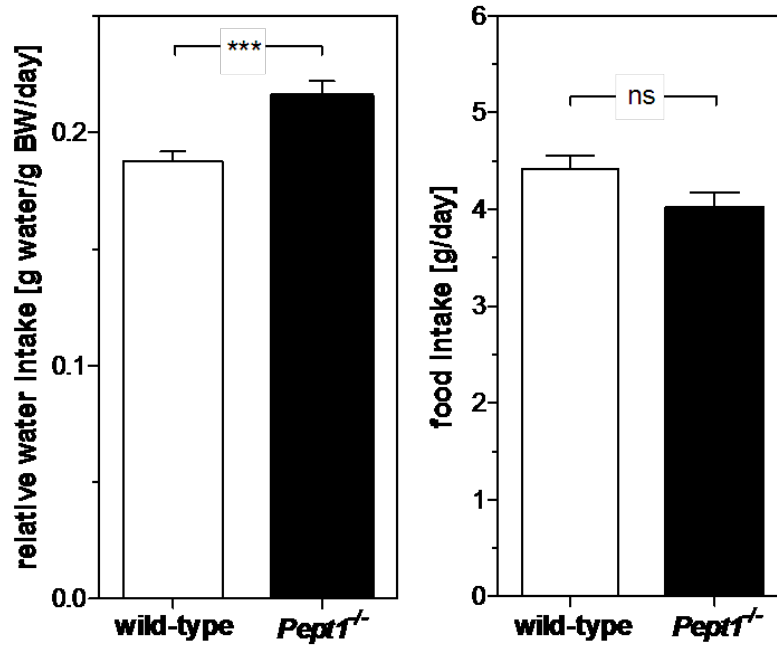
Supplemental Figure 8. Daily food and water intake in wild-type and *Pept1*⁻ᐟ⁻ mice.
Means ± SEM of n=20-24 arte shown, ***p<0.001.

6.2 Supplemental Tables

Supplemental Table 1. Scoring of disease activity index (DAI).
The DAI was modified from Cooper HS et al. [214], calculated by combined assessment of the four parameters weight loss, stool consistency, stool blood content, and appearance.

Score	Weight loss (%)a	Stool consistency	Stool blood content	Appearance
0	None	normal droppings/ or: well formed pellets	none (0)	lively/ normal
1	1-5	loose droppings	traces of blood (10-25)	hunched
2	5-10	pasty stools	bloody (80)	starey coat
3	10-20		200	lethargic
4	>20	liquid stools that adhere to the anus	gross bleeding	apathetic

aThe percentage weight loss was calculated by comparing the weight of each mouse to the baseline weight.

Supplemental Table 2. Individual mouse parameters (body weight, water intake, food intake) of wild-type and *Pept1⁻ᐟ⁻* mice during the 7 days DSS treatment period and controls.

Experiment description: Genotype: wild-type, 2.5% DSS

mouse number	day 0 (110405; 7.30am) weight [g]	water [g]	ohow [g]	day 1 (110407) weight [g]	water [g]	ohow [g]	day 2 (110408) weight [g]	water [g]	ohow [g]	day 3 (110409, 10:00am) weight [g]	water [g]	ohow [g]	day 4 (110410) weight [g]	water [g]	ohow [g]	day 5 (110411) weight [g]	water [g]	ohow [g]	day 6 (110412) weight [g]	water [g]	ohow [g]	day 7 (110413) weight [g]	water [g]	ohow [g]
1	24,13	5,5	6,3	24,8	6,7	6,5	23,63	4,82	4,37	22,95	5,1	4,2	22,36	4,0	3,2	22,87	3,9	3,1	22,69	3,7	2,9	21,1	4,1	3,5
2	22,46	4,1	4,1	22,21	5,0	3,5	21,93	4,54	3,61	21,77	4,3	3,8	22,11	4,7	3,8	21,7	2,8	2,5	20,49	2,7	2,3	16,29	3,5	2,6
3	20,97	3,8	4,2	20,96	5,0	4,1	20,83	4,46	3,5	20,44	4,4	3,7	20,5	3,9	3,7	20,9	3,5	3,3	20,71	3,0	2,7	19,58	3,3	2,8
4	25,34	4,5	4,9	24,91	4,6	4,2	25	4,93	3,84	25,25	5,2	4,1	24,83	4,5	3,4	24,03	2,5	2,1	23,45	2,5	1,8	22,68	3,9	3,1
5	23,64	3,6	3,2	23,68	4,8	3,4	23,17	4,36	3,83	23,46	5,1	4,2	23,65	4,2	3,8	23,2	3,1	3,2	22,82	4,2	2,6	21,2	4,5	2,9
6	22,85	3,9	4,0	22,41	4,6	3,4	22,14	4,08	3,54	21,63	3,8	3,2	21,6	3,7	3,0	21,2	2,7	2,6	20,9	2,1	2,3	18,46	2,7	2,8
7	22,03	3,8	3,0	21,88	4,7	2,9	21,77	4,3	3,2	21,85	5,7	4,4	21,9	4,6	3,5	21,24	3,4	2,3	20,76	3,3	2,1	16,12	2,5	1,7
8	23,63	5,0	4,0	23,12	5,5	4,0	23,09	6,2	4,4	22,73	6,1	4,4	22,51	4,7	3,4	21,96	3,2	2,6	21,09	3,5	2,1	17,7	4,3	2,2
Mean	23,13125	4,2875	4,20375	22,996	5,0975	3,9825	22,695	4,7125	3,78625	22,5	5,0	4,0	22,4	4,3	3,5	22,1	3,1	2,7	21,6	3,1	2,4	19,1	3,6	2,7

Experiment description: Genotype: wild-type, Control, tap water

mouse number	day 0 weight [g]	water [g]	ohow [g]	day 1 (110407) weight [g]	water [g]	ohow [g]	day 2 (110408) weight [g]	water [g]	ohow [g]	day 3 weight [g]	water [g]	ohow [g]	day 4 weight [g]	water [g]	ohow [g]	day 5 weight [g]	water [g]	ohow [g]	day 6 weight [g]	water [g]	ohow [g]	day 7 weight [g]	water [g]	ohow [g]
1	22,09	4,57	4,06	21,25	4,5	4,19	23,18	5,3	4,7	22,74	5,88	4,5	23,58	5,43	4,4	24,1	5,18	4,4	23,88	5,2	4,3	24,02	5,54	4,5
2	21,6	4,84	3,33	22,6	5,3	4,35	22,21	4,3	4,5	21,88	4,03	4,3	23,29	4,3	4	23,85	3,9	5	23,2	4,38	4,5	22,66	4,9	4,1
3	23,66	4,94	5,17	21,13	4,7	4	21,35	4,2	3,5	21,81	4,57	4,7	22,15	4,86	4,8	22,45	4,53	4,3	23,38	4,31	4,7	23,6	4,73	4,5
4	24,27	4,87	5,07	24,85	4,9	4,4	24,96	4,5	4,2	24,77	4,59	4	24,2	5,08	4,3	23,54	4,71	4	23,63	4,59	4	23,46	4,22	4,2
5	22,82	5,20	4,84	23,9	4,3	4,2	23,92	4,0	4,6	23,8	4,3	4,4	24,42	4,22	4,3	24,13	3,98	3,9	23,69	4,28	4,1	24,22	3,87	4
6	22,88	4,70	4,49	22,75	4,74	4,28	23,12	4,47	4,30	23,00	4,68	4,38	23,53	4,78	4,36	23,61	4,45	4,32	23,56	4,55	4,32	23,59	4,65	4,26
Mean	23,275	4,7625	4,49	23,27625	5,60875	3,96	22,695	4,7125	4,30	22,695	4,68	4,38	23,53	4,78	4,36	23,61	4,45	4,32	23,56	4,55	4,32	23,59	4,65	4,26

Experiment description: Genotype: Pept1 -/-, 2.5%DSS

mouse number	day 0 (110405; 7.30am) weight [g]	water [g]	ohow [g]	day 1 (110407) weight [g]	water [g]	ohow [g]	day 2 (110408) weight [g]	water [g]	ohow [g]	day 3 (110409) weight [g]	water [g]	ohow [g]	day 4 (110410) weight [g]	water [g]	ohow [g]	day 5 (110411) weight [g]	water [g]	ohow [g]	day 6 (110412) weight [g]	water [g]	ohow [g]	day 7 (110413) weight [g]	water [g]	ohow [g]
1	21,9	4,57	2,97	23,15	6,76	3,8	23,32	5,86	3,63	22,73	5,53	3,32	22,19	4,97	2,86	22,45	4,33	2,96	21,44	3,17	1,79	17,18	3,41	1,9
2	25,13	4,84	5,49	24,86	5,21	4,3	25,27	5,6	4,16	24,55	4,6	3,04	23,97	4,3	2,3	23,51	2,7	2,3	22,27	2,75	2,19	20,52	3,41	2,68
3	25,1	4,94	4,2	24,76	5,81	3,8	23,88	3,97	3,48	24,85	5,31	4,19	24,89	4,32	3,82	24,18	3,13	2,38	23,14	2,58	2,45	20,42	2,8	2,32
4	23,1	4,33	3,8	22,85	5,08	4,4	22,38	4,3	3,52	23,1	5,55	4,25	23,25	4,04	3,31	22,8	3,09	2,25	21,57	3,91	2,47	19,34	3,66	2,59
5	22,39	4,37	3,54	22,11	4,29	3,28	22,75	5,12	3,85	22,48	5,02	3,6	22,3	4,34	3,05	21,89	3,38	2,74	21,75	4,2	2,64	17,28	1,91	2,01
6	22,78	5,26	3,96	22,53	6,4	3,53	22,41	6,08	3,38	22,2	6,82	3,06	22,03	4,72	3,07	21,36	3,27	2,21	19,62	3,52	1,91	17,77	2,75	1,55
7	21,76	5,14	4,04	21,92	6,02	4,86	21,86	5,52	4,4	21,9	6,25	4,51	21,37	4,36	4,01	20,68	2,77	2,92	20,37	3,46	3,02	18,49	2,84	2,5
8	24,04	4,65	4,68	24,03	5,31	3,75	23,52	5,14	3,84	23,5	5,08	3,91	23,17	4,87	3,95	22,88	3,29	2,67	21,4	3,32	2,51	18,11	2,53	2,34
Mean	23,275	4,7625	4,085	23,27625	5,60875	3,96	23,23	5,20	3,78	23,23	5,52	3,85	22,98	4,42	3,53	22,48	3,09	2,50	21,45	3,39	2,45	18,65	2,84	2,28

Experiment description: Genotype: Pept1 -/-, Control, tap water

mouse number	day 0 weight [g]	water [g]	ohow [g]	day 1 (110407) weight [g]	water [g]	ohow [g]	day 2 weight [g]	water [g]	ohow [g]	day 3 weight [g]	water [g]	ohow [g]	day 4 weight [g]	water [g]	ohow [g]	day 5 weight [g]	water [g]	ohow [g]	day 6 weight [g]	water [g]	ohow [g]	day 7 weight [g]	water [g]	ohow [g]
1	22,3	7,33	3,88	22,94	5,0	3,8	22,57	6,0	3,4	22,45	5,78	4,1	22,71	5,7	4,2	22,65	5,89	3,9	22,3	5,23	4	22,59	5,77	3,8
2	19,21	4,0	3,7	18,27	4,3	4,3	23,93	6,2	4,9	23,7	6,12	4,9	23,56	5,42	4,7	23,41	6,03	4,5	23,7	5,11	4,6	23,82	5,53	4,5
3	20,2	4,4	4,4	24,38	6,3	3,8	25,03	5,4	4,1	25,37	5,77	4,5	25,37	5,16	4,7	25,6	5,87	4,9	25,41	6,43	4,2	25,33	6,02	4,4
4	23,14	5,1	4,3	23,49	4,6	4,4	22,79	4,2	3,8	22,93	4,9	3,9	22,71	4,79	4,1	22,49	5,2	4,3	22,63	4,62	4,4	22,67	4,84	4,1
5	22,27	3,8	4,4	22,86	4,8	4,8	22,43	4,2	5	22,26	5	4,7	22,4	4,04	4,9	22,52	4,98	4,9	22,5	4,01	5,3	22,96	5,13	4,7
Mean	21,42	4,86	4,14	22,33	5,30	4,22	23,35	5,43	4,04	23,34	5,51	4,42	23,35	5,19	4,56	23,33	5,59	4,50	23,31	5,04	4,50	23,38	5,46	4,30

Supplemental Table 3. Colon length of wild-type and *Pept1*$^{-/-}$ mice after 7 days DSS treatment or water control.

wild-type control [cm]	wild-type DSS [cm]	*Pept1*$^{-/-}$ control [cm]	*Pept1*$^{-/-}$ DSS [cm]
7.80	5.40	7.40	6.13
8.00	7.34	7.00	6.63
7.20	7.36	7.23	7.58
7.39	7.81	6.98	6.65
7.20	6.39	7.13	5.95
6.85	5.78		5.81
7.50	5.10		6.20
7.30	6.94		6.63

LIST OF FIGURES

LIST OF TABLES

ABBREVIATIONS

AB	antibody
APS	ammonium persulfate
ATG16L1	autophagy-related protein 16-1
BBMV	brush border membrane vesicles
bp	base pair
CARD	caspase recruitment domains
CD	Crohn's disease
cDNA	complementary DNA
citrobacter	*c.*
Ct	cycle threshold
DAI	disease activity index
DAPI	4′,6-Diamidino-2-phenylindole dihydrochloride
DC	dendritic cell
DC-SIGN	Dendritic Cell-Specific Intercellular adhesion molecule-3-Grabbing Non-integrin
DEPC	Diethylpyrocarbonate
DivCatPre	divalent cation precipitation
DMSO	dimethyl sulfoxide
DRA	downregulated in adenoma
DSS	dextran sulfate sodium
DTT	dithiothreitol
EDTA	Ethylenediamine-tetraaceticacid
EGTA	Ethylene glycol tetraacetic acid
EMSA	electrophoretic mobility shift assay
Endo H	Endoglycosidase H
EPEC	enteropathogenic *Escherichia coli*
ER	endoplasmic reticulum
FDA	Feeding-Drinking-Activity
FITC	Fluorescein isothiocyanate
fMLP	formyl-methionyl-leucine-phenylalanine
GAPDH	glyceraldehyde-3-phosphate dehydrogenase
GlcNAc	N-Acetyl-D-glucosamin
Gly-Sar	glycyl-sarcosine
GWAS	Genome-wide association studies
HE	Hematoxilin-Eosin
hPEPT1	human PEPT1
IBD	inflammatory bowel disease
IEC	intestinal epithelial cells
IF	immunofluorescence
IL	Interleukin
klf4	Krüppel-like factor 4
KO	knockout
KPV	lysine-proline-valine
LP	*Lactobacillus plantarum*
M cells	microfold cells

MDP	muramyl dipeptide (MurNAc-L-Ala-D-isoGln)
mPEPT1	mouse PEPT1
mRNA	messenger RNA
MW	molecular weight
mPEPT1	mouse PEPT1
MPO	myeloperoxidase
MyD88	myeloid differentiation factor 88
Mzf1	myeloid zinc finger 1
NF-κB	nuclear factor κB
NHE	Na+/H+ exchanger
NLRs	NOD-like receptors
NOD	nucleotide-binding and oligomerization domain
ns	not significant
OCTN2	carnitine/ organic cation transporter 2
PAGE	polyacrylamide gel electrophoresis
PBS	phosphate-buffered saline
PEPT1	di- and tripeptide transporter 1
PCR	polymerase chain reaction
PKA	protein kinase A
PKC	protein kinase C
PMSF	phenylmethylsulfonyl fluoride
PNGase F	*N*-linked-glycopeptide-)*N*-acetyl-beta-D-glucosaminyl)-L-asparagine amidohydrolase
POT	proton-coupled oligopeptide transporter
PRRs	pattern recognition receptors
qRT-PCR	quantitative reverse transcriptase-PCR
rPEPT1	rat PEPT1
RT	reverse transcriptase
SD	standard deviation
SDS	sodium dodecylsulfate
SEM	standard error of the mean
SLC	solute carrier
TAE	Tris-Acetat-EDTA
T_H cell	helper T cell
TLR	Toll-like receptor
Tm	melting temperature
TMD	transmembrane domain
TNBS	2,4,6-trinitrobenzene sulfonic acid
TNF	tumor necrosis factor
T_{reg} cell	regulatory T cell
Tri-DAP	L-Ala-γ-D-Glu-*meso*-diaminopimelic acid
UC	ulcerative colitis
UEA	*Ulex europaeus*
WB	Western blot
WT	wild-type
VDR	Vitamin D Receptor

REFERENCES

1. Ganapathy V, Burckhardt G, Leibach FH: **Characteristics of glycylsarcosine transport in rabbit intestinal brush-border membrane vesicles**. *The Journal of biological chemistry* 1984, **259**(14):8954-8959.
2. Fei YJ, Kanai Y, Nussberger S, Ganapathy V, Leibach FH, Romero MF, Singh SK, Boron WF, Hediger MA: **Expression cloning of a mammalian proton-coupled oligopeptide transporter**. *Nature* 1994, **368**(6471):563-566.
3. Boll M, Markovich D, Weber WM, Korte H, Daniel H, Murer H: **Expression cloning of a cDNA from rabbit small intestine related to proton-coupled transport of peptides, beta-lactam antibiotics and ACE-inhibitors**. *Pflugers Arch* 1994, **429**(1):146-149.
4. Liang R, Fei YJ, Prasad PD, Ramamoorthy S, Han H, Yang-Feng TL, Hediger MA, Ganapathy V, Leibach FH: **Human intestinal H+/peptide cotransporter. Cloning, functional expression, and chromosomal localization**. *The Journal of biological chemistry* 1995, **270**(12):6456-6463.
5. Saito H, Okuda M, Terada T, Sasaki S, Inui K: **Cloning and characterization of a rat H+/peptide cotransporter mediating absorption of beta-lactam antibiotics in the intestine and kidney**. *J Pharmacol Exp Ther* 1995, **275**(3):1631-1637.
6. Fei YJ, Sugawara M, Liu JC, Li HW, Ganapathy V, Ganapathy ME, Leibach FH: **cDNA structure, genomic organization, and promoter analysis of the mouse intestinal peptide transporter PEPT1**. *Biochimica et biophysica acta* 2000, **1492**(1):145-154.
7. Kennelly PJ, Krebs EG: **Consensus sequences as substrate specificity determinants for protein kinases and protein phosphatases**. *The Journal of biological chemistry* 1991, **266**(24):15555-15558.
8. Daniel H: **Molecular and integrative physiology of intestinal peptide transport**. *Annu Rev Physiol* 2004, **66**:361-384.
9. Meredith D, Price RA: **Molecular modeling of PepT1--towards a structure**. *J Membr Biol* 2006, **213**(2):79-88.
10. Newstead S, Drew D, Cameron AD, Postis VL, Xia X, Fowler PW, Ingram JC, Carpenter EP, Sansom MS, McPherson MJ *et al*: **Crystal structure of a prokaryotic homologue of the mammalian oligopeptide-proton symporters, PepT1 and PepT2**. *Embo J* 2011, **30**(2):417-426.
11. Lucas M: **Determination of acid surface pH in vivo in rat proximal jejunum**. *Gut* 1983, **24**(8):734-739.
12. Vavricka SR, Musch MW, Fujiya M, Kles K, Chang L, Eloranta JJ, Kullak-Ublick GA, Drabik K, Merlin D, Chang EB: **Tumor necrosis factor-alpha and interferon-gamma increase PepT1 expression and activity in the human colon carcinoma cell line Caco-2/bbe and in mouse intestine**. *Pflugers Arch* 2006, **452**(1):71-80.
13. Tamai I, Nakanishi T, Hayashi K, Terao T, Sai Y, Shiraga T, Miyamoto K, Takeda E, Higashida H, Tsuji A: **The predominant contribution of oligopeptide transporter PepT1 to intestinal absorption of beta-lactam antibiotics in the rat small intestine**. *J Pharm Pharmacol* 1997, **49**(8):796-801.
14. Knutter I, Wollesky C, Kottra G, Hahn MG, Fischer W, Zebisch K, Neubert RH, Daniel H, Brandsch M: **Transport of angiotensin-converting enzyme inhibitors by H+/peptide transporters revisited**. *J Pharmacol Exp Ther* 2008, **327**(2):432-441.
15. Brandsch M, Brandsch C, Ganapathy ME, Chew CS, Ganapathy V, Leibach FH: **Influence of proton and essential histidyl residues on the transport kinetics of the H+/peptide cotransport systems in intestine (PEPT 1) and kidney (PEPT 2)**. *Biochimica et biophysica acta* 1997, **1324**(2):251-262.
16. Doring F, Dorn D, Bachfischer U, Amasheh S, Herget M, Daniel H: **Functional analysis of a chimeric mammalian peptide transporter derived from the**

intestinal and renal isoforms. *The Journal of physiology* 1996, **497 (Pt 3)**:773-779.

17. Watanabe C, Kato Y, Ito S, Kubo Y, Sai Y, Tsuji A: **Na+/H+ exchanger 3 affects transport property of H+/oligopeptide transporter 1**. *Drug Metab Pharmacokinet* 2005, **20**(6):443-451.

18. Thwaites DT, Kennedy DJ, Raldua D, Anderson CM, Mendoza ME, Bladen CL, Simmons NL: **H/dipeptide absorption across the human intestinal epithelium is controlled indirectly via a functional Na/H exchanger**. *Gastroenterology* 2002, **122**(5):1322-1333.

19. Kennedy DJ, Leibach FH, Ganapathy V, Thwaites DT: **Optimal absorptive transport of the dipeptide glycylsarcosine is dependent on functional Na+/H+ exchange activity**. *Pflugers Archiv : European journal of physiology* 2002, **445**(1):139-146.

20. Daniel H, Kottra G: **The proton oligopeptide cotransporter family SLC15 in physiology and pharmacology**. *Pflugers Archiv : European journal of physiology* 2004, **447**(5):610-618.

21. Sterchi EE, Woodley JF: **Peptide hydrolases of the human small intestinal mucosa: distribution of activities between brush border membranes and cytosol**. *Clin Chim Acta* 1980, **102**(1):49-56.

22. Terada T, Sawada K, Saito H, Hashimoto Y, Inui K: **Functional characteristics of basolateral peptide transporter in the human intestinal cell line Caco-2**. *Am J Physiol* 1999, **276**(6 Pt 1):G1435-1441.

23. Ganapathy ME, Huang W, Wang H, Ganapathy V, Leibach FH: **Valacyclovir: a substrate for the intestinal and renal peptide transporters PEPT1 and PEPT2**. *Biochem Biophys Res Commun* 1998, **246**(2):470-475.

24. Hironaka T, Itokawa S, Ogawara K, Higaki K, Kimura T: **Quantitative evaluation of PEPT1 contribution to oral absorption of cephalexin in rats**. *Pharm Res* 2009, **26**(1):40-50.

25. Inui K, Okano T, Maegawa H, Kato M, Takano M, Hori R: **H+ coupled transport of p.o. cephalosporins via dipeptide carriers in rabbit intestinal brush-border membranes: difference of transport characteristics between cefixime and cephradine**. *The Journal of pharmacology and experimental therapeutics* 1988, **247**(1):235-241.

26. Inui K, Tomita Y, Katsura T, Okano T, Takano M, Hori R: **H+ coupled active transport of bestatin via the dipeptide transport system in rabbit intestinal brush-border membranes**. *J Pharmacol Exp Ther* 1992, **260**(2):482-486.

27. Merlin D, Steel A, Gewirtz AT, Si-Tahar M, Hediger MA, Madara JL: **hPepT1-mediated epithelial transport of bacteria-derived chemotactic peptides enhances neutrophil-epithelial interactions**. *J Clin Invest* 1998, **102**(11):2011-2018.

28. Ismair MG, Vavricka SR, Kullak-Ublick GA, Fried M, Mengin-Lecreulx D, Girardin SE: **hPepT1 selectively transports muramyl dipeptide but not Nod1-activating muramyl peptides**. *Can J Physiol Pharmacol* 2006, **84**(12):1313-1319.

29. Dalmasso G, Nguyen HT, Charrier-Hisamuddin L, Yan Y, Laroui H, Demoulin B, Sitaraman SV, Merlin D: **PepT1 mediates transport of the proinflammatory bacterial tripeptide L-Ala-{gamma}-D-Glu-meso-DAP in intestinal epithelial cells**. *American journal of physiology Gastrointestinal and liver physiology* 2010, **299**(3):G687-696.

30. Dalmasso G, Charrier-Hisamuddin L, Nguyen HT, Yan Y, Sitaraman S, Merlin D: **PepT1-mediated tripeptide KPV uptake reduces intestinal inflammation**. *Gastroenterology* 2008, **134**(1):166-178.

31. Groneberg DA, Doring F, Eynott PR, Fischer A, Daniel H: **Intestinal peptide transport: ex vivo uptake studies and localization of peptide carrier PEPT1**. *American journal of physiology Gastrointestinal and liver physiology* 2001, **281**(3):G697-704.

32. Otto C, tom Dieck S, Bauer K: **Dipeptide uptake by adenohypophysial folliculostellate cells**. *Am J Physiol* 1996, **271**(1 Pt 1):C210-217.

33. Shen H, Smith DE, Yang T, Huang YG, Schnermann JB, Brosius FC, 3rd: **Localization of PEPT1 and PEPT2 proton-coupled oligopeptide transporter mRNA and protein in rat kidney**. *Am J Physiol* 1999, **276**(5 Pt 2):F658-665.

34. Agu R, Cowley E, Shao D, Macdonald C, Kirkpatrick D, Renton K, Massoud E: **Proton-coupled oligopeptide transporter (POT) family expression in human nasal epithelium and their drug transport potential**. *Mol Pharm* 2011, **8**(3):664-672.

35. Knutter I, Rubio-Aliaga I, Boll M, Hause G, Daniel H, Neubert K, Brandsch M: **H+-peptide cotransport in the human bile duct epithelium cell line SK-ChA-1**. *American journal of physiology Gastrointestinal and liver physiology* 2002, **283**(1):G222-229.

36. Charrier L, Driss A, Yan Y, Nduati V, Klapproth JM, Sitaraman SV, Merlin D: **hPepT1 mediates bacterial tripeptide fMLP uptake in human monocytes**. *Lab Invest* 2006, **86**(5):490-503.

37. Ruhl A, Hoppe S, Frey I, Daniel H, Schemann M: **Functional expression of the peptide transporter PEPT2 in the mammalian enteric nervous system**. *J Comp Neurol* 2005, **490**(1):1-11.

38. Romano A, Barca A, Kottra G, Daniel H, Storelli C, Verri T: **Functional expression of SLC15 peptide transporters in rat thyroid follicular cells**. *Mol Cell Endocrinol* 2010, **315**(1-2):174-181.

39. Groneberg DA, Doring F, Theis S, Nickolaus M, Fischer A, Daniel H: **Peptide transport in the mammary gland: expression and distribution of PEPT2 mRNA and protein**. *Am J Physiol Endocrinol Metab* 2002, **282**(5):E1172-1179.

40. Teuscher NS, Novotny A, Keep RF, Smith DE: **Functional evidence for presence of PEPT2 in rat choroid plexus: studies with glycylsarcosine**. *The Journal of pharmacology and experimental therapeutics* 2000, **294**(2):494-499.

41. Dieck ST, Heuer H, Ehrchen J, Otto C, Bauer K: **The peptide transporter PepT2 is expressed in rat brain and mediates the accumulation of the fluorescent dipeptide derivative beta-Ala-Lys-Nepsilon-AMCA in astrocytes**. *Glia* 1999, **25**(1):10-20.

42. Meier Y, Eloranta JJ, Darimont J, Ismair MG, Hiller C, Fried M, Kullak-Ublick GA, Vavricka SR: **Regional distribution of solute carrier mRNA expression along the human intestinal tract**. *Drug Metab Dispos* 2007, **35**(4):590-594.

43. Freeman TC, Bentsen BS, Thwaites DT, Simmons NL: **H+/di-tripeptide transporter (PepT1) expression in the rabbit intestine**. *Pflugers Archiv : European journal of physiology* 1995, **430**(3):394-400.

44. Englund G, Rorsman F, Ronnblom A, Karlbom U, Lazorova L, Grasjo J, Kindmark A, Artursson P: **Regional levels of drug transporters along the human intestinal tract: co-expression of ABC and SLC transporters and comparison with Caco-2 cells**. *Eur J Pharm Sci* 2006, **29**(3-4):269-277.

45. Jappar D, Wu SP, Hu Y, Smith DE: **Significance and regional dependency of peptide transporter (PEPT) 1 in the intestinal permeability of glycylsarcosine: in situ single-pass perfusion studies in wild-type and Pept1 knockout mice**. *Drug metabolism and disposition: the biological fate of chemicals* 2010, **38**(10):1740-1746.

46. Ogihara H, Saito H, Shin BC, Terado T, Takenoshita S, Nagamachi Y, Inui K, Takata K: **Immuno-localization of H+/peptide cotransporter in rat digestive tract**. *Biochem Biophys Res Commun* 1996, **220**(3):848-852.

47. Jappar D, Wu SP, Hu Y, Smith DE: **Significance and regional dependency of peptide transporter (PEPT) 1 in the intestinal permeability of glycylsarcosine: in situ single-pass perfusion studies in wild-type and Pept1 knockout mice**. *Drug Metab Dispos*, **38**(10):1740-1746.

48. Ziegler TR, Fernandez-Estivariz C, Gu LH, Bazargan N, Umeakunne K, Wallace TM, Diaz EE, Rosado KE, Pascal RR, Galloway JR *et al*: **Distribution of the**

H+/peptide transporter PepT1 in human intestine: up-regulated expression in the colonic mucosa of patients with short-bowel syndrome. *Am J Clin Nutr* 2002, **75**(5):922-930.

49. Wojtal KA, Eloranta JJ, Hruz P, Gutmann H, Drewe J, Staumann A, Beglinger C, Fried M, Kullak-Ublick GA, Vavricka SR: **Changes in mRNA expression levels of solute carrier transporters in inflammatory bowel disease patients**. *Drug Metab Dispos* 2009, **37**(9):1871-1877.

50. Merlin D, Si-Tahar M, Sitaraman SV, Eastburn K, Williams I, Liu X, Hediger MA, Madara JL: **Colonic epithelial hPepT1 expression occurs in inflammatory bowel disease: transport of bacterial peptides influences expression of MHC class 1 molecules**. *Gastroenterology* 2001, **120**(7):1666-1679.

51. Chen HQ, Yang J, Zhang M, Zhou YK, Shen TY, Chu ZX, Hang XM, Jiang YQ, Qin HL: **Lactobacillus plantarum ameliorates colonic epithelial barrier dysfunction by modulating the apical junctional complex and PepT1 in IL-10 knockout mice**. *American journal of physiology Gastrointestinal and liver physiology* 2010, **299**(6):G1287-1297.

52. Radeva G, Buyse M, Hindlet P, Beaufils B, Walker F, Bado A, Farinotti R: **Regulation of the oligopeptide transporter, PEPT-1, in DSS-induced rat colitis**. *Dig Dis Sci* 2007, **52**(7):1653-1661.

53. Talbot C, Lytle C: **Segregation of Na/H exchanger-3 and Cl/HCO3 exchanger SLC26A3 (DRA) in rodent cecum and colon**. *American journal of physiology Gastrointestinal and liver physiology* 2010, **299**(2):G358-367.

54. Yoshikawa T, Inoue R, Matsumoto M, Yajima T, Ushida K, Iwanaga T: **Comparative expression of hexose transporters (SGLT1, GLUT1, GLUT2 and GLUT5) throughout the mouse gastrointestinal tract**. *Histochem Cell Biol* 2011, **135**(2):183-194.

55. Balen D, Ljubojevic M, Breljak D, Brzica H, Zlender V, Koepsell H, Sabolic I: **Revised immunolocalization of the Na+-D-glucose cotransporter SGLT1 in rat organs with an improved antibody**. *Am J Physiol Cell Physiol* 2008, **295**(2):C475-489.

56. Wolffram S, Block M, Ader P: **Quercetin-3-glucoside is transported by the glucose carrier SGLT1 across the brush border membrane of rat small intestine**. *J Nutr* 2002, **132**(4):630-635.

57. Steinhardt HJ, Adibi SA: **Kinetics and characteristics of absorption from an equimolar mixture of 12 glycyl-dipeptides in human jejunum**. *Gastroenterology* 1986, **90**(3):577-582.

58. Asatoor AM, Cheng B, Edwards KD, Lant AF, Matthews DM, Milne MD, Navab F, Richards AJ: **Intestinal absorption of dipeptides and corresponding free amino acids in Hartnup disease**. *Clin Sci (Lond)* 1970, **39**(1):1P.

59. Hu Y, Smith DE, Ma K, Jappar D, Thomas W, Hillgren KM: **Targeted disruption of peptide transporter Pept1 gene in mice significantly reduces dipeptide absorption in intestine**. *Mol Pharm* 2008, **5**(6):1122-1130.

60. Nassl AM, Rubio-Aliaga I, Fenselau H, Marth MK, Kottra G, Daniel H: **Amino acid absorption and homeostasis in mice lacking the intestinal peptide transporter PEPT1**. *American journal of physiology Gastrointestinal and liver physiology* 2011, **301**(1):G128-137.

61. Chen M, Singh A, Xiao F, Dringenberg U, Wang J, Engelhardt R, Yeruva S, Rubio-Aliaga I, Nassl AM, Kottra G *et al*: **Gene ablation for PEPT1 in mice abolishes the effects of dipeptides on small intestinal fluid absorption, short-circuit current, and intracellular pH**. *American journal of physiology Gastrointestinal and liver physiology* 2010, **299**(1):G265-274.

62. Shiraga T, Miyamoto K, Tanaka H, Yamamoto H, Taketani Y, Morita K, Tamai I, Tsuji A, Takeda E: **Cellular and molecular mechanisms of dietary regulation on rat intestinal H+/Peptide transporter PepT1**. *Gastroenterology* 1999, **116**(2):354-362.

63. Shimakura J, Terada T, Saito H, Katsura T, Inui K: **Induction of intestinal peptide transporter 1 expression during fasting is mediated via peroxisome proliferator-activated receptor alpha**. *American journal of physiology Gastrointestinal and liver physiology* 2006, **291**(5):G851-856.

64. Saito H, Terada T, Shimakura J, Katsura T, Inui K: **Regulatory mechanism governing the diurnal rhythm of intestinal H+/peptide cotransporter 1 (PEPT1)**. *American journal of physiology Gastrointestinal and liver physiology* 2008, **295**(2):G395-402.

65. Maeng HJ, Durk MR, Chow EC, Ghoneim R, Pang KS: **1alpha,25-dihydroxyvitamin D3 on intestinal transporter function: studies with the rat everted intestinal sac**. *Biopharm Drug Dispos* 2011, **32**(2):112-125.

66. Chow EC, Sun H, Khan AA, Groothuis GM, Pang KS: **Effects of 1alpha,25-dihydroxyvitamin D3 on transporters and enzymes of the rat intestine and kidney in vivo**. *Biopharm Drug Dispos* 2010, **31**(1):91-108.

67. Nduati V, Yan Y, Dalmasso G, Driss A, Sitaraman S, Merlin D: **Leptin transcriptionally enhances peptide transporter (hPepT1) expression and activity via the cAMP-response element-binding protein and Cdx2 transcription factors**. *The Journal of biological chemistry* 2007, **282**(2):1359-1373.

68. Dalmasso G, Nguyen HT, Yan Y, Charrier-Hisamuddin L, Sitaraman SV, Merlin D: **Butyrate transcriptionally enhances peptide transporter PepT1 expression and activity**. *PLoS One* 2008, **3**(6):e2476.

69. Nguyen HT, Dalmasso G, Powell KR, Yan Y, Bhatt S, Kalman D, Sitaraman SV, Merlin D: **Pathogenic bacteria induce colonic PepT1 expression: an implication in host defense response**. *Gastroenterology* 2009, **137**(4):1435-1447 e1431-1432.

70. Ashida K, Katsura T, Saito H, Inui K: **Decreased activity and expression of intestinal oligopeptide transporter PEPT1 in rats with hyperthyroidism in vivo**. *Pharmaceutical research* 2004, **21**(6):969-975.

71. Hindlet P, Bado A, Farinotti R, Buyse M: **Long-term effect of leptin on H+-coupled peptide cotransporter 1 activity and expression in vivo: evidence in leptin-deficient mice**. *J Pharmacol Exp Ther* 2007, **323**(1):192-201.

72. Shimakura J, Terada T, Shimada Y, Katsura T, Inui K: **The transcription factor Cdx2 regulates the intestine-specific expression of human peptide transporter 1 through functional interaction with Sp1**. *Biochem Pharmacol* 2006, **71**(11):1581-1588.

73. Shimakura J, Terada T, Katsura T, Inui K: **Characterization of the human peptide transporter PEPT1 promoter: Sp1 functions as a basal transcriptional regulator of human PEPT1**. *American journal of physiology Gastrointestinal and liver physiology* 2005, **289**(3):G471-477.

74. Pugh BF, Tjian R: **Transcription from a TATA-less promoter requires a multisubunit TFIID complex**. *Genes Dev* 1991, **5**(11):1935-1945.

75. Blake MC, Jambou RC, Swick AG, Kahn JW, Azizkhan JC: **Transcriptional initiation is controlled by upstream GC-box interactions in a TATAA-less promoter**. *Mol Cell Biol* 1990, **10**(12):6632-6641.

76. Pohjanpelto P, Holtta E: **Deprivation of a single amino acid induces protein synthesis-dependent increases in c-jun, c-myc, and ornithine decarboxylase mRNAs in Chinese hamster ovary cells**. *Mol Cell Biol* 1990, **10**(11):5814-5821.

77. Dalmasso G, Nguyen HT, Yan Y, Laroui H, Charania MA, Obertone TS, Sitaraman SV, Merlin D: **MicroRNA-92b regulates expression of the oligopeptide transporter PepT1 in intestinal epithelial cells**. *American journal of physiology Gastrointestinal and liver physiology* 2011, **300**(1):G52-59.

78. Pearson R, Fleetwood J, Eaton S, Crossley M, Bao S: **Kruppel-like transcription factors: a functional family**. *Int J Biochem Cell Biol* 2008, **40**(10):1996-2001.

79. Yu T, Chen X, Zhang W, Li J, Xu R, Wang TC, Ai W, Liu C: **Kruppel-like Factor 4 Regulates Intestinal Epithelial Cell Morphology and Polarity**. *PLoS One* 2012, **7**(2):e32492.

80. Li IC, Chan CT, Lu YF, Wu YT, Chen YC, Li GB, Lin CY, Hwang SP: **Zebrafish kruppel-like factor 4a represses intestinal cell proliferation and promotes differentiation of intestinal cell lineages**. *PLoS One* 2011, **6**(6):e20974.

81. Price AB, Morson BC: **Inflammatory bowel disease: the surgical pathology of Crohn's disease and ulcerative colitis**. *Hum Pathol* 1975, **6**(1):7-29.

82. Rao SS, Holdsworth CD, Read NW: **Symptoms and stool patterns in patients with ulcerative colitis**. *Gut* 1988, **29**(3):342-345.

83. **Unusual symptoms of Crohn's disease**. *Br Med J* 1972, **3**(5828):658.

84. Schirbel A, Fiocchi C: **Inflammatory bowel disease: Established and evolving considerations on its etiopathogenesis and therapy**. *J Dig Dis* 2010, **11**(5):266-276.

85. Andersson R, Wang X, Soltesz V: **The significance and potential molecular mechanisms of gastrointestinal barrier homeostasis**. *Scand J Gastroenterol* 1997, **32**(11):1073-1082.

86. Iniguez-Palomares C, Jimenez-Flores R, Vazquez-Moreno L, Ramos-Clamont-Montfort G, Acedo-Felix E: **Protein-carbohydrate interactions between Lactobacillus salivarius and pig mucins**. *J Anim Sci* 2011, **89**(10):3125-3131.

87. Smith CJ, Kaper JB, Mack DR: **Intestinal mucin inhibits adhesion of human enteropathogenic Escherichia coli to HEp-2 cells**. *J Pediatr Gastroenterol Nutr* 1995, **21**(3):269-276.

88. Enss ML, Grosse-Siestrup H, Schmidt-Wittig U, Gartner K: **Changes in colonic mucins of germfree rats in response to the introduction of a "normal" rat microbial flora. Rat colonic mucin**. *J Exp Anim Sci* 1992, **35**(3):110-119.

89. Meslin JC, Fontaine N, Andrieux C: **Variation of mucin distribution in the rat intestine, caecum and colon: effect of the bacterial flora**. *Comp Biochem Physiol A Mol Integr Physiol* 1999, **123**(3):235-239.

90. Van der Sluis M, De Koning BA, De Bruijn AC, Velcich A, Meijerink JP, Van Goudoever JB, Buller HA, Dekker J, Van Seuningen I, Renes IB *et al*: **Muc2-deficient mice spontaneously develop colitis, indicating that MUC2 is critical for colonic protection**. *Gastroenterology* 2006, **131**(1):117-129.

91. An G, Wei B, Xia B, McDaniel JM, Ju T, Cummings RD, Braun J, Xia L: **Increased susceptibility to colitis and colorectal tumors in mice lacking core 3-derived O-glycans**. *J Exp Med* 2007, **204**(6):1417-1429.

92. Wehkamp J, Harder J, Weichenthal M, Schwab M, Schaffeler E, Schlee M, Herrlinger KR, Stallmach A, Noack F, Fritz P *et al*: **NOD2 (CARD15) mutations in Crohn's disease are associated with diminished mucosal alpha-defensin expression**. *Gut* 2004, **53**(11):1658-1664.

93. Wehkamp J, Salzman NH, Porter E, Nuding S, Weichenthal M, Petras RE, Shen B, Schaeffeler E, Schwab M, Linzmeier R *et al*: **Reduced Paneth cell alpha-defensins in ileal Crohn's disease**. *Proc Natl Acad Sci U S A* 2005, **102**(50):18129-18134.

94. Ramasundara M, Leach ST, Lemberg DA, Day AS: **Defensins and inflammation: the role of defensins in inflammatory bowel disease**. *J Gastroenterol Hepatol* 2009, **24**(2):202-208.

95. Vaishnava S, Behrendt CL, Ismail AS, Eckmann L, Hooper LV: **Paneth cells directly sense gut commensals and maintain homeostasis at the intestinal host-microbial interface**. *Proc Natl Acad Sci U S A* 2008, **105**(52):20858-20863.

96. Strobel S, Ferguson A: **Oral tolerance--induction and modulation**. *Klin Padiatr* 1985, **197**(4):297-301.

97. Duchmann R, Kaiser I, Hermann E, Mayet W, Ewe K, Meyer zum Buschenfelde KH: **Tolerance exists towards resident intestinal flora but is broken in active inflammatory bowel disease (IBD)**. *Clin Exp Immunol* 1995, **102**(3):448-455.

98.   Vance RE, Isberg RR, Portnoy DA: **Patterns of pathogenesis: discrimination of pathogenic and nonpathogenic microbes by the innate immune system**. *Cell Host Microbe* 2009, **6**(1):10-21.

99.   Cario E, Rosenberg IM, Brandwein SL, Beck PL, Reinecker HC, Podolsky DK: **Lipopolysaccharide activates distinct signaling pathways in intestinal epithelial cell lines expressing Toll-like receptors**. *J Immunol* 2000, **164**(2):966-972.

100.   Hisamatsu T, Suzuki M, Reinecker HC, Nadeau WJ, McCormick BA, Podolsky DK: **CARD15/NOD2 functions as an antibacterial factor in human intestinal epithelial cells**. *Gastroenterology* 2003, **124**(4):993-1000.

101.   Carneiro LA, Travassos LH, Philpott DJ: **Innate immune recognition of microbes through Nod1 and Nod2: implications for disease**. *Microbes Infect* 2004, **6**(6):609-616.

102.   Chamaillard M, Girardin SE, Viala J, Philpott DJ: **Nods, Nalps and Naip: intracellular regulators of bacterial-induced inflammation**. *Cell Microbiol* 2003, **5**(9):581-592.

103.   Inohara, Chamaillard, McDonald C, Nunez G: **NOD-LRR proteins: role in host-microbial interactions and inflammatory disease**. *Annu Rev Biochem* 2005, **74**:355-383.

104.   Kobayashi K, Inohara N, Hernandez LD, Galan JE, Nunez G, Janeway CA, Medzhitov R, Flavell RA: **RICK/Rip2/CARDIAK mediates signalling for receptors of the innate and adaptive immune systems**. *Nature* 2002, **416**(6877):194-199.

105.   Chung Y, Chang SH, Martinez GJ, Yang XO, Nurieva R, Kang HS, Ma L, Watowich SS, Jetten AM, Tian Q *et al*: **Critical regulation of early Th17 cell differentiation by interleukin-1 signaling**. *Immunity* 2009, **30**(4):576-587.

106.   Siegmund B: **Interleukin-18 in intestinal inflammation: friend and foe?** *Immunity* 2010, **32**(3):300-302.

107.   Tanabe T, Chamaillard M, Ogura Y, Zhu L, Qiu S, Masumoto J, Ghosh P, Moran A, Predergast MM, Tromp G *et al*: **Regulatory regions and critical residues of NOD2 involved in muramyl dipeptide recognition**. *Embo J* 2004, **23**(7):1587-1597.

108.   Laroui H, Yan Y, Narui Y, Ingersoll SA, Ayyadurai S, Charania MA, Zhou F, Wang B, Salaita K, Sitaraman SV *et al*: **L-Ala-g-D-Glu-meso-DAP interacts directly with the leucine-rich region domain of nucleotide-binding oligomerization domain 1, increasing the phosphorylation activity of receptor-interacting serine/threonine-protein kinase 2 and its interaction with nucleotide-binding oligomerization domain 1**. *The Journal of biological chemistry* 2011.

109.   Bell JK, Mullen GE, Leifer CA, Mazzoni A, Davies DR, Segal DM: **Leucine-rich repeats and pathogen recognition in Toll-like receptors**. *Trends Immunol* 2003, **24**(10):528-533.

110.   Hayashi F, Smith KD, Ozinsky A, Hawn TR, Yi EC, Goodlett DR, Eng JK, Akira S, Underhill DM, Aderem A: **The innate immune response to bacterial flagellin is mediated by Toll-like receptor 5**. *Nature* 2001, **410**(6832):1099-1103.

111.   Grabiec A, Meng G, Fichte S, Bessler W, Wagner H, Kirschning CJ: **Human but not murine toll-like receptor 2 discriminates between tri-palmitoylated and tri-lauroylated peptides**. *The Journal of biological chemistry* 2004, **279**(46):48004-48012.

112.   Hemmi H, Takeuchi O, Kawai T, Kaisho T, Sato S, Sanjo H, Matsumoto M, Hoshino K, Wagner H, Takeda K *et al*: **A Toll-like receptor recognizes bacterial DNA**. *Nature* 2000, **408**(6813):740-745.

113.   Zhang G, Ghosh S: **Toll-like receptor-mediated NF-kappaB activation: a phylogenetically conserved paradigm in innate immunity**. *J Clin Invest* 2001, **107**(1):13-19.

114.   Akira S, Takeda K: **Toll-like receptor signalling**. *Nat Rev Immunol* 2004, **4**(7):499-511.

115. Barnich N, Aguirre JE, Reinecker HC, Xavier R, Podolsky DK: **Membrane recruitment of NOD2 in intestinal epithelial cells is essential for nuclear factor-{kappa}B activation in muramyl dipeptide recognition**. *J Cell Biol* 2005, **170**(1):21-26.

116. Clavel T, Haller D: **Bacteria- and host-derived mechanisms to control intestinal epithelial cell homeostasis: implications for chronic inflammation**. *Inflamm Bowel Dis* 2007, **13**(9):1153-1164.

117. Kelly D, Campbell JI, King TP, Grant G, Jansson EA, Coutts AG, Pettersson S, Conway S: **Commensal anaerobic gut bacteria attenuate inflammation by regulating nuclear-cytoplasmic shuttling of PPAR-gamma and RelA**. *Nat Immunol* 2004, **5**(1):104-112.

118. Kobayashi KS, Chamaillard M, Ogura Y, Henegariu O, Inohara N, Nunez G, Flavell RA: **Nod2-dependent regulation of innate and adaptive immunity in the intestinal tract**. *Science* 2005, **307**(5710):731-734.

119. Natividad JM, Petit V, Huang X, de Palma G, Jury J, Sanz Y, Philpott D, Garcia Rodenas CL, McCoy KD, Verdu EF: **Commensal and probiotic bacteria influence intestinal barrier function and susceptibility to colitis in Nod1(-/-);Nod2(-/-) Mice**. *Inflamm Bowel Dis* 2011.

120. Strober W, Murray PJ, Kitani A, Watanabe T: **Signalling pathways and molecular interactions of NOD1 and NOD2**. *Nat Rev Immunol* 2006, **6**(1):9-20.

121. Watanabe T, Kitani A, Murray PJ, Wakatsuki Y, Fuss IJ, Strober W: **Nucleotide binding oligomerization domain 2 deficiency leads to dysregulated TLR2 signaling and induction of antigen-specific colitis**. *Immunity* 2006, **25**(3):473-485.

122. Watanabe T, Kitani A, Murray PJ, Strober W: **NOD2 is a negative regulator of Toll-like receptor 2-mediated T helper type 1 responses**. *Nat Immunol* 2004, **5**(8):800-808.

123. Dziarski R, Gupta D: **Peptidoglycan recognition in innate immunity**. *J Endotoxin Res* 2005, **11**(5):304-310.

124. Schnare M, Barton GM, Holt AC, Takeda K, Akira S, Medzhitov R: **Toll-like receptors control activation of adaptive immune responses**. *Nat Immunol* 2001, **2**(10):947-950.

125. Cooney R, Baker J, Brain O, Danis B, Pichulik T, Allan P, Ferguson DJ, Campbell BJ, Jewell D, Simmons A: **NOD2 stimulation induces autophagy in dendritic cells influencing bacterial handling and antigen presentation**. *Nat Med* 2010, **16**(1):90-97.

126. Saitoh T, Fujita N, Jang MH, Uematsu S, Yang BG, Satoh T, Omori H, Noda T, Yamamoto N, Komatsu M *et al*: **Loss of the autophagy protein Atg16L1 enhances endotoxin-induced IL-1beta production**. *Nature* 2008, **456**(7219):264-268.

127. Cario E: **Toll-like receptors in inflammatory bowel diseases: a decade later**. *Inflamm Bowel Dis* 2010, **16**(9):1583-1597.

128. Vijay-Kumar M, Sanders CJ, Taylor RT, Kumar A, Aitken JD, Sitaraman SV, Neish AS, Uematsu S, Akira S, Williams IR *et al*: **Deletion of TLR5 results in spontaneous colitis in mice**. *J Clin Invest* 2007, **117**(12):3909-3921.

129. Messlik A, Schmechel S, Kisling S, Bereswill S, Heimesaat MM, Fischer A, Gobel U, Haller D: **Loss of Toll-like receptor 2 and 4 leads to differential induction of endoplasmic reticulum stress and proapoptotic responses in the intestinal epithelium under conditions of chronic inflammation**. *J Proteome Res* 2009, **8**(10):4406-4417.

130. Araki A, Kanai T, Ishikura T, Makita S, Uraushihara K, Iiyama R, Totsuka T, Takeda K, Akira S, Watanabe M: **MyD88-deficient mice develop severe intestinal inflammation in dextran sodium sulfate colitis**. *J Gastroenterol* 2005, **40**(1):16-23.

131. Rakoff-Nahoum S, Paglino J, Eslami-Varzaneh F, Edberg S, Medzhitov R: **Recognition of commensal microflora by toll-like receptors is required for intestinal homeostasis**. *Cell* 2004, **118**(2):229-241.

132. Nenci A, Becker C, Wullaert A, Gareus R, van Loo G, Danese S, Huth M, Nikolaev A, Neufert C, Madison B *et al*: **Epithelial NEMO links innate immunity to chronic intestinal inflammation**. *Nature* 2007, **446**(7135):557-561.

133. McGuckin MA, Eri R, Simms LA, Florin TH, Radford-Smith G: **Intestinal barrier dysfunction in inflammatory bowel diseases**. *Inflamm Bowel Dis* 2009, **15**(1):100-113.

134. Steck N, Hoffmann M, Sava IG, Kim SC, Hahne H, Tonkonogy SL, Mair K, Krueger D, Pruteanu M, Shanahan F *et al*: **Enterococcus faecalis Metalloprotease Compromises Epithelial Barrier and Contributes to Intestinal Inflammation**. *Gastroenterology* 2011.

135. Sartor RB: **Therapeutic manipulation of the enteric microflora in inflammatory bowel diseases: antibiotics, probiotics, and prebiotics**. *Gastroenterology* 2004, **126**(6):1620-1633.

136. Hormannsperger G, Haller D: **Molecular crosstalk of probiotic bacteria with the intestinal immune system: clinical relevance in the context of inflammatory bowel disease**. *Int J Med Microbiol* 2010, **300**(1):63-73.

137. Chieppa M, Rescigno M, Huang AY, Germain RN: **Dynamic imaging of dendritic cell extension into the small bowel lumen in response to epithelial cell TLR engagement**. *J Exp Med* 2006, **203**(13):2841-2852.

138. Niess JH, Brand S, Gu X, Landsman L, Jung S, McCormick BA, Vyas JM, Boes M, Ploegh HL, Fox JG *et al*: **CX3CR1-mediated dendritic cell access to the intestinal lumen and bacterial clearance**. *Science* 2005, **307**(5707):254-258.

139. Hue S, Ahern P, Buonocore S, Kullberg MC, Cua DJ, McKenzie BS, Powrie F, Maloy KJ: **Interleukin-23 drives innate and T cell-mediated intestinal inflammation**. *J Exp Med* 2006, **203**(11):2473-2483.

140. Kamada N, Hisamatsu T, Okamoto S, Sato T, Matsuoka K, Arai K, Nakai T, Hasegawa A, Inoue N, Watanabe N *et al*: **Abnormally differentiated subsets of intestinal macrophage play a key role in Th1-dominant chronic colitis through excess production of IL-12 and IL-23 in response to bacteria**. *J Immunol* 2005, **175**(10):6900-6908.

141. Zenewicz LA, Antov A, Flavell RA: **CD4 T-cell differentiation and inflammatory bowel disease**. *Trends Mol Med* 2009, **15**(5):199-207.

142. Mudter J, Weigmann B, Bartsch B, Kiesslich R, Strand D, Galle PR, Lehr HA, Schmidt J, Neurath MF: **Activation pattern of signal transducers and activators of transcription (STAT) factors in inflammatory bowel diseases**. *Am J Gastroenterol* 2005, **100**(1):64-72.

143. Shimoda K, van Deursen J, Sangster MY, Sarawar SR, Carson RT, Tripp RA, Chu C, Quelle FW, Nosaka T, Vignali DA *et al*: **Lack of IL-4-induced Th2 response and IgE class switching in mice with disrupted Stat6 gene**. *Nature* 1996, **380**(6575):630-633.

144. Jacobson NG, Szabo SJ, Guler ML, Gorham JD, Murphy KM: **Regulation of interleukin-12 signalling during T helper phenotype development**. *Adv Exp Med Biol* 1996, **409**:61-73.

145. Niessner M, Volk BA: **Altered Th1/Th2 cytokine profiles in the intestinal mucosa of patients with inflammatory bowel disease as assessed by quantitative reversed transcribed polymerase chain reaction (RT-PCR)**. *Clin Exp Immunol* 1995, **101**(3):428-435.

146. Lakatos L: **Immunology of inflammatory bowel diseases**. *Acta Physiol Hung* 2000, **87**(4):355-372.

147. Weaver CT, Hatton RD, Mangan PR, Harrington LE: **IL-17 family cytokines and the expanding diversity of effector T cell lineages**. *Annu Rev Immunol* 2007, **25**:821-852.

148. Iwakura Y, Ishigame H: **The IL-23/IL-17 axis in inflammation**. *J Clin Invest* 2006, **116**(5):1218-1222.

149. Oppmann B, Lesley R, Blom B, Timans JC, Xu Y, Hunte B, Vega F, Yu N, Wang J, Singh K *et al*: **Novel p19 protein engages IL-12p40 to form a cytokine, IL-23, with biological activities similar as well as distinct from IL-12**. *Immunity* 2000, **13**(5):715-725.

150. Kamada N, Hisamatsu T, Okamoto S, Chinen H, Kobayashi T, Sato T, Sakuraba A, Kitazume MT, Sugita A, Koganei K *et al*: **Unique CD14 intestinal macrophages contribute to the pathogenesis of Crohn disease via IL-23/IFN-gamma axis**. *J Clin Invest* 2008, **118**(6):2269-2280.

151. Neufert C, Pickert G, Zheng Y, Wittkopf N, Warntjen M, Nikolaev A, Ouyang W, Neurath MF, Becker C: **Activation of epithelial STAT3 regulates intestinal homeostasis**. *Cell Cycle* 2010, **9**(4):652-655.

152. Yen D, Cheung J, Scheerens H, Poulet F, McClanahan T, McKenzie B, Kleinschek MA, Owyang A, Mattson J, Blumenschein W *et al*: **IL-23 is essential for T cell-mediated colitis and promotes inflammation via IL-17 and IL-6**. *J Clin Invest* 2006, **116**(5):1310-1316.

153. McGovern D, Powrie F: **The IL23 axis plays a key role in the pathogenesis of IBD**. *Gut* 2007, **56**(10):1333-1336.

154. Goodall JC, Wu C, Zhang Y, McNeill L, Ellis L, Saudek V, Gaston JS: **Endoplasmic reticulum stress-induced transcription factor, CHOP, is crucial for dendritic cell IL-23 expression**. *Proc Natl Acad Sci U S A* 2010, **107**(41):17698-17703.

155. Li MO, Flavell RA: **Contextual regulation of inflammation: a duet by transforming growth factor-beta and interleukin-10**. *Immunity* 2008, **28**(4):468-476.

156. Izcue A, Coombes JL, Powrie F: **Regulatory T cells suppress systemic and mucosal immune activation to control intestinal inflammation**. *Immunol Rev* 2006, **212**:256-271.

157. Powrie F, Carlino J, Leach MW, Mauze S, Coffman RL: **A critical role for transforming growth factor-beta but not interleukin 4 in the suppression of T helper type 1-mediated colitis by CD45RB(low) CD4+ T cells**. *J Exp Med* 1996, **183**(6):2669-2674.

158. Asseman C, Read S, Powrie F: **Colitogenic Th1 cells are present in the antigen-experienced T cell pool in normal mice: control by CD4+ regulatory T cells and IL-10**. *J Immunol* 2003, **171**(2):971-978.

159. Kehrl JH, Wakefield LM, Roberts AB, Jakowlew S, Alvarez-Mon M, Derynck R, Sporn MB, Fauci AS: **Production of transforming growth factor beta by human T lymphocytes and its potential role in the regulation of T cell growth**. *J Exp Med* 1986, **163**(5):1037-1050.

160. Kim JM, Rudensky A: **The role of the transcription factor Foxp3 in the development of regulatory T cells**. *Immunol Rev* 2006, **212**:86-98.

161. Hahm KB, Im YH, Parks TW, Park SH, Markowitz S, Jung HY, Green J, Kim SJ: **Loss of transforming growth factor beta signalling in the intestine contributes to tissue injury in inflammatory bowel disease**. *Gut* 2001, **49**(2):190-198.

162. Fantini MC, Rizzo A, Fina D, Caruso R, Sarra M, Stolfi C, Becker C, Macdonald TT, Pallone F, Neurath MF *et al*: **Smad7 controls resistance of colitogenic T cells to regulatory T cell-mediated suppression**. *Gastroenterology* 2009, **136**(4):1308-1316, e1301-1303.

163. Littman DR, Rudensky AY: **Th17 and regulatory T cells in mediating and restraining inflammation**. *Cell* 2010, **140**(6):845-858.

164. Izcue A, Coombes JL, Powrie F: **Regulatory lymphocytes and intestinal inflammation**. *Annu Rev Immunol* 2009, **27**:313-338.

165. Atarashi K, Tanoue T, Shima T, Imaoka A, Kuwahara T, Momose Y, Cheng G, Yamasaki S, Saito T, Ohba Y *et al*: **Induction of colonic regulatory T cells by indigenous Clostridium species**. *Science* 2011, **331**(6015):337-341.

166. Yu QT, Saruta M, Avanesyan A, Fleshner PR, Banham AH, Papadakis KA: **Expression and functional characterization of FOXP3+ CD4+ regulatory T cells in ulcerative colitis**. *Inflamm Bowel Dis* 2007, **13**(2):191-199.

167. Mizoguchi A, Bhan AK: **A case for regulatory B cells**. *J Immunol* 2006, **176**(2):705-710.

168. Fuss IJ, Heller F, Boirivant M, Leon F, Yoshida M, Fichtner-Feigl S, Yang Z, Exley M, Kitani A, Blumberg RS *et al*: **Nonclassical CD1d-restricted NK T cells that produce IL-13 characterize an atypical Th2 response in ulcerative colitis**. *J Clin Invest* 2004, **113**(10):1490-1497.

169. Madsen KL, Doyle JS, Tavernini MM, Jewell LD, Rennie RP, Fedorak RN: **Antibiotic therapy attenuates colitis in interleukin 10 gene-deficient mice**. *Gastroenterology* 2000, **118**(6):1094-1105.

170. Glocker EO, Kotlarz D, Boztug K, Gertz EM, Schaffer AA, Noyan F, Perro M, Diestelhorst J, Allroth A, Murugan D *et al*: **Inflammatory bowel disease and mutations affecting the interleukin-10 receptor**. *N Engl J Med* 2009, **361**(21):2033-2045.

171. Cho JH: **The genetics and immunopathogenesis of inflammatory bowel disease**. *Nat Rev Immunol* 2008, **8**(6):458-466.

172. Hugot JP, Chamaillard M, Zouali H, Lesage S, Cezard JP, Belaiche J, Almer S, Tysk C, O'Morain CA, Gassull M *et al*: **Association of NOD2 leucine-rich repeat variants with susceptibility to Crohn's disease**. *Nature* 2001, **411**(6837):599-603.

173. Ogura Y, Bonen DK, Inohara N, Nicolae DL, Chen FF, Ramos R, Britton H, Moran T, Karaliuskas R, Duerr RH *et al*: **A frameshift mutation in NOD2 associated with susceptibility to Crohn's disease**. *Nature* 2001, **411**(6837):603-606.

174. Bonen DK, Ogura Y, Nicolae DL, Inohara N, Saab L, Tanabe T, Chen FF, Foster SJ, Duerr RH, Brant SR *et al*: **Crohn's disease-associated NOD2 variants share a signaling defect in response to lipopolysaccharide and peptidoglycan**. *Gastroenterology* 2003, **124**(1):140-146.

175. Anderson CA, Boucher G, Lees CW, Franke A, D'Amato M, Taylor KD, Lee JC, Goyette P, Imielinski M, Latiano A *et al*: **Meta-analysis identifies 29 additional ulcerative colitis risk loci, increasing the number of confirmed associations to 47**. *Nat Genet* 2011, **43**(3):246-252.

176. Franke A, McGovern DP, Barrett JC, Wang K, Radford-Smith GL, Ahmad T, Lees CW, Balschun T, Lee J, Roberts R *et al*: **Genome-wide meta-analysis increases to 71 the number of confirmed Crohn's disease susceptibility loci**. *Nat Genet* 2010, **42**(12):1118-1125.

177. Khor B, Gardet A, Xavier RJ: **Genetics and pathogenesis of inflammatory bowel disease**. *Nature* 2011, **474**(7351):307-317.

178. Zucchelli M, Torkvist L, Bresso F, Halfvarson J, Hellquist A, Anedda F, Assadi G, Lindgren GB, Svanfeldt M, Janson M *et al*: **PepT1 oligopeptide transporter (SLC15A1) gene polymorphism in inflammatory bowel disease**. *Inflamm Bowel Dis* 2009, **15**(10):1562-1569.

179. Falk W, Harvath L, Leonard EJ: **Only the chemotactic subpopulation of human blood monocytes expresses receptors for the chemotactic peptide N-formylmethionyl-leucyl-phenylalanine**. *Infect Immun* 1982, **36**(2):450-454.

180. Anton PA, Targan SR, Shanahan F: **Increased neutrophil receptors for and response to the proinflammatory bacterial peptide formyl-methionyl-leucyl-phenylalanine in Crohn's disease**. *Gastroenterology* 1989, **97**(1):20-28.

181. Buyse M, Tsocas A, Walker F, Merlin D, Bado A: **PepT1-mediated fMLP transport induces intestinal inflammation in vivo**. *Am J Physiol Cell Physiol* 2002, **283**(6):C1795-1800.

182. Chester JF, Ross JS, Malt RA, Weitzman SA: **Acute colitis produced by chemotactic peptides in rats and mice**. *Am J Pathol* 1985, **121**(2):284-290.

183. Ledesma de Paolo MI, Celener Gravelle P, De Paula JA, Panzita MT, Bandi JC, Bustos Fernandez L: **Stimulation of inflammatory mediators secretion by chemotactic peptides in rat colitis model**. *Acta Gastroenterol Latinoam* 1996, **26**(1):23-30.

184. LeDuc LE, Nast CC: **Chemotactic peptide-induced acute colitis in rabbits**. *Gastroenterology* 1990, **98**(4):929-935.

185. Shi B, Song D, Xue H, Li N, Li J: **PepT1 mediates colon damage by transporting fMLP in rats with bowel resection**. *J Surg Res* 2006, **136**(1):38-44.

186. Shi B, Song D, Xue H, Li J, Li N: **Abnormal expression of the peptide transporter PepT1 in the colon of massive bowel resection rat: a potential route for colonic mucosa damage by transport of fMLP**. *Digestive diseases and sciences* 2006, **51**(11):2087-2093.

187. Buyse M, Charrier L, Sitaraman S, Gewirtz A, Merlin D: **Interferon-gamma increases hPepT1-mediated uptake of di-tripeptides including the bacterial tripeptide fMLP in polarized intestinal epithelia**. *Am J Pathol* 2003, **163**(5):1969-1977.

188. Girardin SE, Boneca IG, Viala J, Chamaillard M, Labigne A, Thomas G, Philpott DJ, Sansonetti PJ: **Nod2 is a general sensor of peptidoglycan through muramyl dipeptide (MDP) detection**. *The Journal of biological chemistry* 2003, **278**(11):8869-8872.

189. Vavricka SR, Musch MW, Chang JE, Nakagawa Y, Phanvijhitsiri K, Waypa TS, Merlin D, Schneewind O, Chang EB: **hPepT1 transports muramyl dipeptide, activating NF-kappaB and stimulating IL-8 secretion in human colonic Caco2/bbe cells**. *Gastroenterology* 2004, **127**(5):1401-1409.

190. Higgins LM, Frankel G, Douce G, Dougan G, MacDonald TT: **Citrobacter rodentium infection in mice elicits a mucosal Th1 cytokine response and lesions similar to those in murine inflammatory bowel disease**. *Infect Immun* 1999, **67**(6):3031-3039.

191. Den Hond E, Hiele M, Evenepoel P, Peeters M, Ghoos Y, Rutgeerts P: **In vivo butyrate metabolism and colonic permeability in extensive ulcerative colitis**. *Gastroenterology* 1998, **115**(3):584-590.

192. Ahmad MS, Krishnan S, Ramakrishna BS, Mathan M, Pulimood AB, Murthy SN: **Butyrate and glucose metabolism by colonocytes in experimental colitis in mice**. *Gut* 2000, **46**(4):493-499.

193. Schultz M, Veltkamp C, Dieleman LA, Grenther WB, Wyrick PB, Tonkonogy SL, Sartor RB: **Lactobacillus plantarum 299V in the treatment and prevention of spontaneous colitis in interleukin-10-deficient mice**. *Inflamm Bowel Dis* 2002, **8**(2):71-80.

194. Chen HQ, Shen TY, Zhou YK, Zhang M, Chu ZX, Hang XM, Qin HL: **Lactobacillus plantarum consumption increases PepT1-mediated amino acid absorption by enhancing protein kinase C activity in spontaneously colitic mice**. *J Nutr* 2010, **140**(12):2201-2206.

195. Kannengiesser K, Maaser C, Heidemann J, Luegering A, Ross M, Brzoska T, Bohm M, Luger TA, Domschke W, Kucharzik T: **Melanocortin-derived tripeptide KPV has anti-inflammatory potential in murine models of inflammatory bowel disease**. *Inflamm Bowel Dis* 2008, **14**(3):324-331.

196. Yoon SW, Lee CH, Kim JY, Sung MH, Poo H: **Lactobacillus casei secreting alpha-MSH induces the therapeutic effect on DSS-induced acute colitis in Balb/c Mice**. *J Microbiol Biotechnol* 2008, **18**(12):1975-1983.

197. Netea MG, Ferwerda G, de Jong DJ, Werts C, Boneca IG, Jehanno M, Van Der Meer JW, Mengin-Lecreulx D, Sansonetti PJ, Philpott DJ *et al*: **The frameshift mutation in Nod2 results in unresponsiveness not only to Nod2- but also Nod1-activating peptidoglycan agonists**. *The Journal of biological chemistry* 2005, **280**(43):35859-35867.

198. Dalmasso G, Nguyen HT, Ingersoll SA, Ayyadurai S, Laroui H, Charania MA, Yan Y, Sitaraman SV, Merlin D: **The PepT1-NOD2 Signaling Pathway Aggravates Induced Colitis in Mice**. *Gastroenterology* 2011.

199. Ingersoll SA, Ayyadurai S, Charania MA, Laroui H, Yan Y, Merlin D: **The role and pathophysiological relevance of membrane transporter PepT1 in intestinal inflammation and inflammatory bowel disease**. *American journal of physiology Gastrointestinal and liver physiology* 2011.

200. Wu X, Prasad PD, Leibach FH, Ganapathy V: **cDNA sequence, transport function, and genomic organization of human OCTN2, a new member of the organic cation transporter family**. *Biochemical and biophysical research communications* 1998, **246**(3):589-595.

201. Tamai I, Yabuuchi H, Nezu J, Sai Y, Oku A, Shimane M, Tsuji A: **Cloning and characterization of a novel human pH-dependent organic cation transporter, OCTN1**. *FEBS letters* 1997, **419**(1):107-111.

202. Tamai I, Ohashi R, Nezu J, Yabuuchi H, Oku A, Shimane M, Sai Y, Tsuji A: **Molecular and functional identification of sodium ion-dependent, high affinity human carnitine transporter OCTN2**. *The Journal of biological chemistry* 1998, **273**(32):20378-20382.

203. Noble CL, Nimmo ER, Drummond H, Ho GT, Tenesa A, Smith L, Anderson N, Arnott ID, Satsangi J: **The contribution of OCTN1/2 variants within the IBD5 locus to disease susceptibility and severity in Crohn's disease**. *Gastroenterology* 2005, **129**(6):1854-1864.

204. Fujiya M, Inaba Y, Musch MW, Hu S, Kohgo Y, Chang EB: **Cytokine regulation of OCTN2 expression and activity in small and large intestine**. *Inflamm Bowel Dis* 2011, **17**(4):907-916.

205. Girardin M, Dionne S, Goyette P, Rioux J, Bitton A, Elimrani I, Charlebois P, Qureshi I, Levy E, Seidman EG: **Expression and functional analysis of intestinal organic cation/l-carnitine transporter (OCTN) in Crohn's Disease**. *J Crohns Colitis* 2012, **6**(2):189-197.

206. Yamamoto-Furusho JK, Mendivil-Rangel EJ, Villeda-Ramirez MA, Fonseca-Camarillo G, Barreto-Zuniga R: **Gene expression of carnitine organic cation transporters 1 and 2 (OCTN) is downregulated in patients with ulcerative colitis**. *Inflamm Bowel Dis* 2011, **17**(10):2205-2206.

207. Noble CL, Abbas AR, Cornelius J, Lees CW, Ho GT, Toy K, Modrusan Z, Pal N, Zhong F, Chalasani S *et al*: **Regional variation in gene expression in the healthy colon is dysregulated in ulcerative colitis**. *Gut* 2008, **57**(10):1398-1405.

208. D'Argenio G, Calvani M, Casamassimi A, Petillo O, Margarucci S, Rienzo M, Peluso I, Calvani R, Ciccodicola A, Caporaso N *et al*: **Experimental colitis: decreased Octn2 and Atb0+ expression in rat colonocytes induces carnitine depletion that is reversible by carnitine-loaded liposomes**. *FASEB journal : official publication of the Federation of American Societies for Experimental Biology* 2006, **20**(14):2544-2546.

209. Shekhawat PS, Srinivas SR, Matern D, Bennett MJ, Boriack R, George V, Xu H, Prasad PD, Roon P, Ganapathy V: **Spontaneous development of intestinal and colonic atrophy and inflammation in the carnitine-deficient jvs (OCTN2(-/-)) mice**. *Mol Genet Metab* 2007, **92**(4):315-324.

210. Lee J, Tattoli I, Wojtal KA, Vavricka SR, Philpott DJ, Girardin SE: **pH-dependent internalization of muramyl peptides from early endosomes enables Nod1 and Nod2 signaling**. *The Journal of biological chemistry* 2009, **284**(35):23818-23829.

211. Blasius AL, Arnold CN, Georgel P, Rutschmann S, Xia Y, Lin P, Ross C, Li X, Smart NG, Beutler B: **Slc15a4, AP-3, and Hermansky-Pudlak syndrome proteins are required for Toll-like receptor signaling in plasmacytoid dendritic cells**. *Proc Natl Acad Sci U S A* 2010, **107**(46):19973-19978.

212. Sasawatari S, Okamura T, Kasumi E, Tanaka-Furuyama K, Yanobu-Takanashi R, Shirasawa S, Kato N, Toyama-Sorimachi N: **The solute carrier family 15A4**

regulates TLR9 and NOD1 functions in the innate immune system and promotes colitis in mice. *Gastroenterology* 2011, **140**(5):1513-1525.

213. Kiela PR, Laubitz D, Larmonier CB, Midura-Kiela MT, Lipko MA, Janikashvili N, Bai A, Thurston R, Ghishan FK: **Changes in mucosal homeostasis predispose NHE3 knockout mice to increased susceptibility to DSS-induced epithelial injury**. *Gastroenterology* 2009, **137**(3):965-975, 975 e961-910.

214. Cooper HS, Murthy SN, Shah RS, Sedergran DJ: **Clinicopathologic study of dextran sulfate sodium experimental murine colitis**. *Lab Invest* 1993, **69**(2):238-249.

215. Schmitz J, Preiser H, Maestracci D, Ghosh BK, Cerda JJ, Crane RK: **Purification of the human intestinal brush border membrane**. *Biochim Biophys Acta* 1973, **323**(1):98-112.

216. Hopfer U, Nelson K, Perrotto J, Isselbacher KJ: **Glucose transport in isolated brush border membrane from rat small intestine**. *J Biol Chem* 1973, **248**(1):25-32.

217. Kamath SA, Kummerow FA, Narayan KA: **A simple procedure for the isolation of rat liver microsomes**. *FEBS Lett* 1971, **17**(1):90-92.

218. Bradford MM: **A rapid and sensitive method for the quantitation of microgram quantities of protein utilizing the principle of protein-dye binding**. *Anal Biochem* 1976, **72**:248-254.

219. Bessey OA, Lowry OH, Brock MJ: **A method for the rapid determination of alkaline phosphates with five cubic millimeters of serum**. *J Biol Chem* 1946, **164**:321-329.

220. Rozen S, Skaletsky H: **Primer3 on the WWW for general users and for biologist programmers**. *Methods Mol Biol* 2000, **132**:365-386.

221. Pfaffl MW: **A new mathematical model for relative quantification in real-time RT-PCR**. *Nucleic Acids Res* 2001, **29**(9):e45.

222. Wilson TH, Wiseman G: **The use of sacs of everted small intestine for the study of the transference of substances from the mucosal to the serosal surface**. *J Physiol* 1954, **123**(1):116-125.

223. Sandhu JS, Fraser DR: **Assessment of intestinal permeability in the experimental rat with [3H]cellobiotol and [14C]mannitol**. *Clin Sci (Lond)* 1982, **63**(3):311-316.

224. Tarentino AL, Maley F: **Purification and properties of an endo-beta-N-acetylglucosaminidase from Streptomyces griseus**. *The Journal of biological chemistry* 1974, **249**(3):811-817.

225. Maley F, Trimble RB, Tarentino AL, Plummer TH, Jr.: **Characterization of glycoproteins and their associated oligosaccharides through the use of endoglycosidases**. *Analytical biochemistry* 1989, **180**(2):195-204.

226. Plummer TH, Jr., Elder JH, Alexander S, Phelan AW, Tarentino AL: **Demonstration of peptide:N-glycosidase F activity in endo-beta-N-acetylglucosaminidase F preparations**. *The Journal of biological chemistry* 1984, **259**(17):10700-10704.

227. Klebanoff SJ: **Myeloperoxidase**. *Proc Assoc Am Physicians* 1999, **111**(5):383-389.

228. Winterbourn CC: **Biological reactivity and biomarkers of the neutrophil oxidant, hypochlorous acid**. *Toxicology* 2002, **181-182**:223-227.

229. Midwinter RG, Vissers MC, Winterbourn CC: **Hypochlorous acid stimulation of the mitogen-activated protein kinase pathway enhances cell survival**. *Arch Biochem Biophys* 2001, **394**(1):13-20.

230. Schoonbroodt S, Legrand-Poels S, Best-Belpomme M, Piette J: **Activation of the NF-kappaB transcription factor in a T-lymphocytic cell line by hypochlorous acid**. *Biochem J* 1997, **321 (Pt 3)**:777-785.

231. Fu X, Kao JL, Bergt C, Kassim SY, Huq NP, d'Avignon A, Parks WC, Mecham RP, Heinecke JW: **Oxidative cross-linking of tryptophan to glycine restrains**

matrix metalloproteinase activity: specific structural motifs control protein oxidation**. *The Journal of biological chemistry* 2004, **279**(8):6209-6212.

232. Yan Y, Kolachala V, Dalmasso G, Nguyen H, Laroui H, Sitaraman SV, Merlin D: **Temporal and spatial analysis of clinical and molecular parameters in dextran sodium sulfate induced colitis**. *PLoS One* 2009, **4**(6):e6073.

233. West AB, Isaac CA, Carboni JM, Morrow JS, Mooseker MS, Barwick KW: **Localization of villin, a cytoskeletal protein specific to microvilli, in human ileum and colon and in colonic neoplasms**. *Gastroenterology* 1988, **94**(2):343-352.

234. Lown KS, Mayo RR, Leichtman AB, Hsiao HL, Turgeon DK, Schmiedlin-Ren P, Brown MB, Guo W, Rossi SJ, Benet LZ *et al*: **Role of intestinal P-glycoprotein (mdr1) in interpatient variation in the oral bioavailability of cyclosporine**. *Clin Pharmacol Ther* 1997, **62**(3):248-260.

235. Zimmermann C, Gutmann H, Hruz P, Gutzwiller JP, Beglinger C, Drewe J: **Mapping of multidrug resistance gene 1 and multidrug resistance-associated protein isoform 1 to 5 mRNA expression along the human intestinal tract**. *Drug metabolism and disposition: the biological fate of chemicals* 2005, **33**(2):219-224.

236. Nakamura N, Rabouille C, Watson R, Nilsson T, Hui N, Slusarewicz P, Kreis TE, Warren G: **Characterization of a cis-Golgi matrix protein, GM130**. *J Cell Biol* 1995, **131**(6 Pt 2):1715-1726.

237. Kontoyiannis D, Pasparakis M, Pizarro TT, Cominelli F, Kollias G: **Impaired on/off regulation of TNF biosynthesis in mice lacking TNF AU-rich elements: implications for joint and gut-associated immunopathologies**. *Immunity* 1999, **10**(3):387-398.

238. Kuhn R, Lohler J, Rennick D, Rajewsky K, Muller W: **Interleukin-10-deficient mice develop chronic enterocolitis**. *Cell* 1993, **75**(2):263-274.

239. Sellon RK, Tonkonogy S, Schultz M, Dieleman LA, Grenther W, Balish E, Rennick DM, Sartor RB: **Resident enteric bacteria are necessary for development of spontaneous colitis and immune system activation in interleukin-10-deficient mice**. *Infect Immun* 1998, **66**(11):5224-5231.

240. Rome S, Barbot L, Windsor E, Kapel N, Tricottet V, Huneau JF, Reynes M, Gobert JG, Tome D: **The regionalization of PepT1, NBAT and EAAC1 transporters in the small intestine of rats are unchanged from birth to adulthood**. *J Nutr* 2002, **132**(5):1009-1011.

241. Ohtsubo K, Marth JD: **Glycosylation in cellular mechanisms of health and disease**. *Cell* 2006, **126**(5):855-867.

242. Helenius A, Aebi M: **Intracellular functions of N-linked glycans**. *Science* 2001, **291**(5512):2364-2369.

243. Varki A, Lowe JB: **Biological Roles of Glycans**. In *Essentials of Glycobiology*. 2nd edition. Edited by Varki A, Cummings RD, Esko JD, Freeze HH, Stanley P, Bertozzi CR, Hart GW, Etzler ME. Cold Spring Harbor (NY); 2009.

244. Barnich N, Carvalho FA, Glasser AL, Darcha C, Jantscheff P, Allez M, Peeters H, Bommelaer G, Desreumaux P, Colombel JF *et al*: **CEACAM6 acts as a receptor for adherent-invasive E. coli, supporting ileal mucosa colonization in Crohn disease**. *J Clin Invest* 2007, **117**(6):1566-1574.

245. Hooper LV, Gordon JI: **Glycans as legislators of host-microbial interactions: spanning the spectrum from symbiosis to pathogenicity**. *Glycobiology* 2001, **11**(2):1R-10R.

246. Mack DR, Ahrne S, Hyde L, Wei S, Hollingsworth MA: **Extracellular MUC3 mucin secretion follows adherence of Lactobacillus strains to intestinal epithelial cells in vitro**. *Gut* 2003, **52**(6):827-833.

247. Laboisse C, Jarry A, Branka JE, Merlin D, Bou-Hanna C, Vallette G: **Recent aspects of the regulation of intestinal mucus secretion**. *Proc Nutr Soc* 1996, **55**(1B):259-264.

248. Einerhand AW, Renes IB, Makkink MK, van der Sluis M, Buller HA, Dekker J: **Role of mucins in inflammatory bowel disease: important lessons from experimental models**. *Eur J Gastroenterol Hepatol* 2002, **14**(7):757-765.

249. Pullan RD, Thomas GA, Rhodes M, Newcombe RG, Williams GT, Allen A, Rhodes J: **Thickness of adherent mucus gel on colonic mucosa in humans and its relevance to colitis**. *Gut* 1994, **35**(3):353-359.

250. Sharma R, Schumacher U: **Carbohydrate expression in the intestinal mucosa**. *Adv Anat Embryol Cell Biol* 2001, **160**:III-IX, 1-91.

251. Szentkuti L, Riedesel H, Enss ML, Gaertner K, Von Engelhardt W: **Pre-epithelial mucus layer in the colon of conventional and germ-free rats**. *Histochem J* 1990, **22**(9):491-497.

252. Macfarlane GT, Gibson GR, Cummings JH: **Comparison of fermentation reactions in different regions of the human colon**. *J Appl Bacteriol* 1992, **72**(1):57-64.

253. Walker AW, Duncan SH, McWilliam Leitch EC, Child MW, Flint HJ: **pH and peptide supply can radically alter bacterial populations and short-chain fatty acid ratios within microbial communities from the human colon**. *Appl Environ Microbiol* 2005, **71**(7):3692-3700.

254. Smith EA, Macfarlane GT: **Enumeration of human colonic bacteria producing phenolic and indolic compounds: effects of pH, carbohydrate availability and retention time on dissimilatory aromatic amino acid metabolism**. *J Appl Bacteriol* 1996, **81**(3):288-302.

255. Sellin JH: **SCFAs: The Enigma of Weak Electrolyte Transport in the Colon**. *News Physiol Sci* 1999, **14**:58-64.

256. Kawamata K, Hayashi H, Suzuki Y: **Chloride-dependent bicarbonate secretion in the mouse large intestine**. *Biomed Res* 2006, **27**(1):15-21.

257. Charney AN, Micic L, Egnor RW: **Nonionic diffusion of short-chain fatty acids across rat colon**. *Am J Physiol* 1998, **274**(3 Pt 1):G518-524.

258. Joly F, Mayeur C, Messing B, Lavergne-Slove A, Cazals-Hatem D, Noordine ML, Cherbuy C, Duee PH, Thomas M: **Morphological adaptation with preserved proliferation/transporter content in the colon of patients with short bowel syndrome**. *Am J Physiol Gastrointest Liver Physiol* 2009, **297**(1):G116-123.

259. Walter J, Ley R: **The human gut microbiome: ecology and recent evolutionary changes**. *Annu Rev Microbiol* 2011, **65**:411-429.

260. Carlson RM, Vavricka SR, Eloranta JJ, Musch MW, Arvans DL, Kles KA, Walsh-Reitz MM, Kullak-Ublick GA, Chang EB: **fMLP induces Hsp27 expression, attenuates NF-kappaB activation, and confers intestinal epithelial cell protection**. *American journal of physiology Gastrointestinal and liver physiology* 2007, **292**(4):G1070-1078.

261. Harig JM, Soergel KH, Barry JA, Ramaswamy K: **Transport of propionate by human ileal brush-border membrane vesicles**. *Am J Physiol* 1991, **260**(5 Pt 1):G776-782.

262. Mascolo N, Rajendran VM, Binder HJ: **Mechanism of short-chain fatty acid uptake by apical membrane vesicles of rat distal colon**. *Gastroenterology* 1991, **101**(2):331-338.

263. Rajendran VM, Binder HJ: **Apical membrane Cl-butyrate exchange: mechanism of short chain fatty acid stimulation of active chloride absorption in rat distal colon**. *J Membr Biol* 1994, **141**(1):51-58.

264. Cummings JH: **Short chain fatty acids in the human colon**. *Gut* 1981, **22**(9):763-779.

265. Cummings JH, Pomare EW, Branch WJ, Naylor CP, Macfarlane GT: **Short chain fatty acids in human large intestine, portal, hepatic and venous blood**. *Gut* 1987, **28**(10):1221-1227.

266. Sato T, Mushiake S, Kato Y, Sato K, Sato M, Takeda N, Ozono K, Miki K, Kubo Y, Tsuji A *et al*: **The Rab8 GTPase regulates apical protein localization in intestinal cells**. *Nature* 2007, **448**(7151):366-369.

267. Sugiura T, Kato Y, Wakayama T, Silver DL, Kubo Y, Iseki S, Tsuji A: **PDZK1 regulates two intestinal solute carriers (Slc15a1 and Slc22a5) in mice**. *Drug Metab Dispos* 2008, **36**(6):1181-1188.

268. Marina-Garcia N, Franchi L, Kim YG, Hu Y, Smith DE, Boons GJ, Nunez G: **Clathrin- and dynamin-dependent endocytic pathway regulates muramyl dipeptide internalization and NOD2 activation**. *J Immunol* 2009, **182**(7):4321-4327.

269. Allard JP, Jeejeebhoy KN: **Nutritional support and therapy in the short bowel syndrome**. *Gastroenterol Clin North Am* 1989, **18**(3):589-601.

270. Nightingale JM, Lennard-Jones JE, Walker ER, Farthing MJ: **Jejunal efflux in short bowel syndrome**. *Lancet* 1990, **336**(8718):765-768.

271. Iqbal CW, Qandeel HG, Zheng Y, Duenes JA, Sarr MG: **Mechanisms of ileal adaptation for glucose absorption after proximal-based small bowel resection**. *J Gastrointest Surg* 2008, **12**(11):1854-1864; discussion 1864-1855.

272. Madhavan S, Scow JS, Chaudhry RM, Nagao M, Zheng Y, Duenes JA, Sarr MG: **Intestinal Adaptation for Oligopeptide Absorption via PepT1 After Massive (70%) Mid-Small Bowel Resection**. *J Gastrointest Surg*.

273. Waterman M, Xu W, Stempak JM, Milgrom R, Bernstein CN, Griffiths AM, Greenberg GR, Steinhart AH, Silverberg MS: **Distinct and overlapping genetic loci in crohn's disease and ulcerative colitis: Correlations with pathogenesis**. *Inflamm Bowel Dis* 2011, **17**(9):1936-1942.

274. Charrier L, Merlin D: **The oligopeptide transporter hPepT1: gateway to the innate immune response**. *Lab Invest* 2006, **86**(6):538-546.

275. Hollander D: **Crohn's disease--a permeability disorder of the tight junction?** *Gut* 1988, **29**(12):1621-1624.

ACKNOWLEDGEMENTS

CURRICULUM VITAE

Personal information

Surname, first name	Wünsch, Tilo
Date of birth	02 June 1982
Nationality	German
Contact	Liebenwalder Str. 16
	D-13347 Berlin, Germany
Email	aufbali@gmx.de
Mobile	+49 163 4555444

Education and Training

08/2008 – 10/2011 **PhD student** at Technische Universität München (TUM), Molecular Nutrition Unit, Wissenschaftszentrum Weihenstephan, Freising, Germany

Title: „Colonic expression of the intestinal peptide transporter PEPT1 is not associated with inflammatory bowel diseases in humans and mouse models" (Supervisor: Prof. Daniel, Prof. Haller)

10/2007 – 07/2008 **Diploma thesis** at Charité - Campus Benjamin Franklin, Med. Klinik Nephrologie, Berlin, Germany

Topic: „Effects of hyperglycemia-induced oxidative stress on TRPC channel expression in human monocytes." (Supervisor: Prof. Tepel, Prof. Ristow)

11/2003 – 07/2008 **Diploma in Nutritional Sciences**, Friedrich-Schiller-University Jena, Germany; Course spezialization: Human Nutrition, Nutritional Medicine, Nutrition Physiology, Food Chemistry, Sports and Nutrition

06/2002 general qualification for university entrance
Gymnasium Burgstädt

PUBLICATIONS

Peer-reviewed

1. High Glucose–Induced Oxidative Stress Increases Transient Receptor Potential
   Channel Expression in Human Monocytes.
   Tilo Wuensch, Florian Thilo, Katharina Krueger, Alexandra Scholze, Michael Ristow,
   Martin Tepel. Diabetes. 2010;59:844-9

2. Colonic expression of the peptide transporter PEPT1 is not associated with
   inflammatory bowel diseases.
   Tilo Wuensch, Stephan Schulz, Nicole Lill, Nicola Schaltenberg, Gunnar Loh, Eva
   Rath, Miquel Sans, Ulf Goebel, Balfour R. Sartor, Dirk Haller, Hannelore Daniel. In
   Revision.

Non-peer-reviewed

1. Chronisch entzündliche Darmerkrankungen, Nährstoffaufnahme und PEPT1.
   Tilo Wuensch, Hannelore Daniel, Der Bauchredner, 01/2010

Poster presentations

1. Colonic GLP-1 secretion in response to luminal glucose requires SGLT1.
   Tilo Wuensch, Nicole Lill, Hannelore Daniel; 49. DGE Congress 2012,
   Weihenstephan, Germany

2. Functional Expression of the Peptide Transporter PEPT1 in Healthy Colon Contributes
   to Intestinal Water Absorption.
   Tilo Wuensch, Stephan Schulz, Hannelore Daniel; 48. DGE Congress 2011, Potsdam,
   Germany

3. BCAA Supplementation Improves Recovery from DSS-Induced Colitis in Mice.
   Sina Ullrich, **Tilo Wuensch**, Hannelore Daniel; 48. DGE Congress 2011, Potsdam,
   Germany

4. Hyperglycemia and oxidative stress affect the canonical transient receptor potential
   channel expression in monocytes
   Tilo Wuensch, Florian Thilo, Walter Zidek, Martin Tepel; Hypertension 2008, Berlin,
   Germany

ERKLÄRUNG

Hiermit erkläre ich, dass ich die vorliegende Doktorarbeit selbstständig angefertigt habe. Es wurden nur die in der Arbeit genannten Quellen und Hilfsmittel benutzt. Wörtlich oder sinngemäß übernommenes Gedankengut habe ich als solches kenntlich gemacht.

_____   _____

Ort, Datum   Unterschrift